

CRYSTALLISATION OF PENTAERYTHRITOL

by

John Frederick Rogers

A Thesis submitted to the University of Aston in
Birmingham as a requirement for the Degree of
Master of Science.

Department of Chemical Engineering
University of Aston in Birmingham

April, 1967.

CRYSTALLIZATION OF PENTAMETHYLDIUREA

by

John Frederick Rogers

THE UNIVERSITY OF M.
28 OCT 1969
Sheep 123491
547
Roh

- 3 NOV 1977

Department of Chemical Engineering
University of Aston in Birmingham

April, 1967.

SUMMARY

An analytical method based on the total formaldehyde content of Pentaerythritol (P.E.) was found suitable for the quantitative analysis of an unidentified formal impurity (called Compound X in this work) in P.E. in the absence of other formals. An eutectic was found with P.E. and 40% di - P.E. melting at 185.5°C. The morphology change below 200°C reported by Berlow et al (48) was thought to be, in fact, an eutectic formation due to traces of di - P.E.

A complicated solid/saturated solution phase equilibrium system exists between P.E. and its associated impurities di - P.E. and Compound X in aqueous solution. However, the equilibrium curve for Pure P.E. and P.E. containing respectively 4.73% Compound X,

< 0.1% di - P.E. (Batch A) and 4.3% Compound X, 1.0% di - P.E. (Batch C) could be correlated above 50°C by the equation:-

$$\log_{10} x = 5.072 - \frac{1266}{T}$$

It was found difficult to measure the growth of crystals from fluidised bed experiments by direct crystal measurement as the growth rate of P.E. was so slow; therefore a method was used following the decrease in supersaturation of solution by refractive index measurements, and the crystals were suspended by agitation. The growth rate constants were calculated

assuming a first order growth rate with respect to supersaturation which proved suitable within the limits of experimental accuracy. The growth rate constants \bar{K} obtained for Pure P.E. and Batch A between 50°C and 80°C were correlated by the equations:-

$$\text{Pure P.E. : } \log_{10} \bar{K} = 5.770 - \frac{4025}{T}$$

$$\text{Batch A : } \log_{10} \bar{K} = 13.401 - \frac{6710}{T}$$

with activation energies for growth of 18.4 and 30.65 K cal/g mole for Pure P.E. and Batch A respectively. The growth rates were the same at about 67°C but below this temperature Compound X inhibited the growth.

ACKNOWLEDGEMENTS

The author would like to express his thanks to the following:-

Dr. D.E. Creasy for his invaluable help and supervision throughout the period of this research.

Imperial Chemical Industries, Nobel Division for financial support and help with the chemical analysis.

Professor G.V. Jeffreys for his advice and encouragement.

Mrs. W. Grant for typing the thesis.

Mr. R. Roberts and the technical staff of the Chemical Engineering Department for their assistance and co-operation.

CONTENTS

	PAGE
Introduction	1
Section One - Literature Survey - Crystallisation.	2
1.1. Solubility	2
1.2. Nucleation	6
1.2.1. Primary Nucleation	8
1.2.1.1. Homogeneous Nucleation	8
1.2.1.2. Heterogeneous Nucleation	11
1.2.1.3. Induced Nucleation	13
1.2.2. Secondary Nucleation	15
1.3. Crystal Growth	16
1.3.1. Adsorption Layer Theories	16
1.3.2. Kinetics of Crystal Growth	20
Section Two - Literature Survey - Pentaerythritol	29
2.1. Crystal Structure	29
2.2. Physical Properties	30
2.3. Work done by I.C.I. on P.E. Crystallisation	32
2.4. Impurities in P.E.	33
2.5. Analysis	35
Section Three - Chemical Analysis	40 a
3.1. Introduction	40 a
3.2. Mixture Components	40 a
3.2.1. Pure P.E.	40 a
3.2.2. Di - P.E.	41
3.2.3. Compound X	41
3.2.3.1. Extraction	41
3.2.3.2. Synthesis	41

	PAGE
3.3. Melting Point	44
3.3.1. Apparatus	44
3.3.2. Method	44
3.3.3. Results	45
3.4. Refractive Index	46
3.5. Viscosity	47
3.6. Formaldehyde Content	47
3.6.1. General	47
3.6.2. Total Formaldehyde - Chromotropic Acid Method	48
3.6.2.1. Effect of Heat	48
3.6.2.2. Reagent	49
3.6.2.3. Procedure	49
3.6.3. Adsorbed Formaldehyde	50
3.6.3.1. Reagent	51
3.6.3.2. Procedure	51
3.6.4. Compound X Calibration	52
 Section Four - Preliminary Experiments	 54
4.1. Batch Crystallisation in a stirred vessel	54
4.2. Pilot Plant Oslo cooling crystalliser	55
4.3. Measurement of Crystal Growth in a small scale fluidised bed.	56
4.3.1. Apparatus	56
4.3.2. Size Analysis	57
4.3.3. Procedure	59
4.3.4. Results	61
 Section Five - P.E. Equilibrium in aqueous solution.	 63
5.1. Stability of Compound X in aqueous solution.	63
5.2. Preliminary Solubility Determinations	64
5.2.1. Introduction	64
5.2.2. Rate of Approach to equilibrium	64
5.2.3. Solubility Determination by evaporation	66

	PAGE
5.3. Refractometer Studies	67
5.3.1. Apparatus	67
5.3.2. Experimental Procedure	67
5.3.3. Accuracy	69
5.3.3.1. Instrument Calibration	69
5.3.3.2. Reading Accuracy	70
5.3.3.3. Impurities	71
5.3.4. Calibration Results	71
5.3.5. Nucleation Results	72
5.3.6. Equilibrium Results	73
5.3.7. Anomalous Results	74
5.3.7.1. Batch A	74
5.3.7.2. Batch C	75
 Section Six - Growth Studies by Refractometry	 77
6.1. Growth of Nuclei	77
6.2. Seeded Solutions	78
6.2.1. Introduction	78
6.2.2. Preliminary Tests	79
6.2.3. Metastable Limit	80
6.2.4. Choice of Seed	81
6.2.5. Attrition	82
6.2.6. Theory	85
6.2.7. Results	87
 Section Seven - Discussion and Proposals for Future Work	 91
Conclusions	96
Appendix A (referring to Section 3)	98
Appendix B (referring to Section 4)	104
Appendix C $\text{\textcircled{C}}$ Coulter Counter Particle Size Analyser	106
Appendix D (referring to Section 5)	121
Appendix E (referring to Section 6)	131
Nomenclature	150
References	155

LIST OF TABLES

TABLE		PAGE
1.	Formation of Compound X	98
2.	I.C.I. Analysis of P.E. Batches	99
3.	Melting Points of Binary System P.E./Di-P.E.	100
4.	Melting Points of Binary System P.E./ Compound X	101
5.	Effect of heat on "Formaldehyde Content" analysis.	101
5A.	Comparison of Optical Densities of Table 5	102
6.	Calibration of Spekker absorptiometer.	102
7.	Corrected Optical Density Table.	103
8.	Coulter Counter analysis L.l. before growth.	104
9.	Coulter Counter analysis M.l. after growth.	105
10.	Coulter Counter Data Representation.	114
11.	Calibration of 50 orifice tube.	115
12.	Calibration of 280 orifice tube.	116
13.	Calibration of 560 orifice tube.	117
14.	'F' Scale Expansion Factors for use with 50 tube.	118
15.	'F' Scale Expansion Factors for use with 280 tube.	119
16.	'F' Scale Expansion Factors for use with 560 tube.	120
17.	Rate of Approach to Equilibrium.	121
18.	Concentration equivalent of Specific Gravity at Equilibrium.	122
19.	Solubility Determinations by evaporation	123
20.	Interpolated Calibration of Refractometers	124

TABLE	PAGE	
21 a.	Interpolated Calibration Data - Pure P.E.	125
b.	Interpolated Calibration Data - Batch A.	126
c.	Interpolated Calibration Data - Batch C.	127
d.	Nucleation and Equilibrium Data.	128
22.	Equilibrium Data obtained from growth rate tests.	130
23.	Batch A sieve fraction seed - Effect of stirrer speed.	131
24.	Metastable Limit of Batch A in aqueous solution stirred at 500 r.p.m.	132
25.	Batch A - Comparison of different seed materials.	133
26.	Size Distribution 1. (280 μ tube).	134
27.	Size Distribution 2. (50 μ tube).	135
28.	Combined Size Distribution	136
29 a.	R.32 Pure P.E. Growth at 50.0°C	137
b.	R.27 Pure P.E. Growth at 60.0°C	138
c.	R.29 Pure P.E. Growth at 70.0°C	139
d.	R.30 Pure P.E. Growth at 80.0°C	140
e.	R.34 Repeat R.30. Pure P.E. Grown at 80.0°C.	141
30 a.	R.33 Batch A Growth at 50.0°C	142
b.	R.21 Batch A Growth at 55.0°C	143
c.	R.14 Batch A Growth at 60.0°C	144
d.	R.20 Batch A Growth at 70.0°C	145
e.	R.23 Batch A Growth at 80.0°C	146
31.	Batch C Growth at 60.0°C	147
32.	Batch A. Prepared Seed. Effect of Stirrer Speed.	148

LIST OF FIGURES

FIGURE	FOLLOWING PAGE
1. Condensed Phase Diagram.	2
2. P.E. Crystal Morphology according to Von Groth	29
3. Plan of P.E. structure according to Evans.	29
4. Electrothermal melting point thermometer calibration	99
5. Di - P.E./P.E. Binary melting system	100
6. P.E./Compound X Binary melting system	101
7. Spekker - formaldehyde calibration	102
8. Corrected Optical Density for Compound X	103
9. Size Analysis after batch crystallisation	105
10. Oslo Pilot Plant Crystalliser	55
11. Small Scale fluidised bed apparatus.	56
12. Theoretical P.E. Fluidisation in water.	105
13. Size analysis before and after fluidised bed growth.	105
14. The variation of Specific Gravity with P.E. concentration at 25.0°C.	121
15. Refractometers A and B	67
16. Specimen refractometer calibration curve.	124
17. Temperature correction for partial immersion.	129
18. Calibration for aqueous P.E. solutions (% mass fraction).	129
19. (a) Calibration for aqueous P.E. solutions (% m/v).	129
19. Conversion for concentration units.	130

FIGURE

FOLLOWING
PAGE

20	Nucleation and Equilibrium data (log concentration vs reciprocal temperature).	130	13
21.	Nucleation and Equilibrium data (linear plot).	130	
22 a.	Batch A - seed-sieve fraction 44 - 53 μ	81	
b.	Batch A - prepared seed - sieve fraction 44 - 53 μ .	81	
c.	Batch A - Ball-milled for 20 min - sieve fraction 44 - 53 μ .	81	
d.	Batch A - Ball-milled for 1 h - sieve fraction 44 - 53 μ .	81	
23 a.	Size Distribution (1) - 280 μ orifice tube - after 6 min attrition	134	
b.	Size Distribution (2) - 50 μ orifice tube - after 6 min attrition.	135	
24.	Variation of refractive index with P.E. concentration at constant temperatures.	148	
25.	Variation of growth rate constants with temperature.	148	

INTRODUCTION

During the final production stages in the manufacture of Pentaerythritol (referred to hereafter as P.E. for convenience) the process solution is cooled in a batch crystalliser. This results in a product consisting of agglomerates of a few large crystals and a large number of small ones - see fig. 22a. The amount of this fine material is such (25 mass % < 200 mesh, 18 mass % < 350 mesh) that it is very "dusty" and unpleasant to handle.

The object of the present study was to obtain nucleation and growth data and the effect of various parameters with a view to the design of equipment to produce a dust free uniform sized product. The form of this equipment might possibly be that of a continuous Oslo type cooling crystalliser.

SECTION ONE

LITERATURE SURVEY : CRYSTALLISATION

1.1. Solubility

The first requirement for the study of any crystallisation process is the phase equilibrium diagram. A typical example of the type of diagram obtained for the system pure solute dissolved in pure solvent is shown by the line F.B.D. called the 'solubility' curve in fig. 1. This curve defines the mass of solute which is in equilibrium with a given mass of solvent at various temperatures; the solvent is then said to be saturated with respect to the solute. For systems of more than one solute each must be studied individually. Gibbs' Phase Rule relates the number of components, C, phases P, and degrees of freedom, F of a system by means of the equation,

$$P + F = C + 2$$

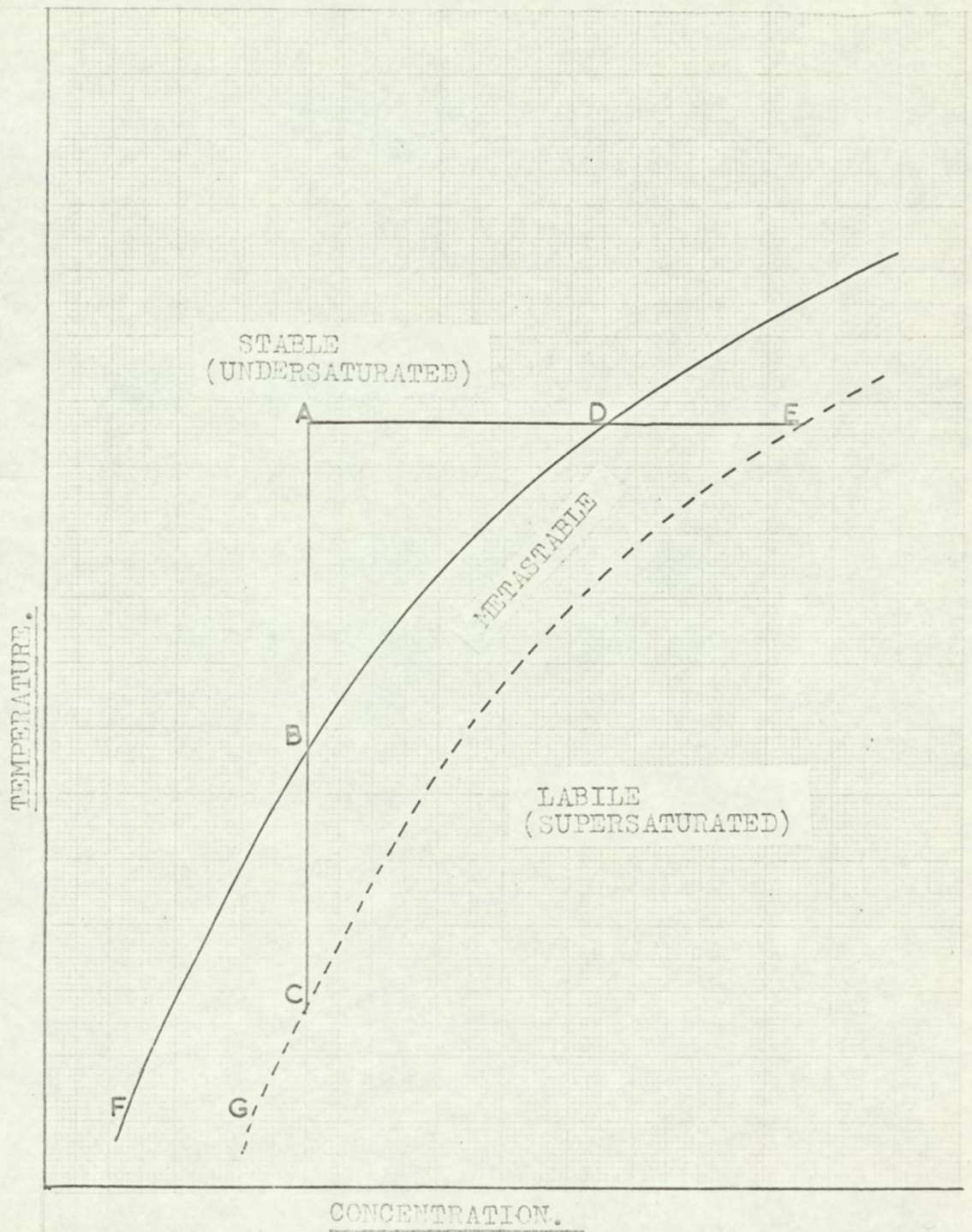
However for "condensed" systems the pressure can be ignored and hence:-

$$P + F^1 = C + 1$$

where F^1 is the number of degrees of freedom, not including pressure.

FIG. 1.

CONDENSED PHASE DIAGRAM.



A solution which contains more dissolved solute than that represented by the saturation composition is termed "supersaturated". Ostwald (1) seems to have been the first to introduce the terms "Labile" and "Metastable" zones which refer to the supersaturated solutions in which homogeneous nucleation will, and will not occur respectively.

Miers (2) did considerable research on this subject by studying the refractive index of solutions. Although he realised that factors such as the rate of cooling had an effect on the limits of supersaturation, he believed that supersolubility was a real property of solutions and melts under ordinary conditions. The supersolubility curve is shown in fig. 1 by the broken line G C E. If a solution of concentration and temperature A is cooled it remains undersaturated until temperature B is reached on the solubility curve. If further cooled it becomes supersaturated until temperature C on the supersolubility curve is reached, after which further cooling will produce spontaneous nucleation. The region between the solubility and supersolubility curves is the metastable supersaturated solution in which crystals are able to grow, but homogeneous nucleation does not normally occur. It is possible to produce supersaturation not only by cooling but also by

evaporation or sometimes by the addition of another solute soluble in the solvent. The concentration then follows line A D E, Fig. 1. Combinations of these three methods are also used on an industrial scale. The supersaturation curve is affected by many variables and is now considered to be a region of supersaturation rather than a definite curve, which is roughly parallel to the solubility curve.

The phenomenon of supersolubility can be explained by the enhanced solubility of fine particles. Ostwald (1) found that if a solute was finely ground before dissolving in water a solubility that was greater than the normal solubility was obtainable. He derived the equation which was later corrected by Freundlich (3) to:-

$$\ln \frac{C_r}{C_\infty} = \frac{2 \sigma V}{R T r}$$

Where C_r and C_∞ are the solubilities of the spherical particles of radius r and ∞ respectively, σ is the surface energy of the solid particle in contact with the solution, V is the molar volume, T is the absolute temperature and R is the gas constant. In the derivation of this equation it was assumed that the particles were spherical, the dissolved solid obeyed the gas laws, and that σ and ρ were independent of particle size. A number of workers

have postulated corrections to the Ostwald - Freundlich equation; e.g: consideration of the energy contributions of edges and corners to the total surface energy; allowance for the degree of dissociation or ionization of the dissolved solid; and the variation of surface energy with particle size. However the equations deduced all postulated a continual increase in solubility with reduction in particle size.

Knapp (4) showed that, if the opposing effect of the electric charge on the surface tension of a particle was considered, the particles were assumed to be isolated charged spheres and their charge independent of size, then the Ostwald - Freundlich equation was modified to:-

$$\ln \frac{C_r}{C_\infty} = \frac{V}{RT} \left(\frac{2\sigma}{r} - \frac{q^2}{8\pi K r^4} \right)$$

Where q is the charge and K the dielectric constant of the medium in which they are dispersed. From this equation the solubility can be shown to have a maximum

when

$$r = \left(\frac{q^2}{4\pi K \sigma} \right)^{1/3}$$

However according to Helmholtz's theory there arises at the interface of disperse particles and the dispersion medium an electrical "double-layer". If then each particle is regarded as a double-layer condenser, its

electrical energy is given by: $\frac{q^2 d}{2Kr(r + d)}$

where q is the quantity of electricity on each layer, d is the distance between the layers and r is the radius.

If d is negligible compared with r this reduces to: $\frac{q^2 d}{2Kr^2}$

The Ostwald - Freundlich equation then becomes:

$$\ln \frac{C_r}{C_\infty} = \frac{V}{RT} \left(\frac{2\sigma}{r} - \frac{q^2 d}{4\pi Kr^5} \right)$$

and the solubility is than a maximum when $r = \left(\frac{5q^2 d}{8\pi k\sigma} \right)^{\frac{1}{4}}$

Dundon (5) found appreciable increases in the solubilities of 0.2μ to 0.5μ particles of PbI_2 , Ag_2CrO_4 , PbF_2 , $SrSO_4$, $BaSO_4$, and CaF_2 , and he found that the solubility rose to a maximum on decreasing the particle size further. Roller (6) studied the solubility of gypsum and found that the solubility rate was proportional to the specific area at sizes above 25μ , that between 25μ and 2.8μ the solubility rate increased more rapidly than the surface exposed and that below 2.8μ the solubility rate began to decrease again.

1.2. Nucleation

Crystallisation is a two step process involving first nucleation and then the growth of the nucleus to macro size. Nucleation involves the activation of smaller unstable particles called embryos. An embryo formed in the metastable region is very small and will dissolve on

on account of the increased solution potential. As the degree of supersaturation is increased the size of the embryo which can be tolerated by the solution decreases to a critical size where the embryo becomes a nucleus possessing sufficient excess surface energy to form a new phase and growth begins.

Two types of nucleation are apparent, Primary nucleation and Secondary nucleation. Most Primary nucleation processes occur heterogeneously as it is extremely difficult if not impossible to avoid extraneous nuclei. Van Hook and Frulla (7) found that by carefully preparing samples of 1 to 5 cm³ of sucrose solution the metastable limit was raised to a supersaturation of about 1.6 (defined by the ratio of the concentration of the supersaturated solution to that at equilibrium) at ordinary temperatures as compared with the previously accepted limit of 1.2. The samples had to be prepared by careful dissolution followed by deactivation of latent nuclei by heating at temperatures at least 20 deg. C above saturation, and after sealing in closed tubes. They then averaged the observations of at least 50 droplets of solution and found that the nucleation rate decreased to a limiting value of about one half the rate observed in the carefully prepared larger samples. These results seem to imply that this

phenomenon is due to the diminished probability of smaller samples containing foreign nuclei. The primary nuclei then grow in the supersaturated solution giving birth to fresh nuclei: this is termed secondary nucleation.

1.2.1. Primary Nucleation

1.2.1.1. Homogeneous Nucleation

When nucleation occurs the transition from the metastable phase to the stable phase represents a decrease in the degree of molecular mobility, a decrease in the free energy of the system and so demands expenditure of energy to create the stable phase. The total quantity of work required to form the stable nucleus is the sum of the work required to form the surface and the work required to form the bulk of the particle.

Gibbs (8) was the first to find that the work of formation of a droplet from its vapour equals one-third of that required to form the surface of the droplet.

The total work required to form a droplet from its vapour, $W = a\sigma - V\Delta P$ where σ is the surface energy per unit area, and r is the radius of the droplet.

$$a = \text{surface area of droplet} = 4\pi r^2$$

$$V = \text{Droplet Volume} = \frac{4\pi r^3}{3}$$

$$\Delta P = \text{Pressure difference in droplet} = \frac{2\sigma}{r}$$

$$\therefore W = \frac{4\pi r^2 \sigma}{3}$$

Similarly for the homogeneous nucleation of a small particle from a solution the excess free energy

ΔG between the particle and the solute in solution is equal to the sum of the surface excess free energy ΔG_s , i.e.: the excess free energy between the surface of the particle and the bulk of the particle; and the volume excess free energy, ΔG_v per unit volume, ΔG_v , i.e.: the excess free energy per unit volume between a very large particle and the solute in solution.

$$\therefore \Delta G = \Delta G_s - V\Delta G_v$$

$$\text{For the spherical particle } \Delta G = 4\pi r^2 \sigma - \frac{4\pi r^3 \Delta G_v}{3}$$

The maximum value of ΔG occurs at a critical size r_c and represents the free energy of formation of the critical nucleus.

At equilibrium $\frac{d\Delta G}{dr} = 0$ and for the above quotation:

$$r_c = \frac{2\sigma}{\Delta G_v}$$

$$\therefore \Delta G_c = \frac{4\pi \sigma r_c^2}{3}$$

It has been shown that the Ostwald - Freundlich equation relates supersaturation, S , to particle size of a spherical particle by:

$$\ln \frac{C_r}{C_\infty} = \ln S = \frac{2\sigma V}{RT r}$$

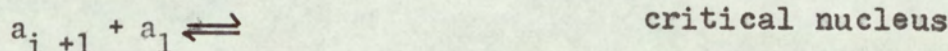
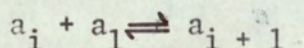
so for the critical spherical nucleus

$$r_c = \frac{2\sigma V}{RT \ln S}$$

and the free energy of formation of the critical spherical nucleus becomes:

$$\Delta G_c = \frac{16\pi\sigma^3 V^2}{3R^2 T^2 (\ln S)^2}$$

Kinetically the formation of nuclei can be assumed to be a series of bimolecular reactions of the form



The rate of nucleation, J , i.e., the number of nuclei formed per unit time per unit volume can be expressed in terms of the Arrhenius reaction velocity equation:

$$J = C \exp\left(\frac{-\Delta G}{RT}\right)$$

where c is a constant of proportionality.

$$\therefore \text{For spherical nuclei } J = C \exp\left(\frac{-16\pi\sigma^3 V^2}{3R^2 T^2 (\ln S)^2}\right) \dots (1)$$

Becker and Doering (9) assumed that embryos of all sizes up to the critical size achieve a non-equilibrium steady-state distribution by growth and decay processes. They introduced a non-equilibrium factor into the equation for the rate of nucleation to allow for the backflux and decrease in embryo population caused by the growth of nuclei.

Becker (10) proposed the nucleation rate equation

$$J = C \exp\left(\frac{-\Delta G_D}{KT} - \frac{\Delta G_C}{KT}\right)$$

Where K is the Boltzmann constant and ΔG_D is the free energy of activation of diffusion. The alternative equations for the nucleation rate have been reviewed (11) (12)(13) but are generally of the form of equation (1), ΔG_D being assumed constant over a limited temperature range.

1.2.1.2. Heterogeneous Nucleation

The presence of a solid impurity in a supersaturated solution can act as a catalyst for nucleation, and it has been shown that homogeneous nucleation is very difficult if not impossible to produce in practice. However, not all impurities in a particular system will act as accelerators and it is in fact possible for some to act as nucleation inhibitors.

The free energy of formation of the critical nucleus for heterogeneous nucleation $\Delta G_C'$ is related to the free energy of formation of the critical nucleus for homogeneous nucleation ΔG_C by: $\Delta G_C' = \phi \Delta G_C$ where ϕ is a factor less than unity.

Volmer (14) has related the factor ϕ to θ which is the angle of contact between the crystalline deposit and the foreign solid surface and is analogous to the angle of wetting in liquid-solid systems:

$$\phi = \frac{(2 + \cos \theta)(1 - \cos \theta)}{4}$$

When $\theta = 180^\circ$, $\phi = 1$ and $\Delta G_C'$ is the same as for homogeneous nucleation.

When $\theta = 0^\circ$, $\phi = 0$ and $\Delta G_C' = 0$

When θ lies between 0° and 180° $\Delta G_C' < \Delta G_C$ and so the impurity acts as a nucleation accelerator.

Preckshot and Brown (15) have studied the effect of crystallographically similar, insoluble, ionic crystals in nucleating quiet supersaturated solutions of Potassium chloride. The time required for nucleation for various fixed degrees of supersaturation were measured conductometrically. They found that for the same time necessary for nucleation, lead sulphide promoted nucleation at a lower degree of supersaturation than an unseeded solution; lead telluride required even less supersaturation; and lead selenide was the most effective.

Telkes (16), working on the nucleation of supersaturated inorganic salt solutions, has added data to strengthen the theory that an additive will accelerate nucleation only if its crystallographic structure and that of the salt to be crystallised agree within 15%.

1.2.1.3. Induced Nucleation

Nucleation can be induced to occur in supersaturated solutions free of extraneous material, below the supersaturation necessary for homogeneous nucleation. This can be done by the effects of external influences such as electric and magnetic fields, ultra-violet light, X-rays, sonic and ultrasonic radiation, cavitations produced by stirring and even the mechanical impact of a stirrer with the vessel walls. Ultrasonic radiation seems to be the most effective although it is not yet used industrially. Two methods of generating ultrasonic waves are in use:

a) Crystals which change shape under the influence of an electric field can be used in conjunction with an alternating current.

b) A ferromagnetic bar is capable of relatively large changes in dimension when it is magnetised. It can be energised by a winding with sinusoidal voltage variation and transduces waves at the same frequency as the voltage.

Ultrasonics when applied to liquids causes cavitations in the liquid alternately producing areas of high and low pressure. The frequency and power of the ultrasonic waves have to be carefully controlled for a particular process, as while the low pressure areas cause embryo coagulation, high intensity ultrasonics break up suspended particles.

Van Hook and Frulla (17) found this effect in the nucleation of sugar solutions. They found that at a supersaturation ratio of 1.1 for which homogeneous nucleation would not occur, a sugar solution would nucleate on momentary irradiation of ultrasonics at a frequency of 8 k.c. and a minimum power input of $100\frac{1}{2}\text{cm}^2$, yielding a prolific crop of crystals. However at 340 k.c. very few crystals developed in the same time.

Mullin and Raven (18) also showed this phenomenon with stirred solutions. They found that the degree of supersaturation necessary for nucleation decreased with increasing stirrer speed only over a limited range, after which there was an increase before again decreasing with further increase in stirrer speed. They suggested that this increase was probably due to the fracture of nuclei at this critical stirrer speed yielding fragments of less than nucleic size.

1.2.2. Secondary Nucleation

If a supersaturated solution is seeded with crystals, nucleation of the solution often occurs. This is termed secondary nucleation.

Melia and Moffitt (20) found that secondary nucleation appeared to be produced by the shearing action of the solution on the crystals and did not normally occur until dendritic type growths appeared on the crystal surface. They also found that these secondary nuclei were themselves capable of producing fresh nuclei.

Strickland - Constable and Mason (19) working on $\text{MgSO}_4 \cdot 7\text{H}_2\text{O}$ distinguished four classes of breeding of nuclei:-

- (i) "Initial breeding" occurred when a seed crystal yielded a shower of small crystals, which were originally attached to it, after immersion in a supersaturated solution.
- (ii) "True breeding" resulted from broken portion of the dendritic or needle-like growth on the original seed.
- (iii) "Splinter breeding" occurred when a needle broke off accompanied by a shower of small crystallites.
- (iv) "Attrition breeding" was that which resulted from agitation.

In general the rate of nucleation will be increased

with increasing supersaturation, increasing agitation and increasing area of crystal seed. But combinations of these effects interfere with each other.

Branson, Dunning and Millard (21) have shown that for continuous crystallisation the rate of nucleation $\frac{dN}{dT} = kS^m$ and they found a value of 3 for m where S is the degree of supersaturation.

Randolph and Larson (22) have reported a value of 4 for m. There are many theories on the factors affecting k and there is a lack of data to confirm the value of m.

1.3. Crystal Growth

The first theories on crystal growth concerned the morphology of the crystals and an historical account of these theories has been made by Buckley (23).

1.3.1. Adsorption - Layer Theories

The following theories have been abstracted from Buckley (23).

"Marc (24) found that as the stirring rate was increased the velocity of growth increased until after a critical rate was reached it remained constant. He considered that at this stage the crystal was covered with an adsorbed layer of molecular dimensions. Volmer (25)

based his theory on the existence of this layer. While studying the growth of mercury crystals from the vapour state at low temperatures he observed the crystals growing layer by layer. He proposed that a molecule arriving at a crystal surface lost only a portion of its latent heat and was thus bound to the surface but had complete mobility on the surface. The adsorbed layer consists then of such molecules frequently colliding with each other forming larger two dimensional particles. When a particle becomes of nucleus dimensions it would attach itself to the crystal lattice. This is called Two Dimensional Nucleation. Volmer assumed that the transfer of the particle from the adsorbed layer to the lattice would be instantaneously made up from the solution. He proposed that the relationship between the growth velocities V_1 and V_2 of two differing lattice planes was given by:

$$\frac{V_1}{V_2} = a \exp \left(\frac{(A_1 - A_2) n}{RT} \right)$$

Where a is a constant, n a factor $\gg 1$, and A_1 and A_2 the heats of adsorption of the two planes. He assumed that the heat of adsorption of a particular lattice plane was proportional to the specific surface energy.

"Brandes (26) making similar assumptions to Volmer considered the surface free energy to have little influence on crystal growth. He considered that the work of

formation of the two dimensional nucleus was the controlling factor for growth, since the growth of the nucleus to complete the lattice plane was very rapid compared with the nucleus formation. The ratio of the growth velocities V_1 and V_2 on planes I and II, where the work of formation of the nucleus is W_1 and W_2 , was given by:

$$\frac{V_{II}}{V_I} = \exp \left(- \frac{(W_2 - W_1)}{KT} \right)$$

"The work of formation was derived on a basis analogous to three dimensional nucleation.

"Bravais (27) postulated that the velocities of growth on lattice planes depends on the densities of the lattice points on the planes. However there are many criticisms to this theory.

"Both Kossel (28) and Stranski (29) proposed theories to account for the way in which atoms or molecules attach themselves to the crystal face. Kossel (28) assumed the crystal to build itself up by the indefinitely continued repetition of the most probably equivalent steps. He showed that it was immaterial to his theory whether the molecular attachments occurred in rows parallel to a cube edge or the diagonal. He expressed the attachment energy ϕ_o as being made up of three components $\phi_o = \phi^1 + \phi^{11} + \phi^{111}$ of which ϕ^1 and ϕ^{11} were tangential to the growth direction and ϕ^{111} was at right angles to the lattice plane. Thus

for the original two dimensional nucleus on a new plane the energy release was that due to ϕ^{111} only. For this particular nucleus he found that for a homopolar crystal the most probable position of attachment is the interior of the plane, followed by the edge and the corner in lower degrees of probability; whereas for an ionic crystal the probability was in the reverse order, i.e. corner > edge > interior. Kossel stated that once the initial nucleus was attached the plane would build up rapidly to completion.

"Stranski (29) working independently and considering the relative work or separation necessary to remove molecules from various positions in the lattice plane came to the same basic conclusions as Kossel."

Frank (30) showed that if a screw dislocation, i.e. one in which the displacement is parallel to the dislocation line, is present in a crystal there is no need for fresh two dimensional nucleation, and so the supersaturation needed for growth is relatively low. The face containing the screw dislocation will then grow perpetually "up a spiral staircase". If there are two such dislocations on a face growth will occur if the supersaturation is raised to a value such that the size of the critical two dimensional nucleus correctly oriented will pass between two points in the positions of the two dislocations.

These theories have given significance to the "Kr factor" which occurs in the kinetic theories (section 1.3.2.) and which makes allowance for the facility with which a surface may incorporate a particle adjacent to it.

1.3.2. Kinetics of Crystal Growth

The following consecutive steps are required in any heterogeneous reaction:-

1. Transport from the medium to the reaction environment.
2. Adsorption on the surface.
3. Orientation in the surface.
4. Desorption of products of reaction.
5. Dissipation of products of reaction.

For crystallisation the last two steps consist of the dissipation of the heat of crystallisation which will be rapid compared with the relatively slow growth rate, and so step 1 is more likely to be rate controlling than 4 or 5. A molecule on arriving at the crystal surface is not necessarily immediately incorporated into the crystal lattice because it may either diffuse away or it may not be at a favourable site. As the orientation of the molecule accounts for the greater part of the entropy change step 3 is more likely to be rate controlling than step 2.

So the two most likely rate controlling steps are:-

1. Transport from the medium to the growing environment.
2. Orientation in the surface.

Diffusion Theories

Noyes and Whitney (31) assumed that the liquid in contact with the crystal was saturated, and that crystallisation was the reverse of dissolution. They assumed that the rate at which a substance dissolves in its own solution was proportional to the difference between the concentration of that solution and the concentration of the saturated solution. Nemst (32) assumed the crystal to be surrounded by a laminar film of liquid of thickness b , through which the solute had to diffuse. Then:

$$\frac{dm}{dt} = DA (C - C^*) / b$$

Where m = mass of solute deposited in time t .

A = Surface area of the crystal.

C = Solute concentration in the bulk of the solution.

C^* = Solute concentration of saturated liquor.

D = Coefficient of diffusion of the solute.

However this equation suffers from the defect that it assumes the liquid in contact with the crystal is saturated, whereas it is known that it is supersaturated.

Mullin (33) has shown how Berthoud (34) and Valetton (35) suggested that there were two steps involved in crystallisation: diffusion to the crystal surface and then a first order 'reaction' when the solute was incorporated into the crystal lattice.

$$\text{Hence } \frac{dm}{dt} = \frac{A (C - C^*)}{\frac{1}{Kd} + \frac{1}{Kr}} \quad \text{--- (1)}$$

Where Kd : Coefficient of mass transfer by diffusion
 Kr : A rate constant for the surface reaction.

Surface Reaction

Cartier et al (36) modified an equation by Amelinckx (37) for the resistance to crystallisation due to the surface reaction. This particle integration rate was based on a statistical determination of the rates of particle attachment and detachment at a crystal face. Cartier et al's modification satisfactorily correlated the particle integration rate data of citric and itaconic acids:

$$\frac{dm}{dt} = K \left(\exp \left(\phi \left(C_f - C \right) \right) - 1 \right) \quad \text{--- (2)}$$

$$\text{Where } \phi = - \frac{1}{kT} \frac{dU}{dC} \quad \checkmark$$

K : particle integration factor

U : attachment energy of the crystallising particles.

C_f : solution concentration at crystal face (%m/v)

C = solution concentration in the bulk liquid (% m/v)

K = Boltzmann's constant.

Hence a plot of $\ln \left(\frac{dm}{dt} + K \right)$ against $C_f - C_l$, where the concentrations are in weight % should give a straight line of slope $\rho\phi$. A value of K has to be determined by trial and error which will give an intercept of $\ln K$. It was found that K and ϕ could be expressed in terms of the absolute temperature.

$$K = \alpha T^{3/2} + \beta$$

$$\rho\phi = B - \frac{A}{T}$$

Where α , β , A and B are constants, and ρ is the solution density.

In order to assess the contribution of each resistance on the growth process it is necessary to try to eliminate one of them. As the thickness of the diffusional film is inversely dependent on the liquid velocity relative to that of the crystal, the diffusional resistance can be made negligible at sufficiently high relative velocities.

Marc (24) studied the effect of agitation on growth rates and found that the degree of agitation had little effect beyond a certain point. The growth rate was then dependent on the second power of supersaturation. However, other workers (38), (39) have found that the rate of growth in well agitated vessels was a linear function of supersaturation.

Cartier et al (36) also studied the effect of agitation and found that at sufficiently high relative velocities the diffusional resistance was insignificant and they were able to correlate their results in the form of equation (2).

McCabe and Stephens (40) studying the rate of growth of copper sulphate pentahydrate crystals in an agitated solution at constant supersaturation found that the rate of growth, r , could be expressed in terms of the relative velocity, u , between crystals and solution, the interfacial growth rate, r_i , and the growth rate at zero velocity, r_o , by the empirical equation:

$$\frac{1}{r_g} = \frac{1}{r_o + \beta u} + \frac{1}{r_i}$$

Where β is a constant.

They found that the growth rate was not affected directly by crystal size, but, at low values of u , r , is markedly influenced by the crystal-solution relative velocity. As u increases the effect of velocity on growth rate diminishes and finally becomes negligibly small. This is consistent with the view that the growth process consists of a diffusion process and a surface reaction in series.

As temperature has a greater influence on the kinetics

of a reaction than on the physical property of the solution, the extent of the resistance to crystallisation presented by the surface reaction can be seen by studying the effect of temperature on the growth rate. The effect is indicated by the value of the activation energy involved.

Van Hook (41) compared the activation energies of viscosity, diffusion and growth, with the conclusion that the former two were considerably less than the third over the normal temperature range. The comparison was made at a constant supersaturation ratio of 1.05 and the three values approached a common low level only at high temperatures. The high activation energy associated with growth was of the order normally associated with purely chemical reactions rather than physical processes.

Rumford and Bain (42) determined the rate of growth of sodium chloride crystals in a fluidised bed for different supersaturations over the range 26 to 73 C. Below 50 C. the rate of growth plotted against supersaturation was non linear showing the growth rate to be surface reaction controlled. Above 50 C. the growth rate was linearly dependent on supersaturation. This could either be a first order surface reaction or diffusion controlled growth. As the activation energy for crystallisation was found to be 5.4 K cal/mole, they considered the growth rate to be diffusion controlled above 50 C. Cooke however in a

discussion (42) disagreed with this conclusion and suggested that the growth rate was diffusion controlled at all temperatures, but the contribution of the surface reaction is greater at lower temperatures and supersaturations. He suggested that if the authors had continued their work for higher supersaturations the curves would have become linear for all temperatures.

Hixon and Knox (43) found the rate of growth coefficients to depend both upon the mass transfer coefficients which varied with fluid velocity and the rate coefficient of the surface reaction. They correlated their results on the growth rates of single crystals of copper sulphate and magnesium sulphate, on a dimensionless basis to allow the mass transfer coefficients to be compared with mass transfer coefficients or heat transfer coefficients in other systems:-

$$\frac{K_d d}{D_m} = \beta \left(\frac{\rho v d}{\mu} \right)^{0.6} \left(\frac{\mu}{M D_m} \right)^{0.3}$$

These are the Sherwood, Reynolds and Schmidt numbers respectively.

Where D_m = Molar diffusivity

d = equivalent diameter of the crystal

v = relative solution - crystal velocity (ft/hr)

ρ = density of solution

μ = viscosity of solution

M = mean molecular weight of the solution

To correlate the data on this basis it was necessary to assume that a resistance was being presented by a surface reaction of first order for magnesium sulphate and of second order for copper sulphate.

Bransom (44) has shown that for a fluidised bed the growth rate $\frac{dr}{dt}$ can be correlated in terms of a modified Reynolds number Re :

$$\frac{dr}{dt} = a (Re)^b S^n$$

Where $Re = 2r \rho_l V_r / \mu$, a = specific growth rate, S = supersaturation, r = crystal equivalent radius, ρ_l = density of liquid, μ = liquid viscosity, and V_r relative velocity.

Using the data of Hixon and Knox (43) he found $n = 1$ for both copper and magnesium sulphate, $b \approx 0.65$ for copper sulphate and $b \approx 0.3$ for magnesium sulphate. He further showed that for a given continuous crystallisation process, μ and ρ_l are constant and V_r varies very little so that

$$\frac{dr}{dt} = a r^b S^n$$

and when the growth rate of crystals is expressed in this form most of the important operating parameters of a continuous crystalliser can be predicted.

Bransom and Palmer (45) working on an Oslo type of

crystalliser found the exponent $b = 1.0$ when calculating average growth rates for a bed of crystals. However when size analyses were done on the individual beds before and after growths it was found that $b = 1.5$. This was explained by the size classification occurring in the bed.

Bennet (46) has used the data of Rumford and Bain (42) to obtain a value of $b = 0.171$ for the same correlation.

However the exponents b and n will vary according to the type of system and the material used.

SECTION TWO

LITERATURE SURVEY : PENTAERYTHRITOL (P.E.)

2.1. Crystal Structure

Von Groth (47) states that P.E. crystals should be tetragonal bipyramids on (001). He showed the morphology as fig. 2.

Berlow, Barth and Snow (48) state that P.E. has a body centred lattice of tetragonal symmetry with two molecules in the unit cell. The crystal has a four-fold alternating axis of symmetry parallel to its c - axis. The dimensions of the P.E. crystal are $a = 6.10\overset{\circ}{\text{A}}$ and $c = 8.73\overset{\circ}{\text{A}}$. The central carbon atom of one molecule in the unit cell is at (0,0,0) and that of the other at $(\frac{1}{2}, \frac{1}{2}, \frac{1}{2})$. The molecular units are so arranged that the Oxygen atoms are in planes perpendicular to the c - axis. The oxygen atoms of four neighbouring molecules are arranged in the form of a square whose sides are inclined 10° to the a_1 and a_2 axes. In P.E. the C-C bond length is $1.50\overset{\circ}{\text{A}}$, the C-O bond length is $1.46\overset{\circ}{\text{A}}$ and the O-O bond length is $2.69\overset{\circ}{\text{A}}$. The short distance between the oxygen atoms is regarded as an indication of hydrogen bonding. There is marked cleavage along the (001) plane which has been attributed to the linking together in sheets of the P.E. molecules. Shinod et al (49) give revised bond lengths as CC : $1.548 \pm 0.011\overset{\circ}{\text{A}}$

FIG. 2.

P. E. CRYSTAL MORPHOLOGY..... VON GROTH [47]

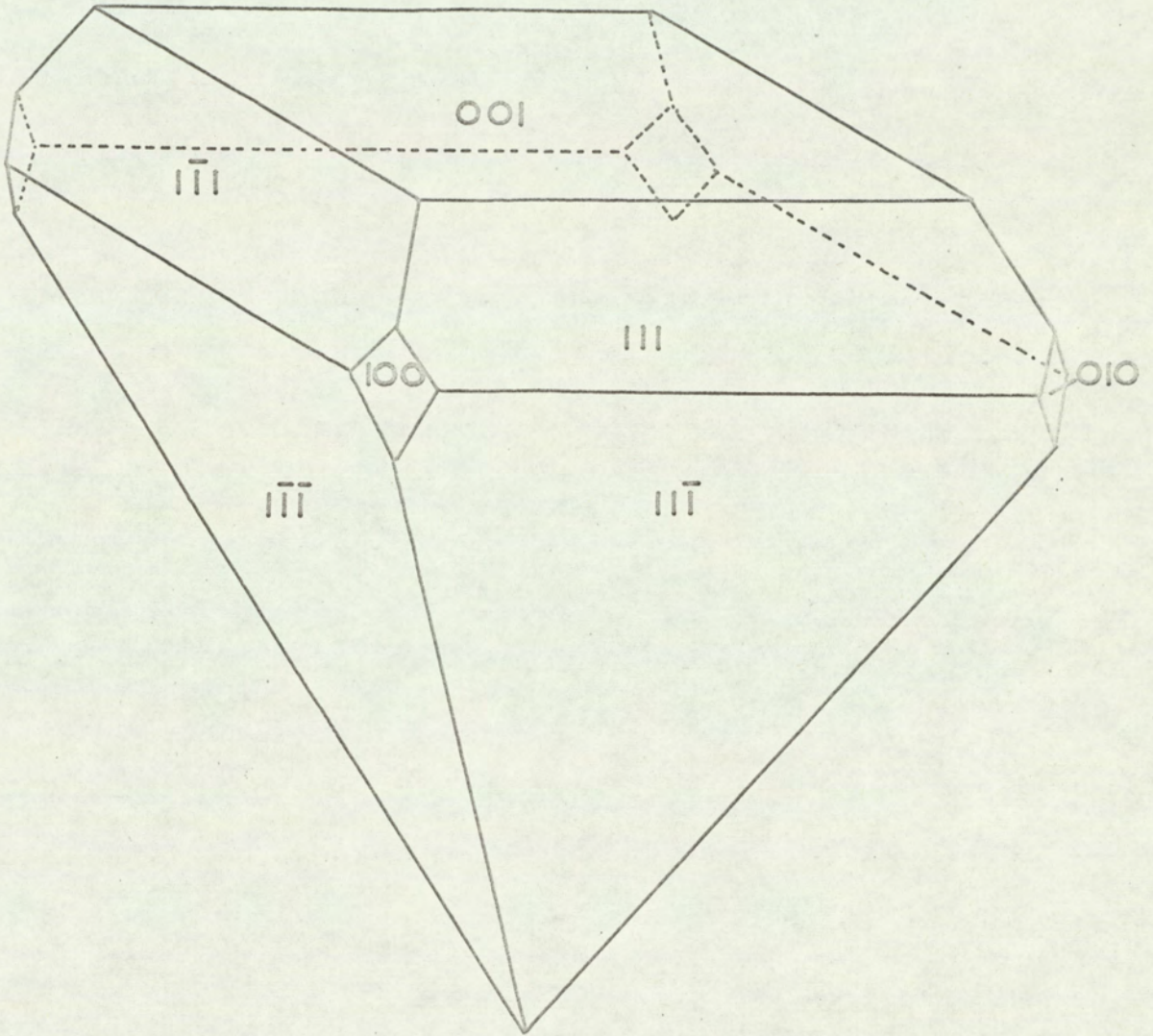
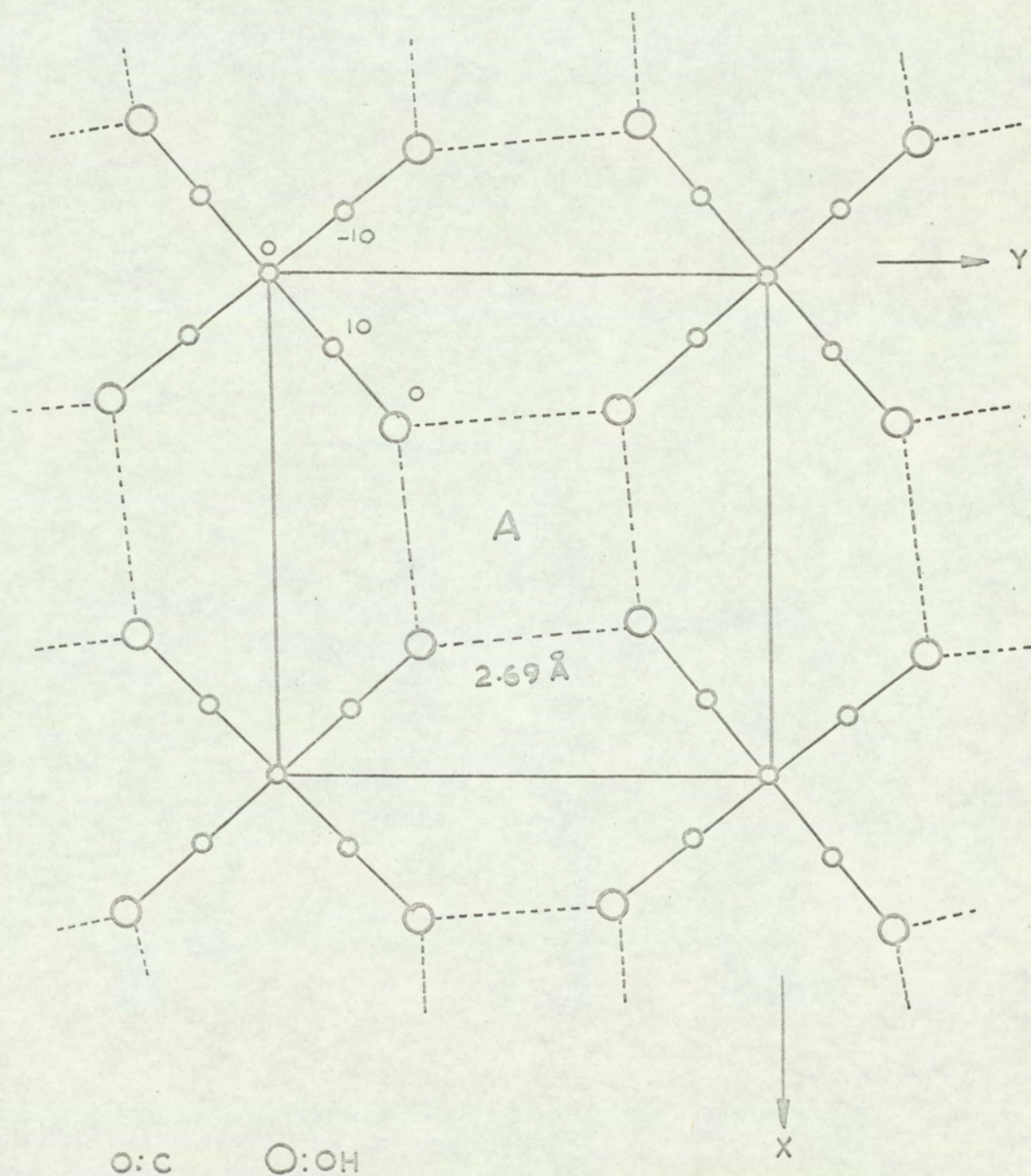


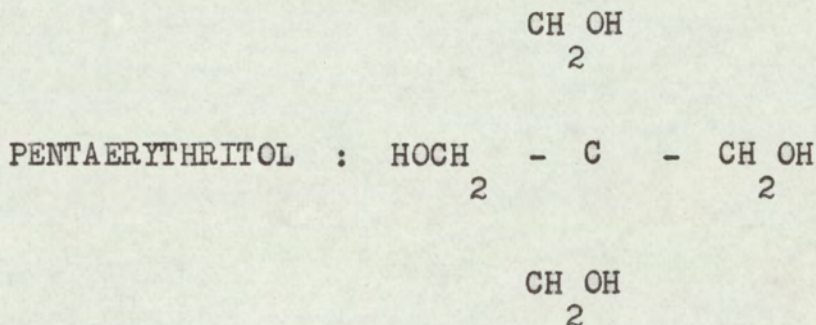
FIG. 3.

Plan of one layer of the tetragonal structure of Pentaerythritol $C(CH_2OH)_4$ projected on a plane perpendicular to the Z axis. The heights of the atoms in one molecule are indicated in units of $c/100$ and hydrogen bonds are represented by broken lines.



and $C-O = 1.425 \pm 0.014 \text{ \AA}$. Evans (50) gives a plan of one layer of the tetragonal structure of P.E. projected on a plane perpendicular to the z axis (fig. 3.).

2.2. Physical Properties



Berlow et al (48) state that P.E. is a polyhydric alcohol with four primary hydroxyl groups arranged compactly around a central carbon atom. It is an odourless, white crystalline compound which is non-hygroscopic, practically non-volatile and stable in air. Its density is 1.396 g/cm^3 . The entropy of transition of P.E. is 22.8 e.u., its entropy of fusion is 3.2 e.u., and its entropy of sublimation is 60.8 e.u.

The diffusion coefficient of P.E. in water at 20°C is $0.573 \text{ cm}^2/\text{sec}$. at a normality of 0.4 and $0.589 \text{ cm}^2/\text{sec}$. at a normality of 0.2.

P.E. is moderately soluble in cold water, 5.6% m/m at 20°C and freely soluble in hot water, 30.5% m/m at 80°C ; it is only slightly soluble in alcohols and other organic

liquids.

I.C.T. (51) has reported the heat of combustion as 661 K-cal/mole and the equivalent conductance as 1.71 @ 25 °C and 0.06 g. mol./dm³.

According to Bradley and Cotson (52) the vapour pressure of P.E. ranges from 2.12×10^{-5} cm. Hg at 106.4 °C to 52.4×10^{-5} cm. Hg at 135.1 °C and is represented by the equation $\text{Log } p = 15.17 - \frac{7528}{T}$. Nitta et al (53) stated that the vapour pressure of P.E. is given by $\text{log } p = 14.525 - \frac{6861}{T}$. Bright and Carson (54) give the heats of solution of P.E. in water as:-

g. mol P.E./500 g. mol. Water	Differential molar heat of solution K cal/g. mol. solute.
0.381	- 5.48
1.216	- 5.17
2.117	- 5.25
3.025	- 5.34

Where the thermochemical sign convention is used,
i.e. - absorption of heat.

Berlow et al (48) have recorded the variously reported melting points of P.E. as ranging from 256 °C to 265.5 °C. They state that P.E. exhibits a polymorphic

transformation variously reported between 180^o C and 192^o C. Wyler and Wernett (55) report that P.E. forms a eutectic with 35% Di - P.E. melting at 190^o C.

2.3. Work done by I.C.I. on P.E. Crystallisation

McLean and Fort (56) investigating the crystallisation of P.E. found that a higher yield of purer material was obtained by crystallisation from hot liquor rather than cold. They thought this to be due to the solubility of the impurities increasing at a greater rate with rise in temperature than that of P.E.

Jackson and Gilmore (57) found on the laboratory scale that a decrease in the speed of stirring and in the initial rate of cooling during crystallisation resulted in the production of larger crystals of P.E. McCallum (58) also found that stirring had the greatest physical effect on the crystallisation of P.E. and that the best results were obtained with very slow stirring speeds. He found that the sugars from the manufacture of P.E. inhibited crystallisation and that this could be remedied by acidifying the solution to a pH of 2 or less and boiling. The presence of the acid was not necessary for crystal growth, however, and the solution could be neutralised immediately after boiling. The result was a product of much larger crystals. He continued this work (59)

labelling the inhibiting by-product of formaldehyde and P.E. as "Compound X" and compared the crystal and dust formation of (a) P.E. containing 4% Compound X; (b) P.E. treated with an iron exchange resin which reduced Compound X to 1%; and (c) P.E. after removing Compound X by boiling with 10% Hydrochloric acid. The results obtained showed a correlation between the dust and crystal size of P.E. and the presence of Compound X.

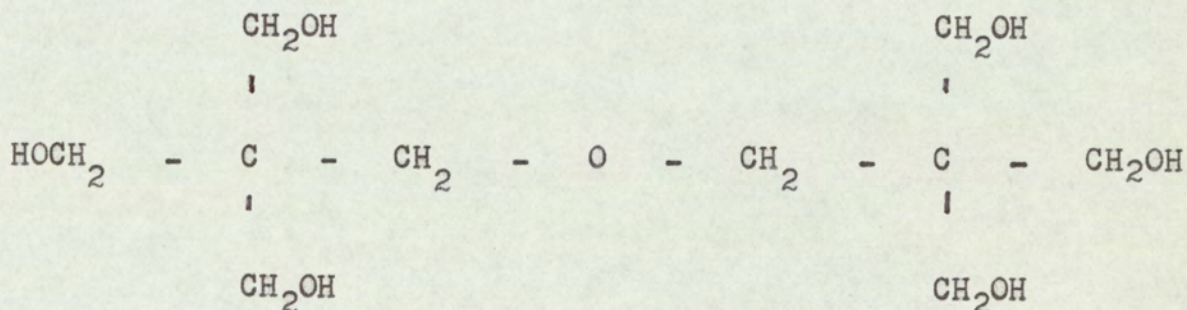
Whetstone (60) suggested that either (a) the preferential rate of deposition on the (001) face should be reduced by introducing into the solution some compound to compete with the P.E. in solution in effecting hydrogen - bond formation with - CH₂OH groups already in the plane to form large tabular crystals; or (b) that the deposition on the (001) face and possibly on the (100) and (010) faces should be reduced by additives which will become adsorbed on the surfaces and thus present to the P.E. molecules in solution a temporary layer of incompatible molecules. McCallum (60) tried this habit modification using "Nonic 218" (polyethylene glycol tert-dodecylthioether) and found that the crystals assumed a tabular habit but they did not appear to be any larger than before modification.

2.4. Impurities in P.E.

There are two main impurities in I.C.I. P.E., namely

di - P.E. and compound X. The amount of di - P.E. present varies from 0% to about 2% whereas compound X is usually about 4%.

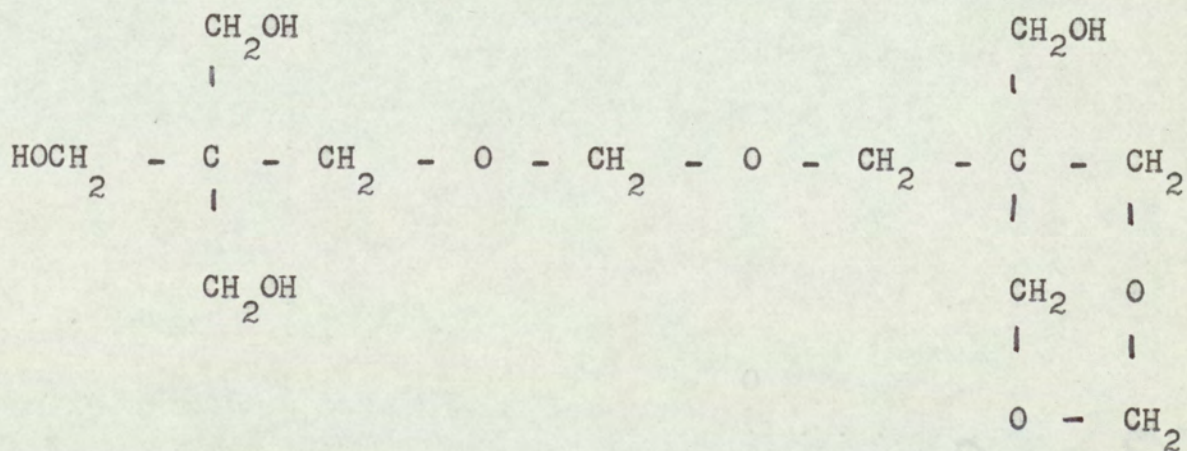
Di - P.E.: This is an ether having the formula:



Compound X: Wilson and Williams (61) found that compound X gave equivalent amounts of P.E. and its monoformal when treated with acid. The hydroxyl content of this compound X was 26% and its molecular weight between 265 and 270.

They suggested that compound X could be one of the two following compounds:

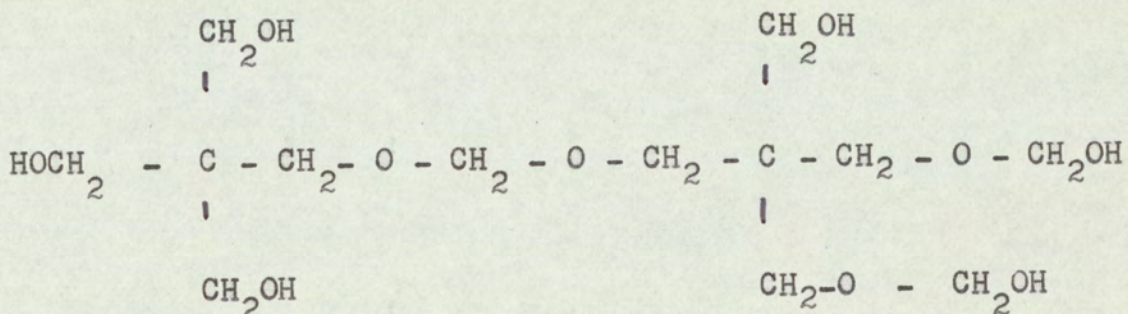
i) Bis pentaerythritol formal cyclic formal.



Molecular Weight = 296

Hydroxyl Content = 23%

ii) Dimethyl formaldehyde bipentaerythritol acetal.

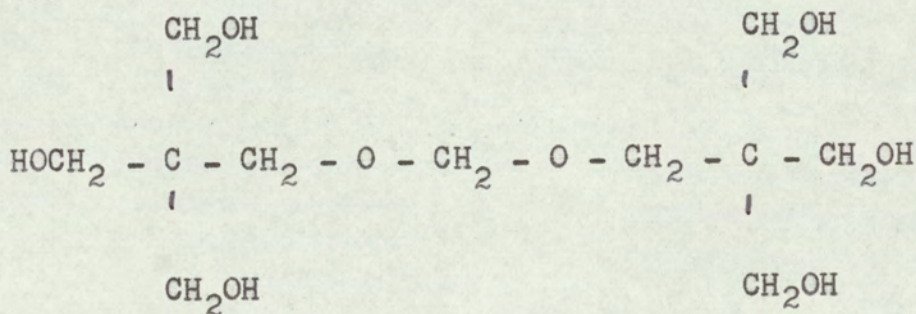


Molecular Weight = 344

Hydroxyl Content = 30%

Competitor's products have a similar impurity to compound X and this has been reported (62) (63) as:

iii) Bis pentaerythritol monoformal.



Molecular Weight = 284

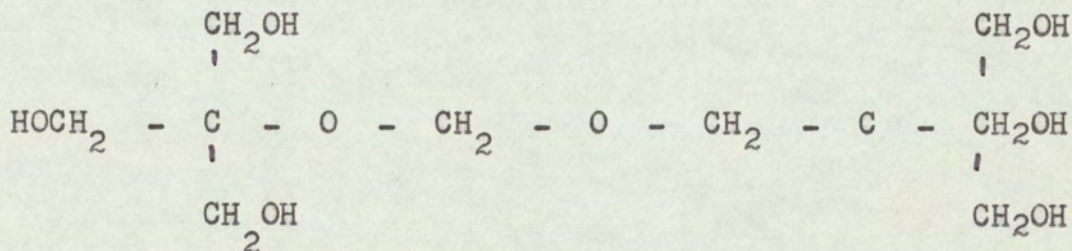
Hydroxyl Content = 35.9%

Although this has a molecular weight nearer to that found for compound X, the hydroxyl content is higher.

Barth and Snow (64) have reported a similar impurity

which they identified by carbon and hydrogen determinations, hydroxyl value, molecular weight and saponification value as:

iv) Formaldehyde bipentaerythritol acetal

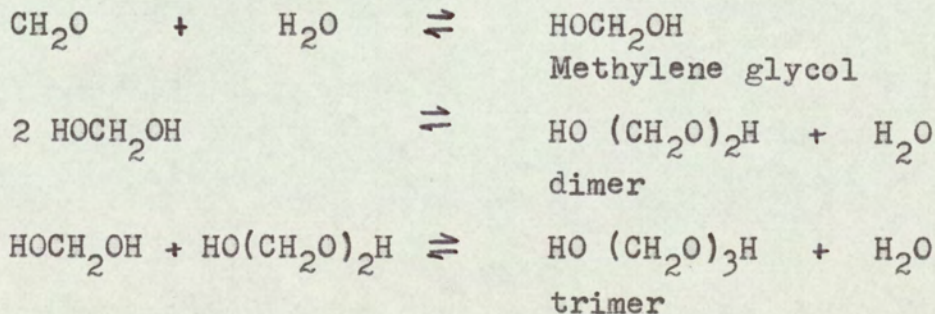


Molecular Weight : 270

Hydroxyl Content : 37.8%

Again the hydroxyl value is higher than that reported by Wilson and Williams (61). However it has since been found (65) that the method used for hydroxyl determination is unreliable in the presence of sugars found in purge liquors.

The degree of polymerisation of formaldehyde in aqueous solution can be expressed in the form of the following reversible reactions:



Salkind et al (62) have proposed two possible sequences of reactions which account for the formation of di - P.E. and bis - P.E. monoformal. The first is based on the fact that very little formaldehyde exists in aqueous solution as free HCHO but it is mostly in the hydrated form. The reaction proceeds by splitting out water between these polymers and acetaldehyde. In the sequence of reactions methylene glycol forms P.E., the hydrated dimer forms di - P.E. and the trimer by a similar sequence forms bis - P.E. monoformal. The other proposed sequence recognises the low concentration of HCHO in aqueous solutions but considers its high reactivity compared to that of its polymers. The formaldehyde reacts with acetaldehyde to form acrolein two molecules of which then react with methylene glycol to form bis - P.E. monoformal.

2.5. Analysis

Berlow et al (48) state that the analysis of technical P.E. generally includes the following determinations: P.E. content, melting range, hydroxyl content, ash content, acidity, moisture content, water solubility, colour and physical state. The method given for the determination of P.E. content is the Benzal method based on the formation of the di - benzylidene acetal

which is relatively insoluble in a dilute aqueous methanolic solution of hydrochloric acid containing benzaldehyde. Spirek and Strouts (66) give some modifications of this method which they report as suitable for P.E. in the presence of up to 15% Di - P.E. It was found however by Sprek and Williams (67) that formaldehyde found in reaction liquors caused low results and sugars found in purge liquor caused high results with this procedure. They suggested the use of chromatographic extraction of P.E. using celite as adsorbent and acetone as solvent followed by the benzilidene procedure. The results were found to be about 2% lower than the analysis by exhaustive crystallisation followed by benzaldehyde condensation, but it was nevertheless shown that this method was the more accurate.

Macinnes and Allan (68) described a nitration test for the determination of P.E. concentration, but this method is inaccurate and should only be performed by an experienced operator because of the explosive nature of the tetranitrate.

Murray, Brooks and Williams (69) applied differential refractometry to saturated aqueous solutions of P.E. They found that this was a good analysis method for P.E./Di - P.E. mixtures, but for technical grade P.E.

Compound X was present which had a far greater effect on the refractive index than di - P.E. Colorimetric methods were examined in some detail for the determination of di - P.E. (59) and it was found that triacetyl hydroxyquinone reacts with di - P.E. in the presence of HCl to give a yellow solution which could be used as an indication of di - P.E. in P.E./di - P.E. mixtures. However, strong interference was encountered with the presence of Compound X.

Murray et al (69) reported that infra-red analysis had been examined without success. The spectra of P.E. and di - P.E. were too similar to enable the small amounts of di - P.E. encountered to be evaluated. Compound X also interfered.

Wilson and Williams (61) studied the application of gradient elution chromatography to the examination of P.E. purge liquor for the study of the closely related and rather unstable constituents. The method involved the use of a relatively weak adsorbent, cellulose, with solvent extraction using first a poor solvent, petroleum ether, which was automatically gradually diluted with a good solvent. As the extraction proceeded, a series of fractions were collection with the aid of an automatic fraction collector. The fractions were examined by paper

strip chromatography. They showed that P.E. purge liquor contained very little P.E. monoformal and no detectable amount of diformal.

Murray et al (69) showed that the colorimetric method based on the reaction of formaldehyde with chromotropic acid in concentrated sulphuric acid which on heating produces an intense violet colour, can be used for the detection of formaldehyde in technical P.E. It was found that the effect of P.E. on this method was nil, the effect of di - P.E. only very slight and that the determination of formals by this method was almost theoretical.

The present I.C.I. analytical method (70) involves acetylation of the P.E. and examination of the resulting product in a high temperature gas chromatograph. The analysis gives a direct measurement of the di - P.E. content, and as Compound X had never been obtained pure to calibrate the G.C.R. the amount present is stated in terms of the equivalent amount of di - P.E.

SECTION THREE

CHEMICAL ANALYSIS

3.1. Introduction

As a high temperature chromatograph, as used by I.C.I. for the determination of compound X and di - P.E. was not available, an alternative analytical method was sought. Compound X and di - P.E. are the only two major impurities in the I.C.I. P.E. and it was hoped to develop a method using a combination of iso-physical properties of the ternary composition system. For this work it was necessary to produce synthetic mixtures of known composition.

3.2. Mixture Components

3.2.1. Pure P.E.

This was produced by dissolving sufficient commercial P.E. in 10% (W/V) HCl to form a saturated solution at its boiling point. The solution was refluxed for 1 h, cooled to 0°C, filtered and washed in ice cold water. This procedure was then repeated and the resulting P.E. recrystallised from distilled water. The product was then washed with successive quantities of ice cold water and dried in an oven. Its purity was confirmed by I.C.I. as being essentially 100% P.E.

3.2.2. Di - P.E.

This was obtained as the commercial product "DIPENTEK". It was analysed by I.C.I. as containing 4.0% compound X but no detectable amount of P.E.

3.2.3. Compound X

3.2.3.1. Extraction

The method of Barth and Snow (64) was used in an attempt to extract compound X from technical P.E. as follows.

Technical grade P.E. (400 g) containing 4.7% compound X was dissolved in water at 25 °C and the mother liquor (containing a higher percentage of compound X) removed and evaporated to dryness. The resulting crystals were boiled with ten times their own weight of n - propanol. The insoluble P.E. was filtered off and the mother liquor concentrated and chilled, producing 20 g of crystal product. This product was analysed by I.C.I. as containing 15% compound X instead of nearly 100% expected on a yield basis.

3.2.3.2. Synthesis

Murray et al (69) found that the amount of compound X in P.E. could be increased by heating with 1% aqueous formaldehyde solution.

An attempt was made to produce compound X by refluxing P.E. with 40% formaldehyde solution. It was found that the amount of compound X present in the P.E. in fact decreased and this was thought to be due to the inhibiting effect of the methanol present as a stabiliser. The slight decrease may have been equivalent to that obtained by simple recrystallisation from water.

Walker (71) has recorded the various equilibria, for different pH ranges, occurring in dilute and concentrated aqueous formaldehyde solutions. He also reported that excellent yields of formals were obtained by heating alcohols with paraformaldehyde at 100°C in the presence of ferric chloride. In view of the uncertainty of the composition of compound X, tests were carried out under different conditions of pH and formaldehyde concentration, and with ferric chloride added in an attempt to synthesise the compound. The P.E. used initially contained 4.7% compound X and < 0.1% di - P.E. Formaldehyde was added in the form of paraformaldehyde (a mixture of low molecular weight polyoxymethylene glycols). The results as analysed by I.C.I. are shown in Table 1. (Appendix A.)

All 20% formaldehyde solutions were cloudy at first but cleared after about twenty minutes. This was probably due to the slow depolymerisation rate. For

these solutions the concentration used of 70% P.E. was not sufficiently high for the P.E. to crystallise out when cooled to room temperature so more P.E. had to be added. This was possibly due to the formation of P.E. monoformal which will not normally crystallise. It appears that the critical condition for the synthesis of compound X by the reaction of P.E. with formaldehyde is the long reflux time. The pH of the solution did not appear to affect the formation of compound X although the presence of ferric chloride seemed to favour the formation of di - P.E.

It can be seen from table 1 that sample 11 achieved the largest increase in compound X, although this contained 0.5% di - P.E. as well as possible unknown formals and adsorbed formaldehyde. It was decided therefore to use a batch of P.E. (M 214, Bag 490), Batch A, containing an unusually high concentration of compound X and < 0.1% di - P.E. to study the properties of mixtures up to the concentration in the batch. In view of the uncertain reproducibility of the I.C.I. analytical method a number of samples of Batch A were sent for analysis giving an average result of 4.73% compound A and 0.1% di - P.E. (Table 2 Appendix A) upon which all subsequent experiments were standardised.

3.3. Melting Point

3.3.1. Apparatus

The apparatus used was a standard Electrothermal melting point apparatus in series with a voltage regulator for finer temperature control. The thermometer was divided in 1 deg. C. for the range 0 °C to 360 °C and was calibrated with pure substances of known melting points, fig. 4, Appendix A. The apparatus was equipped with three holes to accommodate the 100 mm. x 2.0 mm. capillary tubes provided.

3.3.2. Method

I.C.I. (70) state that the temperature should be raised at 10 deg. C./min. and this rate gradually reduced after 200 °C, so that from approximately 10 deg. C below the expected melting point the rate is closely controlled at 1 deg. C./min. Two temperatures should be taken:-

- a) The temperature at which there is a first appearance of liquid.
- b) The temperature at which crystals completely disappear and the liquid becomes clear.

If the temperature range is greater than 2 deg. C, both temperatures should be reported.

However, a eutectic composition was found with P.E.

and di - P.E. which made temperature (a) constant for all mixtures containing di - P.E. So temperature (b) was the only temperature characteristic of the composition. This was studied by grinding samples to finer than 150 mesh, filling the capillary tubes to a depth of about 3 mms. and placing them in the holes provided. The melting point of each sample was then done in triplicate.

The rate of heating had to be reduced to 0.3 deg.C/min. at 5 C below the expected melting point.

3.3.3. Results

An eutectic composition was found with the binary system P.E./ di - P.E. at 40% di - P.E. which melted at 185.5 C, (Table 3, and fig. 5, Appendix A.). Wyler and Wernet (72) have reported that P.E. forms an eutectic with 35% di - P.E. melting at 190 C. The discrepancy could have been due to the 4% compound X present in the di - P.E. The melting points of the binary P.E./ Compound X system were examined up to 15% Compound X. (Table 4, and Fig. 6. Appendix A.) The source of compound X used for these tests was the product of the extraction with n - propyl alcohol in which di - P.E. is completely insoluble. It was found that it was increasingly difficult to detect the eutectic temperature with increasing compound X, and for the 15% compound X test there was no detectable change below about 200 C.

Berlow et al (48) report that P.E. exhibits a polymorphic transformation variously reported between 180°C and 192°C but no mention is made of the eutectic composition. Although the crystal morphology of the sample containing 15% compound X was not examined during the melting tests there was no obvious physical change below 200°C, while the "pure" P.E. (< 0.1% di-P.E.) with possible traces of di - P.E. did show the eutectic temperature.

The ternary melting system P.E./di - P.E./Compound X was briefly examined but the technique found to be unsatisfactory for use in the analysis of P.E. with the amount of impurities normally encountered.

3.4. Refractive Index

Murray et al (69) applied differential refractometry to saturated aqueous solutions of P.E. They found that this was a good analytical method for P.E./di - P.E. mixtures but that compound X had a far greater effect on this method than di - P.E. However as they used saturated solutions this could be expected as compound X enhances the solubility of P.E. in aqueous solutions. Tests were done to examine the effect of impurities on the refractive index of solutions of constant strength. A High Accuracy Abbe Refractometer was used and solutions

of 3 gms./100 gms. water and 7 gms./100 gms. water were examined at 25°C. It was found, however, that although the refractometer gave the refractive index to five decimal places, its sensitivity was only good to four decimal places. This did not give sufficient discrimination for the solutions analysed, although it was found that the effects of di - P.E. and compound X were approximately of the same order and this method could possibly be used in conjunction with another test if a more accurate refractometer was used.

3.5. Viscosity

It was thought possible that the presence of the high molecular weight compound X might increase the viscosity of P.E. in aqueous solution. Aqueous solutions of constant strength were made up containing various compositions of compound X and di - P.E. Viscosities were examined at 25°C with a size 25 Cannon-Fenske viscometer, but they were identical for the quantities of impurities studied.

3.6. Formaldehyde Content

3.6.1. General

Murray et al (69) found that the "formaldehyde" content of P.E. could be found by a colorimetric method based on the reaction of formaldehyde with chromotropic

acid in conc. sulphuric acid when, on heating, an intense violet colour is formed. They thought this to be due to both free formaldehyde adsorbed on the solid and also possibly combined formaldehyde in the form of formals and Compound X. They studied the effect of P.E. monoformal and P.E. biformal on this method and found that whereas theoretically 20% and 37.5% formaldehyde should be obtained respectively the actual formaldehyde values obtained were 17% and 32% respectively. However P.E. monoformal does not readily crystallise and as Wilson and Williams (61) found that P.E. purge liquor contained very little P.E. monoformal and no detectable amount of P.E. diformal, it was thought that the effect on the colorimetric method due to adsorbed formals would be negligible. So this colorimetric analysis has been modified for greater reproducibility with the view to establishing an accurate determination of the combined formaldehyde content due to compound X and adsorbed free formaldehyde.

3.6.2. Total Formaldehyde : Chromotropic Acid Method

3.6.2.1. Effect of Heat

The biggest factor found effecting the reproducibility of the method was the time and temperature of heating the sample with the chromotropic acid and

concentrated sulphuric acid. It was found that when heated at 90^o C compound X took more than half an hour to completely break down, although if the heating was prolonged the reagent blank discoloured. The variation of optical density with the time of heating at 90^o C is shown in tables 5 and 5A, App. A. Although these results serve as an indication of the variation of optical density with the time of heating, it was found impossible to obtain reproducible results in an oven because of the temperature distribution in the oven and the inadequacy of the temperature control. Hence all samples were heated for exactly one hour in an oil bath at 90^o C and compared with a reagent blank similarly treated.

3.6.2.2. Reagent

The reagent had to be freshly prepared before use. 0.9 g. of the pure sodium salt of chromotropic acid were dissolved in 25 ml. water and 50 mg. of pure stannous chloride added. The mixture was well shaken and centrifuged for 30 minutes at 3,500 r.p.m. The clear liquid was then pipetted off ready for use.

3.6.2.3. Procedure

1.000 g. of the P.E. sample was accurately weighed and dissolved in 100 mls. of distilled water. 1 ml. of this solution was transferred with a pipette to

a 50 ml. volumetric flask. 1 ml. of the chromotropic reagent was added and then 10 mls. of 95% sulphuric acid was added cooling the flask in ice. The flask was heated in an oil bath at 90°C for 1 hour, cooled in cold water and made up to 50 ml. with distilled water, continually mixing and cooling during dilution.

The optical density was measured by comparison with a reagent blank treated in the same way, measured at a wave-length of 570 $m\mu$ in $\frac{1}{2}$ cm. cells using a "SPEKKER" absorptiometer with Kodak No. 6 filters.

The absorptiometer was calibrated by treating 1 ml. of known concentration formaldehyde solutions in the same way as the 1 ml. of P.E. solution. The calibration is shown Table 6, and fig. 7. appendix A.

3.6.3. Adsorbed Formaldehyde

It was thought possible to determine the amount of adsorbed formaldehyde affecting the colorimetric analysis by using the Sodium Sulphite method for formaldehyde determination. This method involves the use of a very dilute acid only in the final titration, and as no heat is applied this would not be sufficient to break down the compound X present. It was found later (section 5) that in fact compound X is relatively stable

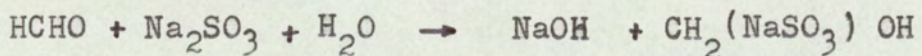
in aqueous solution and does not break down to P.E. and formaldehyde very easily.

3.6.3.1. Reagent

The sodium sulphite solution was prepared by dissolving 126 g. of anhydrous sodium sulphite in distilled water and making up the volume to 1 litre.

3.6.3.2. Procedure

Fifty ml. of the sodium sulphite solution were placed in a 500 ml. Erlenmeyer flask. A few drops of thymolphthalein indicator were added and the solution neutralised with $\frac{N}{100}$ hydrochloric acid until the blue colour had disappeared. The 99 ml. of the original 1 g. P.E./100 ml. H₂O solution remaining after the colorimetric test were transferred to the flask. The formaldehyde present reacts with the sodium sulphite to form the formaldehyde - bisulphite addition product:-



The resulting mixture was titrated slowly with the standard $\frac{N}{100}$ hydrochloric acid to complete discoloration. One ml. of normal acid is equivalent to 0.03003 g. formaldehyde. The per cent formaldehyde in the sample is hence given by the equation:

$$\% \text{ HCHO} = \frac{\text{acid titer} \times \text{Normality of acid} \times 3.003}{\text{Weight of Sample}}$$

$$\text{and HCHO mg./ml. solution} = \% \text{ HCHO} \times \frac{1}{10}$$

3.6.4. Compound X Calibration

The formaldehyde equivalent of the optical density obtained for the total formaldehyde content in the colorimetric test is known from the formaldehyde calibration of the instrument. fig. 7. The effect of the adsorbed formaldehyde, found from the sodium sulphite method, on the optical density is the product of the ratio of the adsorbed formaldehyde to equivalent formaldehyde and the optical density. If this is subtracted from the optical density the corrected optical density is assumed to be due to Compound X only, in the absence of other formals. The calibration of compound X in terms of the corrected optical density is shown, table 7 and fig. 8, appendix A.

To ascertain whether any appreciable quantities of formals were adsorbed on Batch A, the sample was finely ground and washed in water at 20 C for 12 hours. The resulting P.E. was analysed to contain 4.38% compound X, this small loss of 0.35% compound X could have been due to the compound X being more soluble in water than P.E., but it was assumed that the amount of adsorbed formals was

negligible.

Di - P.E. gave an equivalent of 1.88% compound X by this method. As I.C.I. have analysed this di - P.E. as containing 4.0% compound X, the effect of di - P.E. on this method can be neglected.

By extrapolation Batch B (Bag P.8) was analysed by this method to contain 4.82% compound X. The average of I.C.I.'s analyses gave a composition of 4.9% compound X. Batches A, B and C (containing 4.3% Compound X and 1.0% di - P.E.) were used as the source materials for the later experimental work.

SECTION FOUR

PRELIMINARY EXPERIMENTS

4.1. Batch Crystallisation in a stirred vessel.

As I.C.I.'s present method of crystallisation involves cooling hot concentrated product liquors in batch operated stirred tanks, to ambient temperature, the effect of controlling the growth temperature was investigated. A 30% m/v Batch A solution was made up, held at 90 C for complete dissolution and cooled in a flask while gently stirred. The flask was held at the nucleation temperature of 54 C for 24 h and the product filtered under vacuum at 50 C. The crystals were washed with two batches of water at 0 C, dried at 60 C and sieve analysed. Each sieve fraction was examined under a microscope (x 70) and all fractions were found to consist of agglomerates: the large agglomerate particles were composed of particles about 1/5 the agglomerate diameter the smaller agglomerate particles consisted of crystals about 1/3 the agglomerate diameter. Only in the - 350 mesh size were large numbers of discrete crystals seen, and this fraction also contained small irregular crystals which were presumably the "dust" produced when the large aggregates were broken down. The size analysis of the product is shown B.C.T. 1, fig. 9, Appendix B.

A similar test was done on a 30% m/v Batch C solution which was grown for 3 hours at the nucleation temperature of 55.3^o C. The product was given one wash with ice water and one with acetone, and then dried at 60^o C. The sieve analysis is shown B.C.T. 2, fig. 9, appendix B. Although the size distribution appears similar to B.C.T. 1 the microscope indicated that in the smaller size fractions agglomeration was limited and many well shaped crystals were observed. The smallest crystals were again about 20 μ diameter, but there was practically no material smaller than this at all. This is in contrast to the original, Batch C, feed which contained a large amount of exceedingly small irregular crystals.

4.2. Pilot Plant Oslo cooling crystalliser (fig.10)

A 6 in. diameter pilot plant Oslo type cooling crystalliser was available which had not been commissioned. An attempt was made to operate this with P.E. but was unsuccessful for the following reasons:

- a) The crystalliser had been built from standard glass (Q.V.F.) sections and had a hemi-spherical base. The bulk of the seed bed would not fluidise in this base but formed a solid cake with a small cone shaped fluidised bed at its centre.
- b) The cooler was of too large a diameter and tended

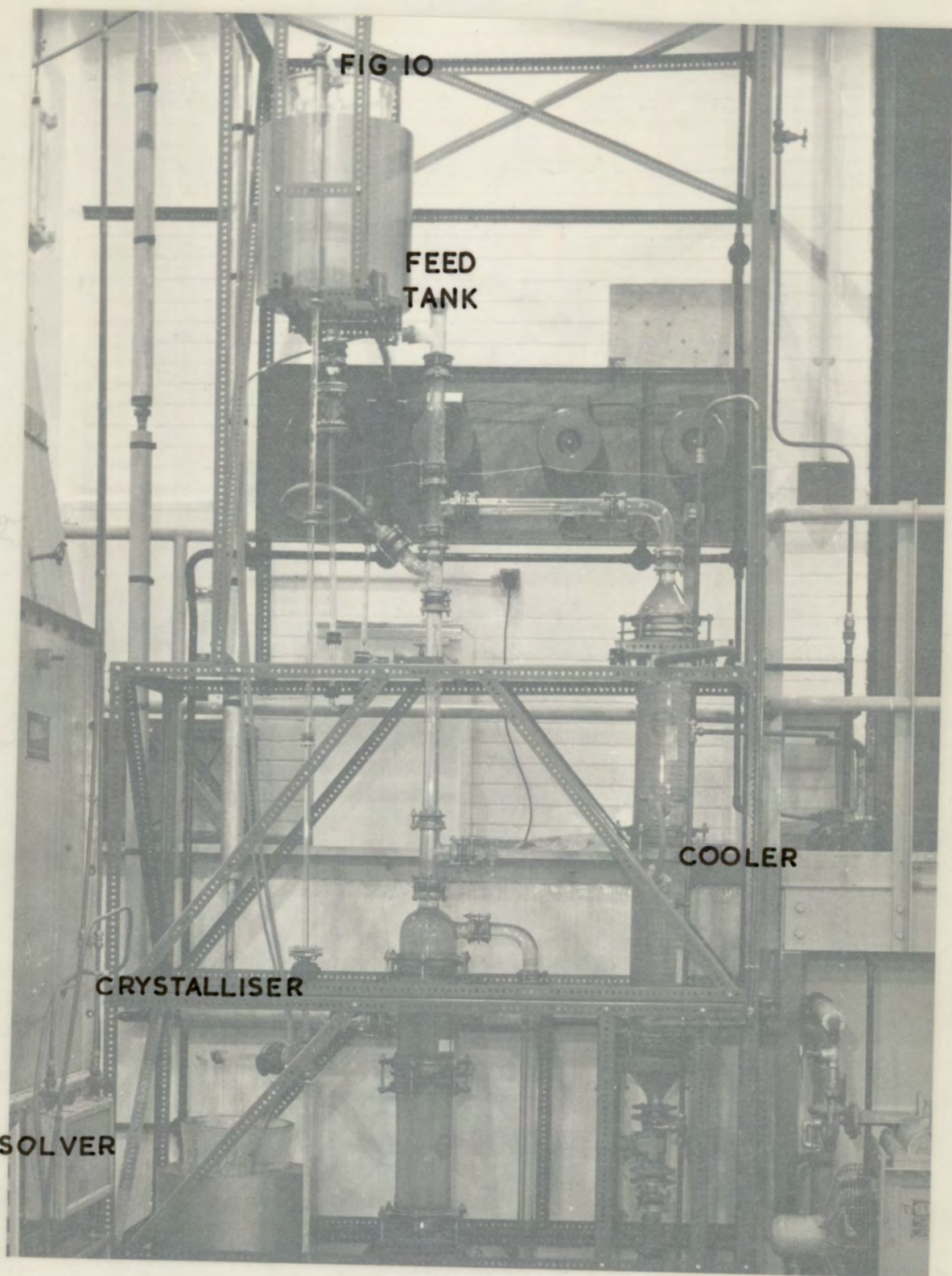


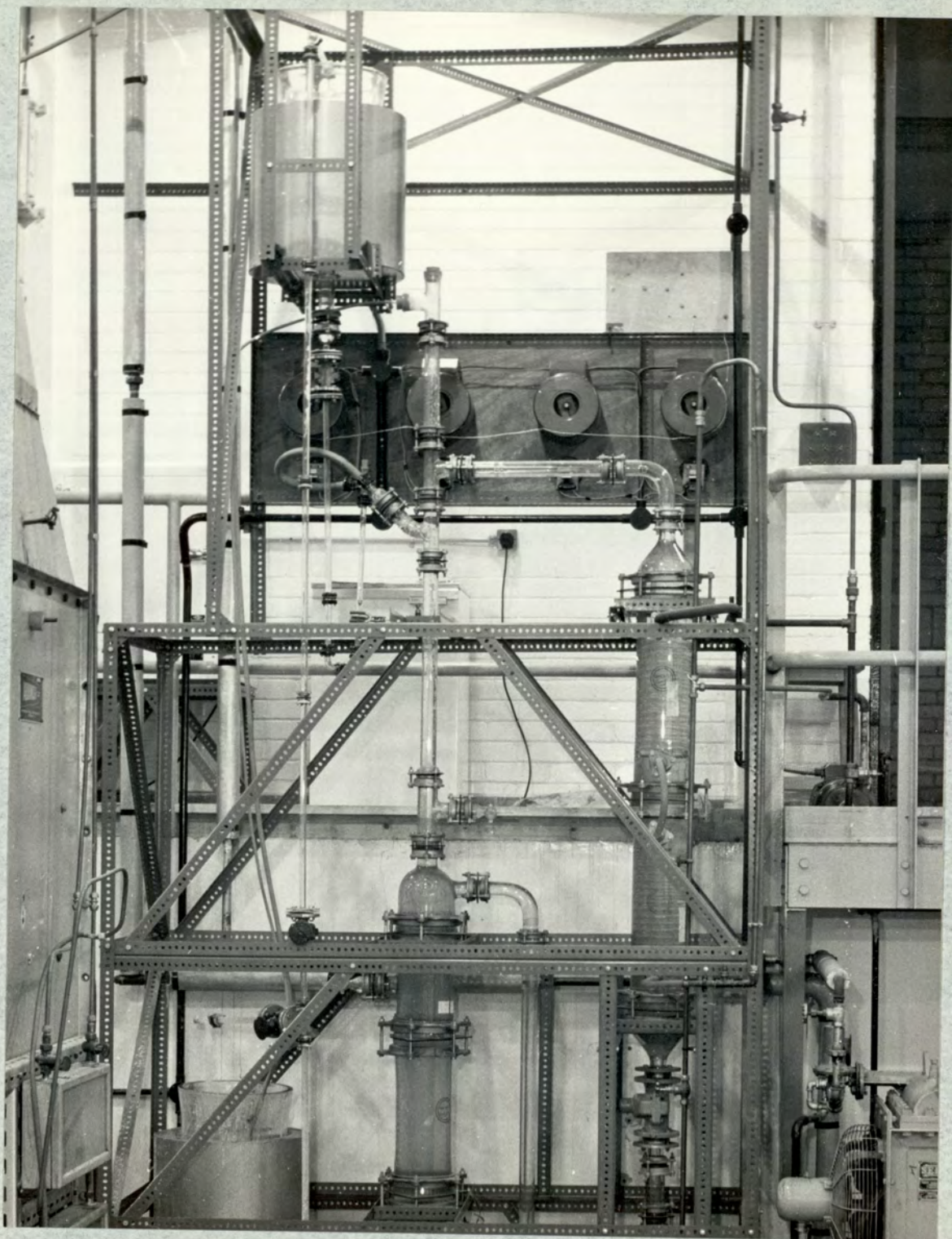
FIG 10

FEED
TANK

COOLER

CRYSTALLISER

DISSOLVER



to build up its own fluidised bed from transported fines.

c) Although the cooling water could be recirculated so that any degree of supersaturation could be produced as desired without excessive temperature drop at the heat transfer surface, it was found that the growth rate of P.E. was so slow that there was very little loss of supersaturation of the recirculated liquor. Hence heating tape was required to compensate for natural cooling losses when operated above room temperature.

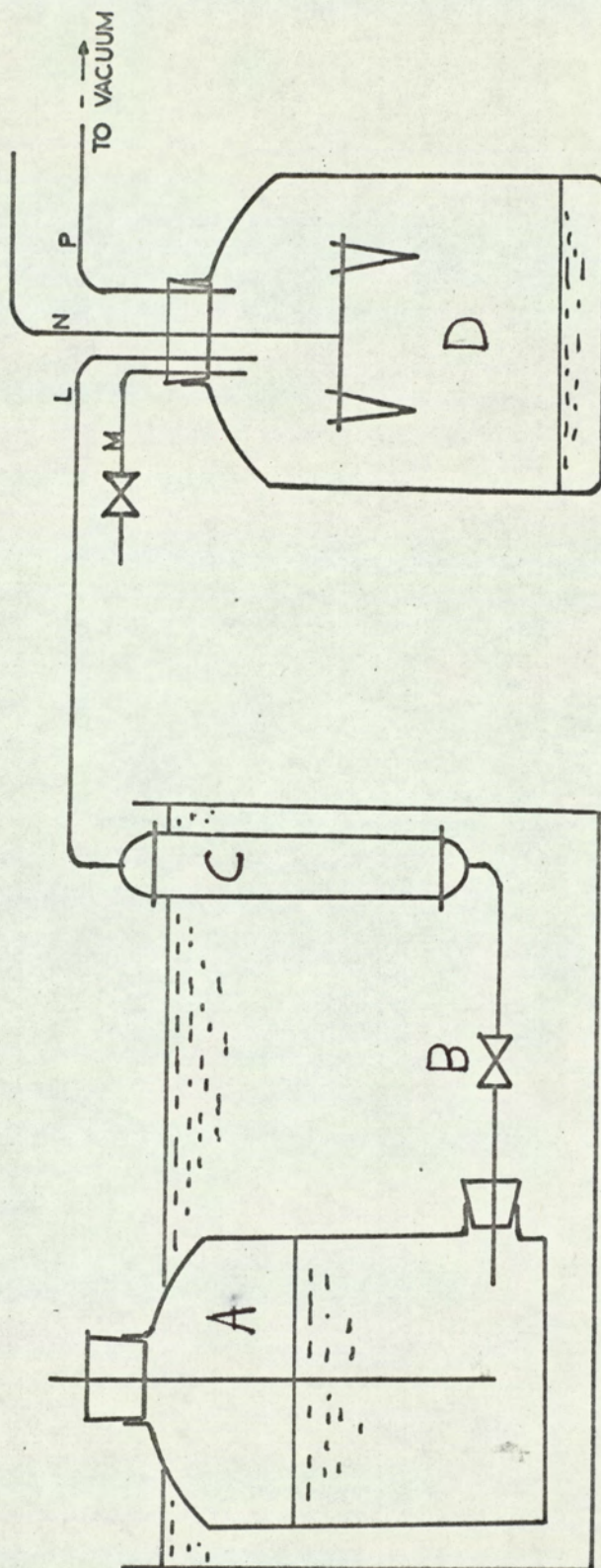
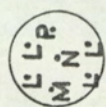
d) There was no rapid control of the mother liquor concentration. The only check on the concentration was by removing samples and evaporating to dryness, by which time the addition of too much feed had produced homogeneous nucleation.

4.3. Measurement of Crystal Growth in a small-scale fluidised bed.

4.3.1. Apparatus

Fig. 11 shows a sketch of the apparatus used. A supersaturated solution was placed in the 2 litre feed aspirator A and throttled through a needle valve, B, which had an extended spindle for ease of use, through the $\frac{5}{8}$ " diameter crystalliser body, C, into the receiving vessel D. Flow was due to the pressure drop created by a vacuum pump. The apparatus A, B and C was immersed in

FIG. II. FLUIDISED BED APPARATUS



an oil bath thermostatically controlled to ± 0.01 deg. C. Four such sets of apparatus were used in parallel, each connected to the receiving vessel D. Receiver D had a controlled air bleed M which together with the valves B allowed a fine control of the liquid flow rates. The flow rates were measured by manouvering graduated tubes, attached to a glass arm, N, in the receiver, into the paths of the individual liquid outlets. The effect of the head of feed liquid on the flow rate was prevented by placing a tube open to the atmosphere through the aspirator stopper. Items A, B and C were connected by neoprene tubing; C and D were connected by thick walled rubber tubing wound with heating tape.

The crystal bed was supported by a No. 4 porosity (5 - 15 μ pore diameter) sintered glass disc sealed round its edge by an O - ring clamped by brass plates between two neoprene gaskets. Both epoxy resins and impact adhesives were found unsatisfactory for sealing the disc.

4.3.2. Size Analysis

A size analysis of the fluidised beds was made before and after each run by means of a 'Coulter Counter' particle size analyser (Appendix C). This instrument determines the number and size of particles suspended in an electrically conductive liquid by passing a measured

volume of suspension through a small orifice having an immersed electrode on either side. If the largest particle diameter is less than 40% of the aperture diameter and its length is shorter than that of the aperture, it can be shown that the change in aperture resistance is directly proportional to the particle volume.

$$\text{i.e. } \Delta R = \frac{\rho_0 V}{A^2} \left(\frac{1}{1 - \frac{\rho_0}{\rho}} - \frac{a}{A} \right)^{-1}$$

where ΔR = the change in resistance produced by the particle.

ρ_0 = the electrolyte resistivity.

ρ = the particle resistivity.

V = the particle volume.

A = the orifice area normal to the axis.

a = the projected area, parallel to the orifice axis, of the particle as it is oriented in passing through the orifice.

Hence for a given sample and electrolyte, all factors on the right hand side of the equation will be constant except V and a which change with particle size. Now if the particle diameter is restricted to less than about 40% of the orifice diameter, the factor $\frac{a}{A}$ will be negligible and ΔR will be directly proportional to the particle volume V .

As the particles pass through the orifice the voltage pulses they produce are amplified and fed to a threshold circuit having an adjustable threshold level. If this level is reached or exceeded by a pulse, the pulse is counted. By pre-calibrating the threshold circuit and taking a series of counts at selected threshold levels, data are obtained for plotting a cumulative size distribution.

Before plotting the counts are corrected for coincident particle passages and for the background count due to the particles present in the electrolyte. To keep the coincidence corrections at a moderate level it is necessary to have a very high dilution. For the P.E. crystals counted this was found to be approximately 0.01 g. of crystals in 250 ml. of electrolyte. The electrolyte used was first filtered through a 0.45 μ porosity Millipore membrane filter to keep the background count as low as possible.

4.3.3. Procedure

Solutions of known concentrations were made up and placed in the four feed aspirators A, with the two thermostatically controlled oil baths set to the same temperature. The calculated theoretical limits for the fluidisation of P.E. crystals in water are shown in figure

12, appendix B. From preliminary tests it was found that crystals $\langle 44 \mu$ diameter were very difficult to fluidise, however a small seed size was necessary to enable the Coulter Counter to be used for size analysis, so a close cut seive fraction 64 - 75 μ seed size was used. As the seed was ground Pure P.E. preliminary growths were done for one hour in a beaker of supersaturated solution at the temperature of operation to obtain the usual crystal morphology. The crystals were then allowed to settle, the liquor filtered off and saturated solution added. The suspension was divided into four volumes and a size analysis done on each. The suspensions were then transferred to the crystalliser tubes, C, and the vacuum applied drawing supersaturated solutions through to receiver D where the flow rates were measured. Manometers were initially used before the crystallising tubes as flow indicators but found unsatisfactory due to the very low flow rates used. The crystal bed expansions were used as indications of constant flow rates, assuming negligible growth, throughout the runs. For the higher temperature runs transference of the seed after preliminary growths was found unsatisfactory and the preliminary growths were done in the crystallising tubes. Sampling of the beds in the crystallising tubes was done using a 1/16" bore stainless steel tube preheated

to the temperature of operation. The average of three samples was taken for each size analysis.

4.3.4. Results

Growth rates were measured for Pure P.E. at four different supersaturations at 25 °C and 40 °C at fluidisation rates of 1 cm³/min. for a period of five hours. However no detectable growths were obtained, the changes in size analysis being within the limits of accuracy of the sampling procedure and the Coulter Counter.

Several attempts to measure the growth rate of both Pure P.E. and Batch A material at 60 °C and 70 °C were made but difficulty was experienced in maintaining properly fluidised beds. In fact all runs agglomerated causing channelling in less than two hours and no measurable growth was obtained during this time. A run was done on Batch A at 80 °C which lasted one hour before agglomerating and again no growth was apparent. A possible cause was later thought to be due to the nature of the seed of Batch A and a run was done at 70.0 °C using specially prepared seed (Section 6.2.4.) fluidised with 28% m/v P.E. at a rate of 4 cm³/min. The run lasted 2½ hours during which time the bed agglomerated several times and was broken up manually. No preliminary growth

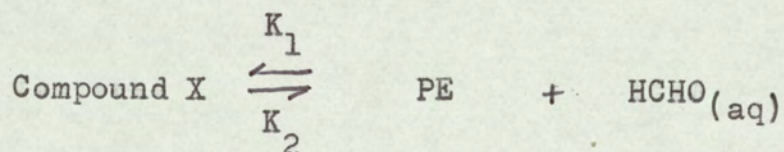
was attempted for this run and the size analyses obtained before and after, L 1 and M 1, respectively are shown tables 8 and 9 and fig. 13 (Appendix B). These two curves were typical of the results obtained with the fluidised bed growth experiments.

SECTION FIVE

P.E. EQUILIBRIUM IN AQUEOUS SOLUTION

5.1. Stability of Compound X in aqueous solution

As compound X could be synthesised with formaldehyde and P.E. in aqueous solution, and in view of the sequence of reactions for bis - P.E. monoformal proposed by Salkind (62) an attempt was made to obtain information on the overall decomposition reaction rate constant K_2 expressed by:



An almost saturated solution of Batch A P.E. was made up and placed in a flask in an oil bath maintained at 90.0^o C. The flask was purged with a stream of nitrogen at a rate of approximately 3 ft³/h. The concentration was kept constant by periodically adding water. Samples were sent to the analytical laboratories of I.C.I. after 40 ft³ and 60 ft³ of nitrogen had been used. The results of this test were within the limits of analytical accuracy for Compound X. The experiment was repeated sampling periodically until 200 ft³ of Nitrogen had been used. The samples were analysed by the 'Formaldehyde Content' method

described in Section 3.6. The results were again within the limits of analytical accuracy (i.e: approx. $\pm 0.2\%$ compound X). Hence it was assumed that compound X does not easily decompose in aqueous solution below 90^o C.

5.2. Preliminary Solubility Determinations

5.2.1. Introduction

Equilibrium of solute in solvent can either be approached from undersaturation or from supersaturation. It was hoped to attain equilibrium of P.E. solutions quickly by using ultrasonics, and for this purpose an ultrasonic probe was used which was immersed in the solution and emitted ultrasonic waves at a fixed frequency of 20 Kc/s. However, the heat generated raised the temperature of the solution being studied by several degrees in a few minutes. The ultrasonic probe could not be used, therefore, to attain equilibrium from undersaturation although it was found to be a very effective nucleator for supersaturated systems, the smaller the degree of supersaturation, the longer it being necessary to apply the ultrasonics. It was also found that even when the solutions were nucleated with the ultrasonics it took days to attain equilibrium unless they were stirred.

5.2.2. Rate of approach to equilibrium

To study the effect of impurities on the attainment

of equilibrium the following method was used.

A supersaturated solution was made up of 20g. P.E./100 g. water and dissolved at about 50°C. It was allowed to attain the desired equilibrium temperature of 25°C in a thermostatically controlled water bath and the ultrasonic probe was applied to nucleate the solution. Once nucleation had occurred the solution was stirred at a constant speed. The specific gravity of the solution was then measured periodically to find the time necessary to attain equilibrium at this temperature. To measure the specific gravity the stirrer was stopped, the solution was filtered out using an immersion filter into a double jacketed vessel through which water at 25.0°C was circulated and the weight of a sphere totally immersed in the solution was measured using a sensitive balance. By comparison with the weight in air and in water at 25°C the specific gravity could be calculated. The variation of specific gravity with time for different P.E. mixtures is shown Table 17. It can be seen that the presence of Compound X makes the attainment of equilibrium much slower and that the value obtained is not the same when approached from undersaturation as from supersaturation. This test was repeated with the same result, and a complicated system similar to the NaCl - Na₄Fe(CN)₆ - H₂O system (73) was anticipated.

The graph of specific gravity at 25.0 C ^o vs P.E. concentration is shown in fig. 14 and the equilibrium values obtained are shown in table 18. These values have been shown (points G) in the equilibrium diagram fig. 20.

5.2.3. Solubility by evaporation

In order to determine the solubilities of P.E. with its associated impurities in water at various temperatures, supersaturated solutions at the particular temperature were made up, nucleated with the ultrasonic probe and stirred in a beaker, immersed in a thermostatically controlled oil bath, for about 12 hours. Approximately 10 ml. of the solution was then pipetted out using a pipette preheated to the appropriate temperature through an immersion filter and transferred to a crucible. The weight of the solution was recorded and the water was evaporated off in an oven at 90 C. ^o The results of these solubility determinations are shown table 19 and have been included (points S) in the equilibrium diagram fig. 20. This method, however, was not found to be very satisfactory for solubility determinations at high temperatures as the solutions easily crystallised out in the pipette on transference and inaccuracies were caused through evaporation before weighing.

5.3. Refractometer Studies

As it had been found Section 3.4. that the refractive index of aqueous P.E. solutions was not very sensitive to the impurities normally encountered in commercial P.E., this property was studied for suitability of concentration measurements.

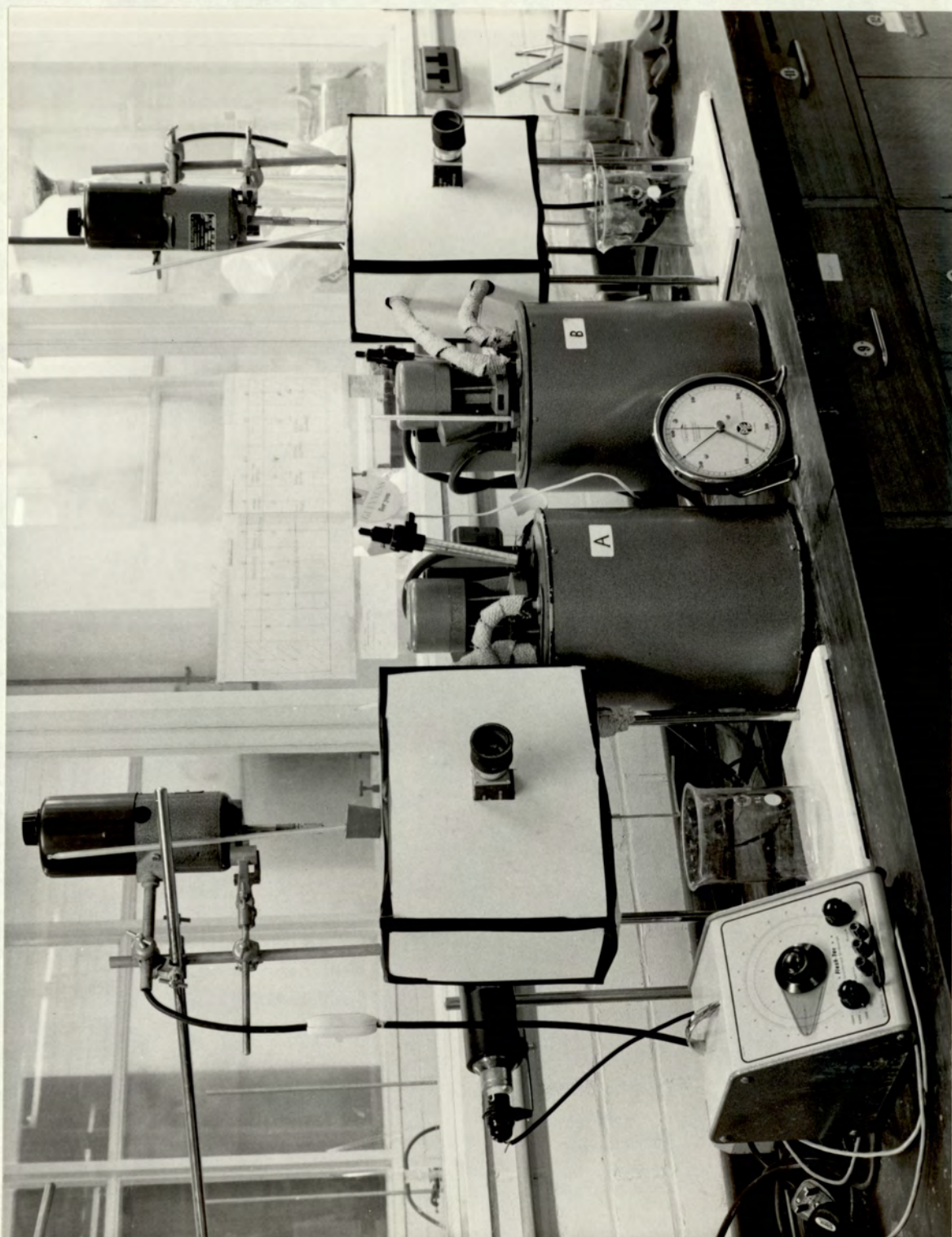
5.3.1. Apparatus. (Fig. 15)

Two standard Bellingham and Stanley in-line refractometers (Nos: 583215 and 583213) were used having scales indicating 0 - 40% sugar at 20 C. Water jackets were fitted round the body castings and supplied with water from Townsen and Mercer TU 3 thermostat circulating units. The refractometers were mounted in frames with sodium lamps behind them. The lower port of each refractometer was sealed with a rubber bung having a glass tube and plug for draining purposes fitted flush with the inside of the casting. A rubber bung fitted with a thermometer and with a hole large enough to accommodate a small stirrer could be inserted in the top port of each refractometer. The capacity of the instruments was about 300 cm³.

5.3.2. Experimental Procedure

The approximate amount of P.E. required was

FIG. 15 REFRACTOMETERS



accurately weighed out and washed into a 250 cm³ volumetric flask which had been selected for having the volume line very low on the neck to allow for expansion. The volume was made up to 250 cm³ with distilled water taking care to eliminate air bubbles. The flask was warmed until the P.E. had dissolved and the refractometer was brought up to ca. 70 C or higher for more concentrated solutions. When the solution was at about the same temperature as the instrument it was poured in and the stirrer started. The temperature was then raised to 80 - 90 C to ensure solution of any nuclei formed during the addition of the solution and then cooling was commenced.

Readings of the refractive index (as indicated % sugar) and temperature were taken every 5 minutes and plotted as shown in the specimen calibration curve (fig. 16). The TU 3 unit gave a convenient temperature rise of slightly less than 1 deg. C./min. and the cooling rate under natural convection was of the same order at the higher temperatures. To maintain the cooling rate at the lower temperatures however it was necessary to use mains water in the cooling coils of the TU 3 unit. Finally the solution was reheated to about 70 C ready for the next test.

In cases where nucleation occurred during cooling

the temperature was held at the nucleation temperature for a while in order to get some qualitative value of the growth rate (section 6), this was sometimes so rapid that readings could usefully be taken every half minute. The thermostat was then set at some desired temperature and held until no change in refractive index occurred. In this way it was possible to obtain nucleation and equilibrium data at the same time as the calibration.

5.3.3. Accuracy

5.3.3.1. Instrument Calibration

In terms of indicated % sugar the calibration is of course as accurate as the experimental technique allows, but to convert the readings to actual refractive index and make them more universally useful further calibration is required. The following three points were used (74) and are compared with the published data table (20).

		Equivalent % Sugar	Indicated % Sugar on A (ie.no. 583215)	Indicated % Sugar on B (ie.no. 583213)
Distilled Water	$n_D^{20} = 1.3330$	0	0.4	0.05
Analar Acetone	$n_D^{19.4} = 1.3589$	16.9	18.0	17.75
Analar Acetic Acid	$n_D^{22.9} = 1.3715$	24.5	25.1	25.25

The mean refractive index change for both sugar and P.E. aqueous solutions is approximately the same at ca. 0.0015 per 1%.

5.3.3.2. Reading Accuracy

The thermometer used was graduated in 0.1 deg. C which was more than sufficient in view of the accuracy to which the refractometer could be read and the slope of the calibration graph fig. 16.

The steam point and the transition of hydrated sodium sulphate were checked and found to be within 0.1 C of the expected values for total immersion of the thermometers. The correction for partial immersion, as used with the refractometers, is shown in fig. 17. Also shown (fig. 17) is the calculated correction obtained from the equation $y = e (T_o - t) L(76)$ assuming t varying between 22 C and 30 C. Where y = correction to be added to T_o ; T_o = observed temperature C; $e = 0.000156$ (apparent expansion of Hg in glass); and L = length of emergent mercury column expressed in degrees.

The refractometer scale was graduated to 1% (sugar) and could be estimated to 0.1% with ease. With practice it was found possible to estimate to 0.05% but it was then found that a parallax error was introduced

at this limit. In this respect it was found that the focusing of the instrument was important and also sensitive to temperature (which was close to the solution temperature). This indicates that P.E. solution concentration could be determined to $\pm 0.05\%$ ($\Delta n : \text{ca. } 0.00015$) as expected from section 5.1. the calibration curve could be retraced on heating with the same result as negligible impurity decomposition takes place. It was also found that with the rubber bung in the top port there was no change in the refractive index due to evaporation even after being held for 14 hours at 80.0°C .

5.3.3.3. Impurities

The calibration was based on the three materials, Pure P.E., Batch A and Batch C. The calibration curves, as expected, were almost identical for the three materials the average correction necessary to convert a reading from Pure P.E. to Batch A being to add - 0.16% and to Batch C being to add - 0.11%. Since these corrections are of the same order as the accuracy of the readings they were neglected and the calibration curve given in fig. 18 is the average of the results for all three materials.

5.3.4. Calibration Results

The concentrations of the solutions tested were converted to % mass fraction assuming the density of water at room temperature, $\rho_w = 0.998 \text{ g/cm}^3$ and the density of P.E. $\rho_s = 1.395 \text{ g/cm}^3$ (see fig. 19). The calibration data were then interpolated at intervals of refractive index of 0.001 using the calibration table 20. These data (tables 21A, B and C) were then used to construct the final calibration curve fig. 18.

5.3.5. Nucleation Results

The presentation in the refractometer eyepiece is a dark field which when focused correctly has a sharp edge with a bright field. It was observed that in the tests in which homogeneous nucleation occurred the hair - line structure observed in the bright field would disappear and the bright field lose its brilliance quite suddenly and several degrees before there were any signs of the presence of nuclei to the naked eye. It was assumed that this disappearance of the hair - line structure gave an accurate indication of the nucleation temperature.

The Ostwald - Freundlich equation (p.4) suggests that homogenous nucleation data might be correlated on a basis of log concentration ν_0 reciprocal absolute temperature as with equilibrium data. This has been

done fig. 20 and the correlation then transposed to a linear plot fig. 21.

The equations of the nucleation curves are:

McCallum's data (Plant P.E. in Mother liquor):

$$\log_{10} x = 2.659 - \frac{339}{T}$$

$$\text{Pure P.E.: } \log_{10} x = 2.289 - \frac{633}{T}$$

$$\text{Batch A and Batch C P.E.: } \log_{10} x = 3.112 - \frac{545}{T}$$

$x = \% \text{ mass fraction}$ $T = \text{degrees Kelvin}$

5.3.6. Equilibrium Results

The study of equilibrium in nucleated solutions was considered ideal since the very large surface area of crystal available for growth should permit rapid approach to the equilibrium concentration value. The collected data are given in table 21 and fig. 20. It is apparent from this graph that for impure P.E. equilibrium was approached very slowly below ca. 45°C . Even a change in the slope of the equilibrium line would not account for the scatter of results in this region. Above this temperature equilibrium was effectively reached in $\frac{1}{2}$ hour or even less at the higher temperatures. The results of the impure material at the higher temperatures are very similar to those

of Cooke (75) who used P.E. of "better than 99.6% purity". The results of the pure P.E. (which analysed as better than 99.9% purity) gave a straight line identical to that of Cooke. The equilibrium values obtained from the growth experiments (section 6) table 22 have also been included (points R) on the equilibrium diagram fig. 20.

The equations to the equilibrium curves are given below:

McCallum's data (Plant P.E. in mother liquor):

$$\log_{10} x = 4.195 - \frac{939}{T}$$

$$\begin{array}{l} \text{Cooke's Data, Pure P.E. } \\ \text{Batch A, Batch C } \left. \begin{array}{l} \text{ } \\ \text{ } \end{array} \right\} \log_{10} x = 5.072 - \frac{1266}{T} \\ \text{ } \left. \begin{array}{l} \text{ } \\ \text{ } \end{array} \right\} \text{ } \end{array}$$

x = % mass fraction

T = degrees Kelvin

5.3.7. Anomalous Results

5.3.7.1. Batch A

As equilibrium values overlapped according to whether they were approached from undersaturation or supersaturation in the specific gravity studies (5.2.2.) checks were made on the equilibrium values found by refractometry at different temperatures. At 70°C the equilibrium value obtained on refractometer A from supersaturation was found to be 17.8% (sugar) compared

with 17.9% obtained from undersaturation. Similarly at 80 C the equilibrium value approached from supersaturation was 22.15% compared with 22.3% approached from undersaturation. This overlap was as expected from the specific gravity measurements at 25 C and no dependence was found on the initial degree of supersaturation.

5.3.7.2. Batch C

Aqueous solutions of Batch C were studied in refractometer B at 60 C with unexpected results. It was found that whereas a seeded 24.0% m/v solution (R.31) grown for 21 h gave a value of 14.4% (sugar) a similar solution nucleated at 40 C and grown for 15 h at 60 C gave a value of 15.2% (sugar). This same solution nucleated with ultrasonic waves at 60 C and grown for 40 h gave a value of 15.0% (sugar). A solution of about 30% m/v was stirred from supersaturation for 18 h giving a value of 14.7% (sugar). 10 g of extra Batch C seed was added and stirred for a further 4 h with no change. The solution was cooled to 22.5 C for a few hours and the equilibrium value at 60 C when then approached from undersaturation was 15.1% (sugar). The solution was held at 30 C for 24 h and the equilibrium value obtained when again approached from undersaturation at 60 C for 72 h was 14.8% (sugar). There appears to

exist a complicated four component system possibly dependent on the nucleation temperature, the degree of supersaturation and whether equilibrium is approached from supersaturation or undersaturation.

SECTION SIX

GROWTH STUDIES BY REFRACTOMETRY

6.1. Growth of Nuclei

During the nucleation experiments (section 5) the temperature was held at the nucleation temperature for a while in order to obtain some qualitative value of the growth rate. However because of the considerable variation in the number of nuclei produced, affected by a number of uncontrollable factors no correlation was found in the results. An attempt was made to differentiate between nucleation and growth by doing a size analysis with the Coulter analyser on the nucleated solution. As the weight of solid thrown out of solution was known from the refractometer readings, an accumulative number oversize analysis could be calculated. If this could be done at different time intervals any fresh nucleation occurring during the process could be allowed for and the growth of the original nuclei measured. This growth has to be related to the average supersaturation between readings so a reading would be necessary for each small decrease in concentration. This method was found impractical however as the refractometer readings of concentration were not accurate enough and the decrease in concentration following nucleation was far too rapid

to allow size analyses to be done at the necessary time intervals (it being necessary to analyse with the 50 μ tube immediately after sampling).

6.2. Seeded Solutions

6.2.1. Introduction

Jenkins (39) used refractometry for the measurement of the velocity of crystallisation using an immersion refractometer in a cell seeded with crystals. Whittier and Gould (77) and Van Hook (78) used this method for the measurement of the velocity of crystallisation of sucrose but used an Abbé refractometer to follow the decrease in solution concentration. There are however practical difficulties involved in using an Abbé refractometer for this purpose and it is not thought possible to prevent evaporation of the solution on transference. The in-line refractometer used for the growth studies was similar to Jenkins' refractometer cell. It was found necessary to polish the stainless steel walls and prism holder otherwise the nature of this surface encouraged crystal attachment, decreasing the area of crystals available for growth. Jenkins (39) used 1 g of seed crystals as the unit of surface for crystal growth. It was thought preferable to do a size analysis on the seed to correlate the results on an

actual surface area for more universal comparison.

6.2.2. Preliminary Tests

A close cut sieve fraction $44 - 53\mu$ size was used as seed. The small size being chosen so that a slower stirrer speed would be necessary for complete suspension. It was found that 2 g of seed was most convenient for accurate following of the concentration change without obscuring the sodium light. After the first few runs a size analysis on the product crystals revealed a large amount of fine material present. This could have been due to nucleation induced by the stirrer over the time of the experiment, secondary nucleation produced by seeding the solutions or attrition of the crystals. To minimise this last effect the flat bladed stirrer was changed for a marine type propeller made to fit the refractometer. The front wall of the refractometer containing the prism was unscrewed and temporarily replaced with a perspex front. The minimum stirrer speed necessary for complete suspension of $75 - 89\mu$ crystals was then observed to be about 200 r.p.m. (measured with a stroboscope) compared with 1000 r.p.m. necessary with the flat blade. The effect of the stirrer speed on the growth rate of $44 - 53\mu$ Batch A sieve fraction is shown in table 23. The growth rate

constants K^1 were calculated using 1 g of seed crystals as the unit of surface area as the degree of attrition at different stirrer speeds was not known. From a consideration of this table 500 r.p.m. seemed to be an appropriate speed to work with, as there is very little change of growth with stirrer speed between 400 r.p.m. and 600 r.p.m. and so the diffusional resistance is considered to be very small. The faster growth at 750 r.p.m. could have been due to excessive attrition producing a larger surface area available for growth.

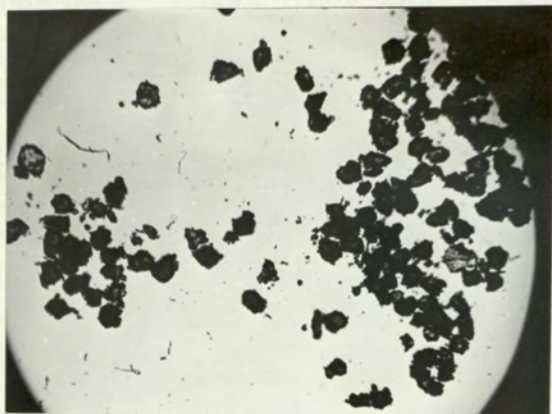
6.2.3. Metastable Limit

The initial tests used a high supersaturation of about 7.0% m/v. Although this is not high enough for spontaneous nucleation, nucleation could have been induced by the agitation over the period of the runs. A 22.5% m/v solution of Batch A was made up in order to study the effect of the supersaturation on the time taken to nucleate, under agitation at 500 r.p.m. The results are shown table 24. Between each nucleation the solution was redissolved at 90 °C under agitation for about an hour. From a consideration of the results it was considered safest to work with supersaturations of less than about 4% m/v.

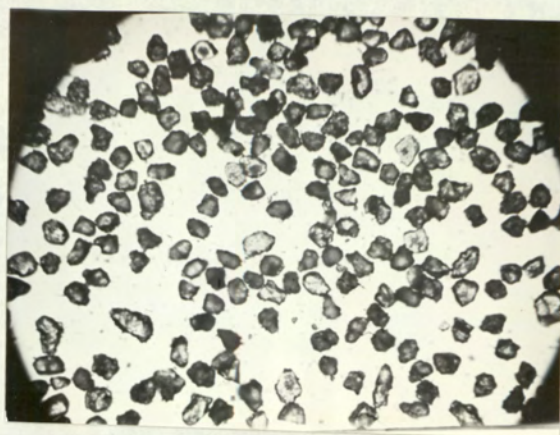
6.2.4. Choice of Seed

A lot of fine material was still found to be present in the product crystals after growth even though low supersaturations and a propeller type stirrer was used. This was then considered to be due to the nature of the seed. It had previously been observed that the manufactured product consisted of agglomerates of crystals with small crystals attached around the surface and it had been found possible to obtain a better product (B.C.T. 2 section 4.1.) by controlling the growth temperature and washing the product with acetone. The growth rate of the Batch A sieve fraction was compared with the sieve fraction 44 - 53 μ of product prepared in a similar way to that of B.C.T. 2 and with the 44 - 53 μ sieve fraction of Batch A material ball milled for 20 minutes and 3 hours respectively. The results are shown in table 25. It was hoped that ball-milling the P.E. would break up the agglomerates, but it was found that the growth was faster after 20 min milling than before and even faster after 3 h milling. This could possibly be due to static electricity created by the milling holding together agglomerates of very fine particles so that the true surface area was in fact much greater than that based on the sieve fraction size. On examination of the different seed materials figures

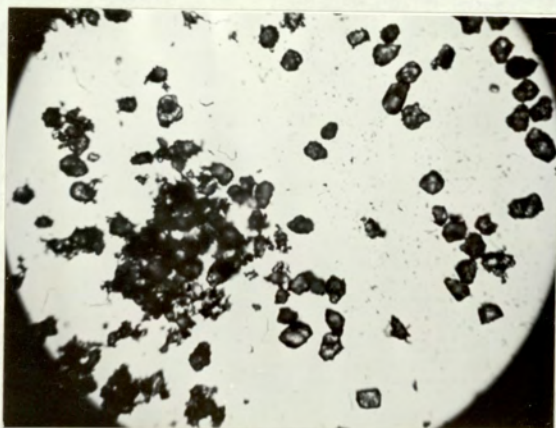
FIG 22 BATCH A SEED 44-53 μ



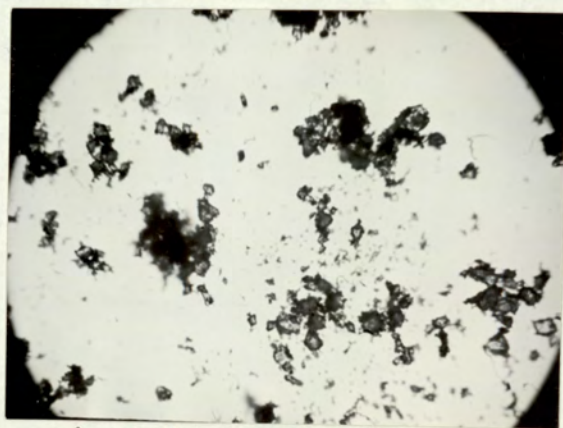
a SIEVE FRACTION



b PREPARED SEED



c MILLED FOR 20MINS



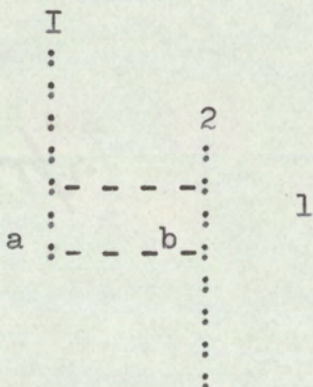
d MILLED FOR 3h

22 A, B, and D it was thought that the slow growth of the prepared seed was due to less attrition, hence a smaller surface area available for growth. This "prepared seed" was used for all further growth tests.

6.2.5. Attrition

In order to correlate results on a basis of the actual surface area available for growth it was necessary to determine the rate of increase in surface area due to attrition only. This was done by suspending 2 g of 44 - 53 μ sieve fraction prepared Batch A seed in 250 cm³ of Batch A solution saturated at 25.0^o C in the refractometer and agitating at 500 r.p.m. Samples were taken with a 1/16" bore stainless steel tube at different times and analysed with the Coulter Counter using a 280 μ orifice tube (table 26). As the analysis was not complete at the bottom threshold limit for the 280 μ orifice tube it would have had to be used in conjunction with the 50 μ orifice tube. It was not, however, satisfactory to change tubes during the analysis of a sample, or to have large particles present when using the 50 μ orifice tube. To obtain a combined size distribution the attrition test was repeated, after doing size distributions (1) with the 280 μ orifice tube in the first test. Samples were taken after the same time intervals as with the first test, dispersed with the

ultrasonics in the pre-filtered electrolyte and then filtered through a $14\mu \pm 3\mu$ duralon Millipore Filter. The size distribution (2) then obtained with the 50μ orifice tube was combined with the 280μ orifice tube distribution (1) in the following way:



If $X =$ Converted No. % oversize on the combined scale.

$Y =$ No.% Oversize on distribution (1) 280μ

$Z =$ No.% Oversize on distribution (2) 50μ

$$1. \quad X = \frac{Y \times 100}{100 + (100 - 1)\left(\frac{a}{b}\right)} \quad \%$$

$$2. \quad X = \frac{100 + (z - 1)\left(\frac{a}{b}\right)}{100 + (100 - 1)\left(\frac{a}{b}\right)} \times 100 \quad \%$$

As the duralon filter was only $\pm 3\mu$ this had to be allowed for when combining the distributions. This was done by selecting "b" as the difference in the values of the number % oversize between 10μ and the lower limit of size distribution 1. Similarly "a" equivalent to "b"

is the difference in the values between the lower limit of the size distribution (1) and 10μ . These values of a and b had to be obtained graphically. Typical graphs of the size distributions obtained are shown figures 23 (a) and (b). The table of the size distributions (2) obtained with the 50μ orifice tube is shown table 27 and the combined size distributions table 28. The specific surface area was calculated from each combined size distribution and is shown table 28. As there was very little increase in area over the first 20 h after the initial 6 mins the growth rate calculations were based on the specific surface after 6 mins. Pure P.E. was assumed to behave similarly and the size distribution of the seed sample and its specific surface after the first 10 minutes attrition is shown table 28. Due to external influences affecting the Coulter Counter at the lower threshold limits with the 50μ orifice tube the size distribution could only be obtained for diameters $> 1.88 \mu$ with the Batch A seed and $> 2.50 \mu$ at the time of the Pure P.E. analysis. The effect of the number of particles below these limits on the specific surface calculated is not known. The specific surface of Batch A seed after 6 mins attrition based on size distribution 1 (i.e. $> 6.22 \mu$) is $1110 \text{ cm}^2/\text{g}$ compared with $1295 \text{ cm}^2/\text{g}$ based on the combined

size distribution. The error in specific surface could possibly be of this order (i.e. 20%).

6.2.6. Theory

Using the general growth rate equation

$\frac{dc}{dt} = -KA (c - c_{\infty})$ where c is the concentration of solution at any time t , c_{∞} the equilibrium concentration, A the actual area of crystal seed and K the velocity constant. The growth rate is assumed to be first order with respect to the supersaturation.

If A is assumed constant over a small time increment t_1 to t_2 .

$$\text{Then } K = \frac{2.303}{(t_2 - t_1) A} \log \frac{c_1 - c_{\infty}}{c_2 - c_{\infty}}$$

If the crystals are assumed to growth without altering their shape then the ratio of the area A_2 at

time t_2 to A_1 at time t_1 is:
$$\frac{A_2}{A_1} = \left(\frac{M_1 + dM}{M_1} \right)^{\frac{2}{3}}$$

where M_1 is the mass of crystals at time t_1 and dM is the increase of crystal mass from time t_1 to t_2 .

The area A then used in the integrated equation is the average of these areas A_1 to A_2 .

It is shown fig. 24 that the relationship of Indicated % Sugar of refractometer A to % P.E.(m/v) is linear over the concentration changes examined. Therefore

the ratio $\frac{n_1 - n_\infty}{n_2 - n_\infty}$ can be used directly instead of

$\frac{c_1 - c_\infty}{c_2 - c_\infty}$ in the equation, where n is the refractive

index in Indicated % Sugar.

Now, $c\% \text{ m/v} = \frac{\frac{m}{\rho_s} \times 100}{\frac{m}{\rho_s} + V}$ where V = volume of solvent
 m = mass of solute in solution

$$\therefore dm = \frac{dc}{100V} \left(\frac{m}{\rho_s} + V \right)^2$$

In this instance $\frac{m}{\rho_s} + V = 250$

$$\therefore dm = \left(\frac{250^2}{250 - \frac{m}{\rho_s}} \right) \frac{dc}{100}$$

Hence the velocity constant can be calculated from:

$$K = \frac{2.303}{(t_2 - t_1)} \left(\frac{2}{A_1 + A_2} \right) \log \frac{n_1 - n_\infty}{n_2 - n_\infty}$$

K can be compared to K_L where $\frac{dr}{dt} = K_L (c - c_\infty)$ and to K_m where $\frac{dm}{dt} = -K_m A (c - c_\infty)$ by the conversion shown in Appendix E.

The relationship between the velocity constant K and the absolute temperature, T , can be expressed by the Arrhenius equation

$$\frac{d \ln K}{dT} = \frac{E}{RT^2}$$

Hence $\ln K = \ln A - \frac{E}{RT}$

Where A is a constant, R is the gas constant and E the activation energy for growth.

Therefore a plot of $\ln K$ against $\frac{1}{T}$ should give a straight line of slope $-\frac{E}{R}$ and intercept $\ln A$ if the Arrhenius equation applies.

6.2.7. Results

The initial concentrations % m/v recorded in tables 23, 25, 29, 30, 31, 32 are those which were accurately prepared. This does not necessarily agree with that obtained from the refractometer reading and the equation from fig. 24, due to experimental error. However after the initial reading all concentrations were obtained from the equation obtained from fig. 24 over the concentration range and at the temperature of the experiment. The first increment was not included in the averaged growth rate constant anyway as it was considered that the crystal morphology was not constant during initial growth. The values of the growth rate constants for each run have been averaged, \bar{K} , with the following exceptions:

- 1) Results including the first 25% increment on the initial mass.
- 2) Results where $n_2 \gg n_\infty + 0.5$ Indicated % Sugar.

3) Results where $t_2 > 1500$ mins.

Exception (1) was because it was considered that this mass increment would be necessary before the seed, undergoing attrition in the first few minutes, would obtain its usual crystal morphology. Exception (2) was because a small error in n_∞ made a large difference to the ratio $\frac{n_1 - n_\infty}{n_2 - n_\infty}$ when n_1 and n_2 approached n_∞ . Exception (3) was because of the attrition effect, the crystal area could no longer be assumed constant in the absence of growth after this time.

The standard deviation from the mean \bar{K} has been calculated for each run using: Standard Deviation =

$$\pm \sqrt{\frac{\sum (K - \bar{K})^2}{n - 1}}$$

where n is the number of individual growth rate constants K used in obtaining the mean \bar{K} . It can be seen that the standard deviations are higher at the higher temperatures. This is possibly due to the fact that the refractometer readings were more sensitive to the instrument focus at high temperatures.

The generally high standard deviations could be expected due to the difficulty in estimating 0.1% Sugar on the refractometer scale. However these errors are largely self-compensating when averaged assuming the first

order equation to be correct.

Although an error in the initial area determination is cumulative throughout each run, errors in each area increment due to the concentration conversion are largely self compensating, provided the equation obtained from fig. 24 is accurate. An error in this equation would produce a trend in the growth rate constants, increasing or decreasing with supersaturation.

The results of Pure P.E. are shown in tables 29 a, b, c, d and e. Since run R.30 (table 29 d) was suspect as the Pure P.E. was splashed with oil, it was repeated, (table 29 e) with freshly purified material. The contrast shows the great inhibiting effect of traces of oil on the growth rate. The activation energy obtained from these results for pure P.E. is 18.4 k cal/g. mole. The results plotted as $\log \bar{K}$ vs $\frac{1}{T}$ (fig. 25) fit a linear correlation of $\log_{10} \bar{K} = 5.770 - \frac{4025}{T}$ for $80^\circ\text{C} > T > 50.0^\circ\text{C}$. The results for Batch A, tables 30 a, b, c, d and e are also plotted on fig. 25. and fit the linear correlation $\log_{10} \bar{K} = 13.401 - \frac{6710}{T}$ with an activation energy $E = 30.65$ K cal/g. mole for $80^\circ\text{C} > T > 50.0^\circ\text{C}$. The growth constants for Batch C containing 1.0% di - P.E. at 60.0°C and 500 r.p.m. are shown table 31. This run was done using seed prepared

similarly to that used in the Batch A runs, and the area was assumed to be the same as the Batch A seed for the purpose of the calculations. This result is inconclusive.

SECTION SEVEN

DISCUSSION AND PROPOSALS FOR FUTURE WORK

When studying the physical properties of P.E. and its associated impurities, in an attempt to establish a chemical analytical test, it became apparent from the melting point tests that the change below 200^o C, reported by Berlow et al (48) as a morphology change, was in fact due to a eutectic formed between P.E. and di - P.E. This was further investigated and found to be at 185.5^o C as compared with 190^o C found by Wyler and Wernet (55). Although the melting point test was found unsatisfactory for the measurement of impurities it could still be used as an indication of the purity of P.E. The method established for the analysis of Compound X based on the "formaldehyde content" was satisfactory for the I.C.I. product where the amount of adsorbed formals was negligible but would be useless for intermediate production stages with the presence of mono and di - formals. Although this method was calibrated on the I.C.I. analysis, the I.C.I. analytical method for Compound X was itself calibrated on the di - P.E. analysis as no method of isolating Compound X has yet been found. The analytical methods investigated for di - P.E. all suffered interference by the presence of Compound X. Attempts were made to extract Compound X

with 1.4 Dioxan and with n - propanol but no simple single stage method was found. However as the I.C.I. product contains only small quantities of di - P.E. and as Compound X was considered to have the greater effect on the crystallisation of P.E. the analysis was not pursued.

More work is necessary to establish the equilibrium distribution of the impurities in P.E. between the crystals and the mother liquor in aqueous solution. In order to do this it is necessary to obtain equilibrium from a very low initial supersaturation. This was tried by using an ultrasonic probe but the heat generated raised the solution temperature and hence the solubility. Agitation with a stainless steel stirrer was also found to be unsuccessful for low initial supersaturations. A change in the distribution of the impurities at ca. 45°C could possibly account for the unexpected results (shown in fig. 20) with the equilibrium determinations. Also if it is assumed that the impurities distort the crystal lattice somewhat, then this could also account for the slow growth rates found below 45°C in the crystal growth in nucleated solutions (section 6.1.)

Bransom (79) has demonstrated the necessity for a knowledge of the growth kinetics in a fluidised bed for

the design of a classifying crystalliser. The experiments on the fluidised bed apparatus, however, were unsuccessful due to the slow growth rate which was below the limit of resolution of the Coulter Counter size analyser. Also the beds agglomerated when operated at 60 C and above causing channelling. This was thought to be due to the nature of the seed (having small crystallites attached to the parent crystals) even though the voidage was about 0.83. More work is necessary on the preparation of suitable seed for a fluidised bed. The run at 70 C with Batch A (fig. 13) showed negligible crystal growth in 2½h. However if this had obeyed the rate constant obtained from R.20 table 30 d an increase in diameter of the order of 16μ would be expected in the same time. This implies that a large diffusional resistance was present in the fluidised bed tests. The effect of stirrer speed on the growth rate of the "prepared seed" was examined (table 32) and a greater effect was found than on the ordinary Batch A seed (table 23). This effect could either have been due to an increase in seed area because of further attrition at the higher stirrer speeds, and/or the effect of a lower diffusional resistance. Because of the results (table 23) with the Batch A seed which contained less firmly agglomerated crystals than the prepared seed, it was assumed that the effect of stirrer

speed was due to attrition and the diffusional resistance to the growth rate at 500 r.p.m. is very small.

As the errors in the calculations of K from the refractive index estimations were largely self-compensating a main possible source of error was the area determination. Since it was found that after the initial 6 min there was negligible attrition over the first 20 h when stirred at 500 r.p.m. in saturated solution, it was assumed that this was also true during crystal growth tests. However there was no simple method of checking the validity of this assumption. The variation of specific surface with time could only be taken as an indication of the effect of stirrer speed since only one sample was taken for each analysis; whereas, for the specific surface calculation after the initial 6 min attrition an average of 3 samples was taken. It can be seen from fig. 23 that a large source of error is in the "a" and "b" determinations from the graph which would make an appreciable difference to the $\frac{a}{b}$ ratio used in combining the size analyses. This could possibly have been improved by determining the exact thresholds needed on the Coulter Counter to obtain "a" and "b" and averaging many counts at these thresholds. More work is also necessary to widen the Coulter Counter size range. If electrical interferences and atmospheric dust

are carefully screened it should be possible to increase the range to a lower limit of about 0.45μ .

Immersion refractometers have now been obtained with arbitrary scales - 5 to +105 (with facilities to measure to 0.1 units and estimate 0.01 units) equivalent to 0 - 20% Sugar on the refractometers (A and B) used in this work. These will allow smaller concentration changes to be measured with greater accuracy. More work is necessary on the effect of crystal size and stirrer speed on the growth rate. It is planned to build an improved fluidised bed apparatus in which tests can be performed for longer times without agglomerating. It is then hoped to obtain the information necessary for the redesign of the Oslo pilot plant crystalliser and determine the optimum operating conditions.

CONCLUSIONS

1. The morphology change below 200^o C, reported by Berlow et al (48) appears to be, in fact, an eutectic formed between P.E. and traces of di - P.E.
2. The eutectic formed between P.E. and di - P.E. was found to contain 40% m/m di - P.E. and melted at 185.5^o C (c.f. 190^o C with 35% di - P.E. reported by Wyler and Wernet (55)). The di - P.E. used in these tests was analysed by the "Formaldehyde Content" method as containing 1.88% Compound X, which may account for the slightly lower eutectic temperature.
3. The "Formaldehyde Content" analytical method is suitable for the analysis of Compound X in the absence of other formals.
4. A complicated solid/saturated solution equilibrium system exists between P.E. and its associated impurities di - P.E. and Compound X in aqueous solution.
5. The equations of the nucleation curves of P.E. in aqueous soln are:

$$\text{Pure P.E.} \quad : \quad \log_{10} x = 2.289 - \frac{633}{T}$$

$$\begin{array}{l} \text{Batch A (4.73\% Compound X; } < 0.1\% \text{ di - P.E.) } \\ \text{Batch C (4.3\% Compound X; } 1.0\% \text{ di - P.E.) } \end{array} \left. \vphantom{\begin{array}{l} \text{Batch A} \\ \text{Batch C} \end{array}} \right\} \log_{10} x = 3.112 - \frac{545}{T}$$

6. The equations of the equilibrium curves of P.E. in aqueous solution are:

$$\left. \begin{array}{l} \text{Pure P.E. and} \\ \text{Batch A, Batch C} \end{array} \right\} \log_{10} x = 5.072 - \frac{1266}{T} \quad \left. \begin{array}{l} \\ \\ \end{array} \right\} \begin{array}{l} \\ \\ > 50^{\circ} \text{ C} \end{array}$$

7. The growth rate constants \bar{K} obtained for Pure P.E. ($80^{\circ} \text{ C} > T > 50^{\circ} \text{ C}$) were correlated by the equation:

$$\log_{10} \bar{K} = 5.770 - \frac{4025}{T}$$

with an activation energy for growth of 18.4 K cal./g. mole.

8. The growth rate constants \bar{K} obtained for Batch A (4.73% Compound X; < 0.1% di - P.E.) for $80^{\circ} \text{ C} > T > 50^{\circ} \text{ C}$ were correlated by the equation:

$$\log_{10} \bar{K} = 13.401 - \frac{6710}{T}$$

with an activation energy for growth of 30.65 K cal./g. mole.

9. The growth rates of Pure P.E. and Batch A are the same at 77° C but below this temperature the presence of compound X reduces the growth rate.

Appendix

A P P E N D I X A

TABLE 1 : FORMATION OF COMPOUND X

Sample no.	PE (g)	HCHO (g)	Buffer Vol (pH) (cm ³)	Other	Reflux (h)(°C)	Yield (g)	Product	
							%di-PE	% X
8	70	10	8.2 50	2g FeCl ₃	0.75	14	1.1	1.8
9	35	10	water 50		0.5	-		
	+35				0.5	45	<0.1	4.4
10	35	1	water 50		0.5	15	<0.1	4.3
11	70	10	water 50		40	21	0.5	25
12	35	10	50	N.H ₂ SO ₄	1.0 90	-		
	+35		(1.0)		0.5 90	25	0.5	3.8
13	70	10	4.0 50		2.0 90			
					0.5 100	37	<0.1	7.0
14	70	10	5.4 50		0.5	43	<0.1	2.8
15	70	10	8.2 50		1.0	38	<0.1	4.3
16	35	1	(1.0) 50	N.H ₂ SO ₄	1.0 90	25	<0.1	1.0
17	35	1	4.0 50		2.0	25	<0.1	5.6
18	35	1	5.4 50		1.0	19	<0.1	4.9
19	70	10	water 50	2g FeCl ₃	0.75	9	0.4	0.9

TABLE 2 : I.C.I. ANALYSIS OF P.E. BATCHES

BATCH A : BAG 490. M. 214

SAMPLE No.	DATE	%Di-P.E.	%COMPOUND X	AVERAGE COMPOUND X
-	9. 9.65	< 0.1	5.4	4.73
1	19.11.65	-	4.1	
20	10. 2.66	< 0.1	5.2	
23	16. 5.66	-	4.2	
24	16. 5.66	-	4.6	
27	16. 5.66	-	2 x 2.4 4.8	
28	16. 5.66	-	2 x 2.4 4.8	

BATCH B : P. 8

-	-	< 0.1	7.9	?
21	10. 2.66	< 0.1	3.3	?
25	16. 5.66	-	5.0	4.98
26	16. 5.66	-	4.9	
29	16. 5.66	-	2 x 2.4 4.8	
30	16. 5.66	-	2 x 2.6 5.2	

BATCH C

-	-	1.0	4.3	
---	---	-----	-----	--

FIG.4 ELECTROTHERMAL MELTING POINT CALIBRATION

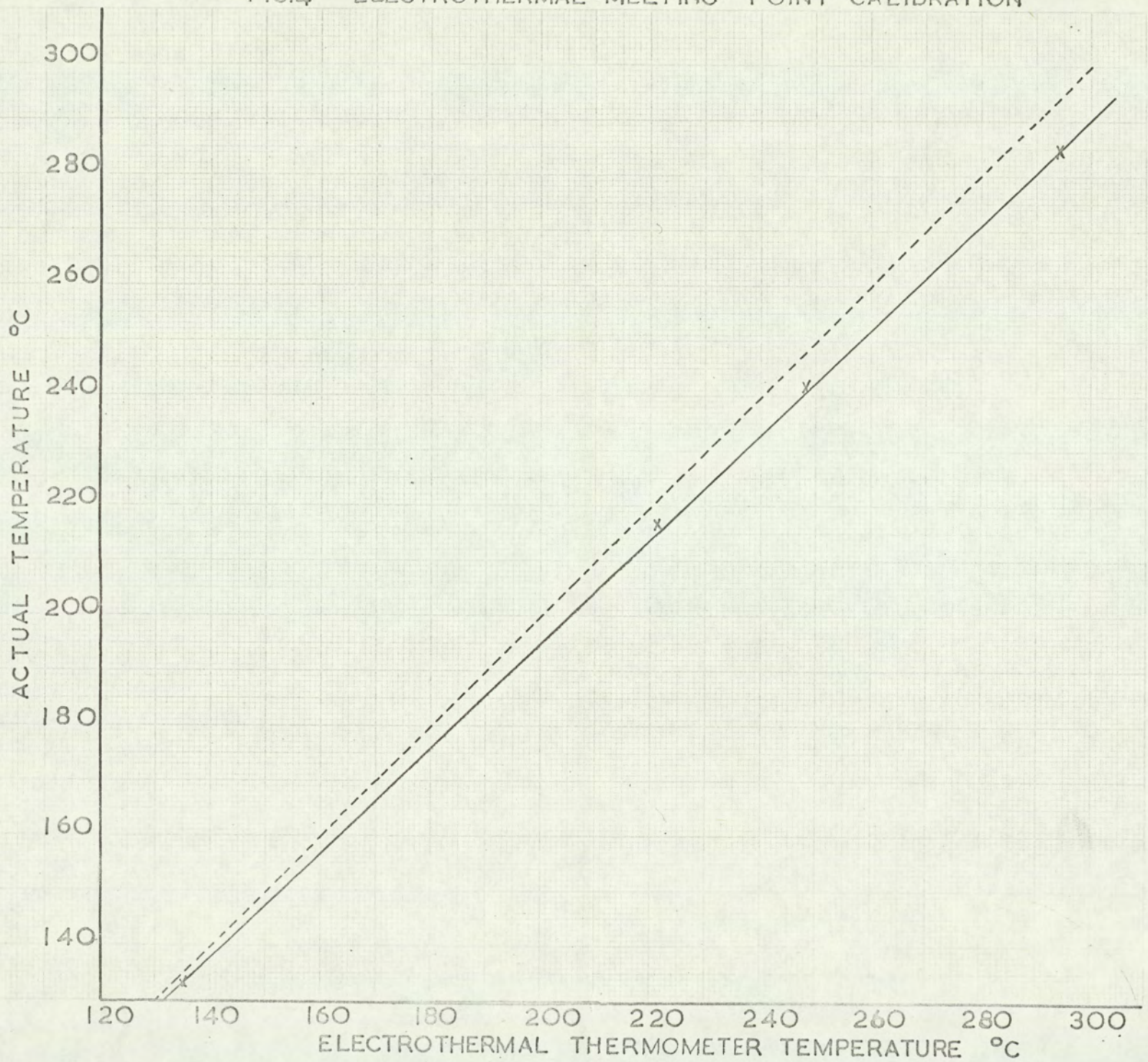


TABLE 3 : MELTING POINTS OF BINARY SYSTEM P.E./Di-P.E.

Composition	Melting temperature (b)	Composition	Melting temperature (b)
Pure P.E.	259°C	P.E. + 36% Di-P.E.	186.5°C
+ 0.1% Di-P.E.	259°C	+ 38% Di-P.E.	186°C
+ 0.5% Di-P.E.	259°C	+ 40% Di-P.E.	185.5°C
+ 1% Di-P.E.	257.5°C	+ 42% Di-P.E.	186.5°C
+ 2% Di-P.E.	255°C	+ 45% Di-P.E.	188°C
+ 5% Di-P.E.	242.5°C	+ 50% Di-P.E.	192.5°C
+ 10% Di-P.E.	224.5°C	+ 60% Di-P.E.	199.5°C
+ 20% Di-P.E.	201°C	+ 80% Di-P.E.	208°C
+ 30% Di-P.E.	187°C	+ 100% Di-P.E.	219.5°C
+ 35% Di-P.E.			

FIG. 5. DI-PE./PE. BINARY MELTING SYSTEM

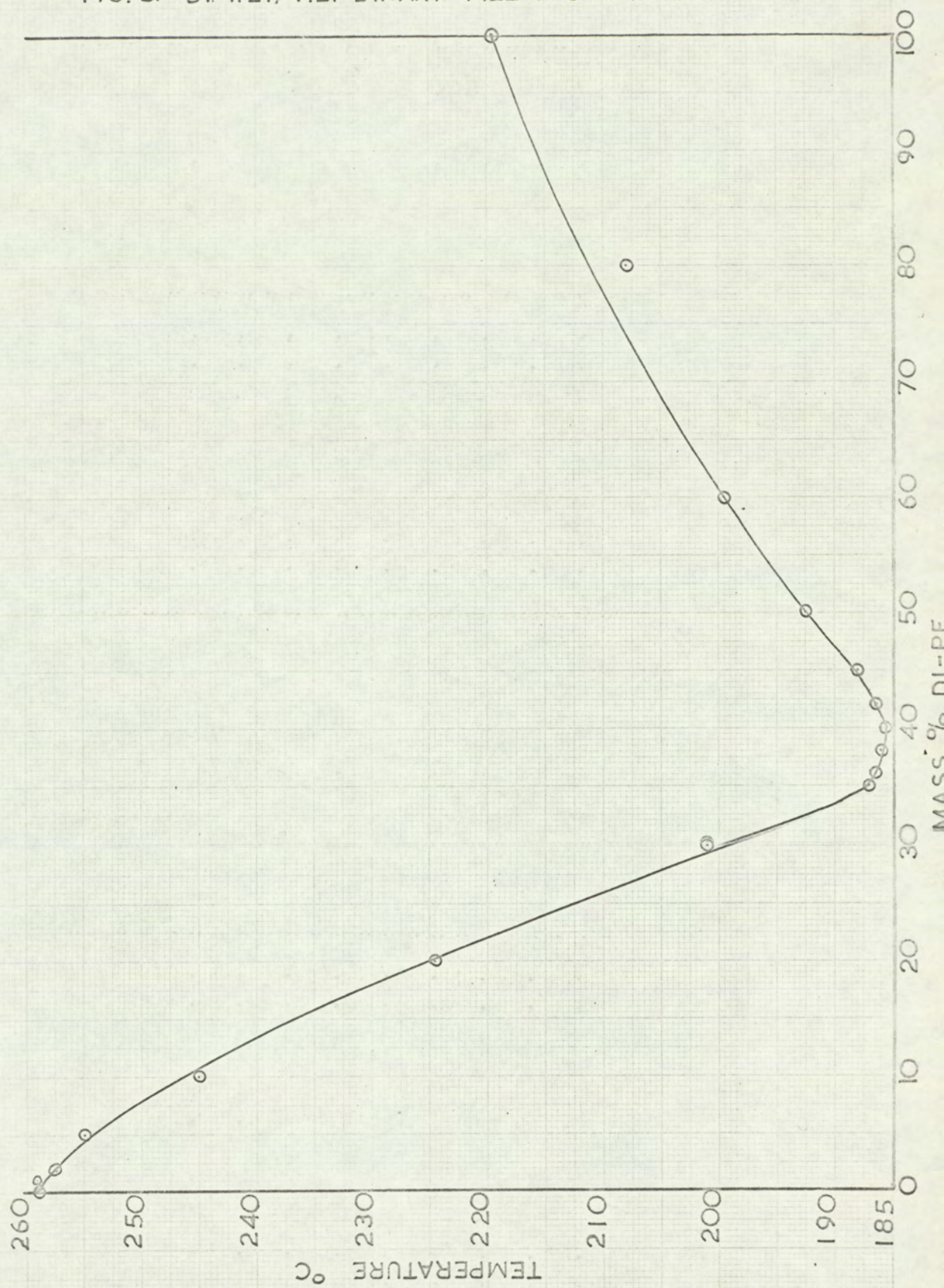


TABLE 4 : MELTING POINTS OF BINARY SYSTEM P.E./
COMPOUND X

Composition	Melting temperature (b)
Pure P.E. + <0.1% CompoundX <0.1% Di-P.E.	259 ^o C
P.E. + 3% Compound X	257 ^o C
P.E. + 6% Compound X	254.5 ^o C
P.E. + 9% Compound X	251.5 ^o C
P.E. + 12% Compound X	247 ^o C
P.E. + 15% Compound X	240.5 ^o C

TABLE 5 : EFFECT OF HEAT ON FORMALDEHYDE
CONTENT ANALYSIS

Sample	Time of sample in oven at 90 ^o C
66 1 P.E. + 4.73% Comp $\frac{1}{2}$ X	$\frac{1}{2}$ hour
2 Reagent Blank	$\frac{1}{2}$ hour
3 P.E. + 4.73% Comp. X	1 hour
4 Reagent Blank	1 hour
5 P.E. + 4.73% Comp.X	2 hours
6 Reagent Blank	2 hours
7 P.E. + 4.73% Comp. X	4 hours
8 Reagent Blank	4 hours
9 P.E. + 4.73% Comp. X	5 hours
10 Reagent Blank	5 hours
11 P.E. + 4.73% Comp. X	6 hours
12 Reagent Blank	6 hours

FIG. 6
P.E./COMPOUND X BINARY MELTING SYSTEM

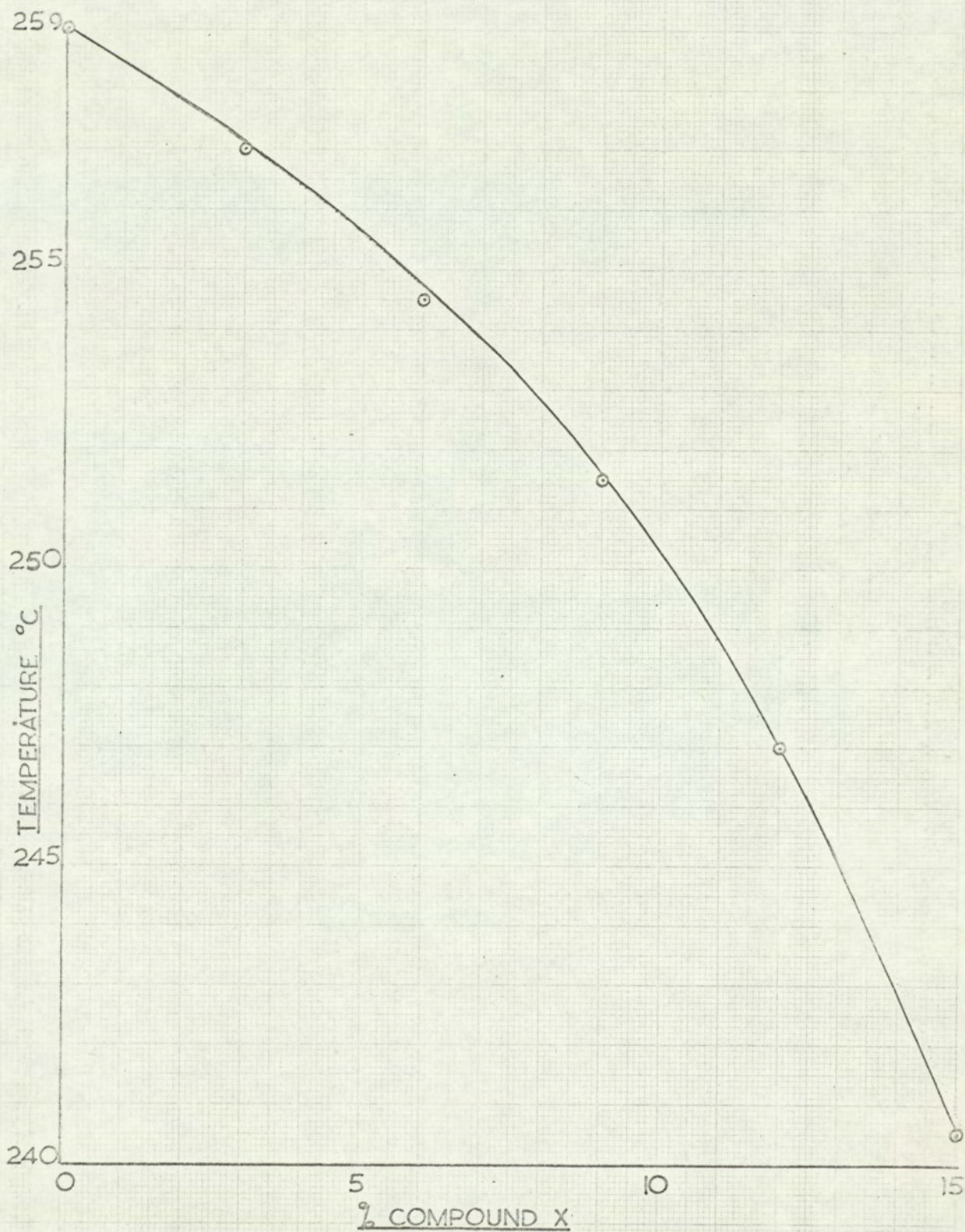


TABLE 5A : COMPARISON OF OPTICAL DENSITIES OF TABLE 5

Comparison	Optical Density	Comparison	Optical Density
1 and 2	0.210		
3 and 4	0.290	3 and 2	0.280
5 and 6	0.275	5 and 2	0.330
7 and 8	0.263	7 and 2	0.405
9 and 10	0.222	9 and 2	0.390
11 and 12	0.195	11 and 2	0.400

TABLE 6 : CALIBRATION OF SPEKKER

Formaldehyde concentration (mg/ml solution)	Optical Density ($\lambda = 570m\mu$ $\frac{1}{2}$ cm cell)
0.005	0.020
0.010	0.040
0.020	0.070
0.030	0.118
0.040	0.142
0.050	0.118
0.060	0.202
0.070	0.240
0.080	0.278
0.090	0.298

FIG. 7

SPEKKER ABSORPTIOMETER FORMALDEHYDE CALIBRATION

$\lambda = 570 m\mu$ $\frac{1}{2}$ cm cell

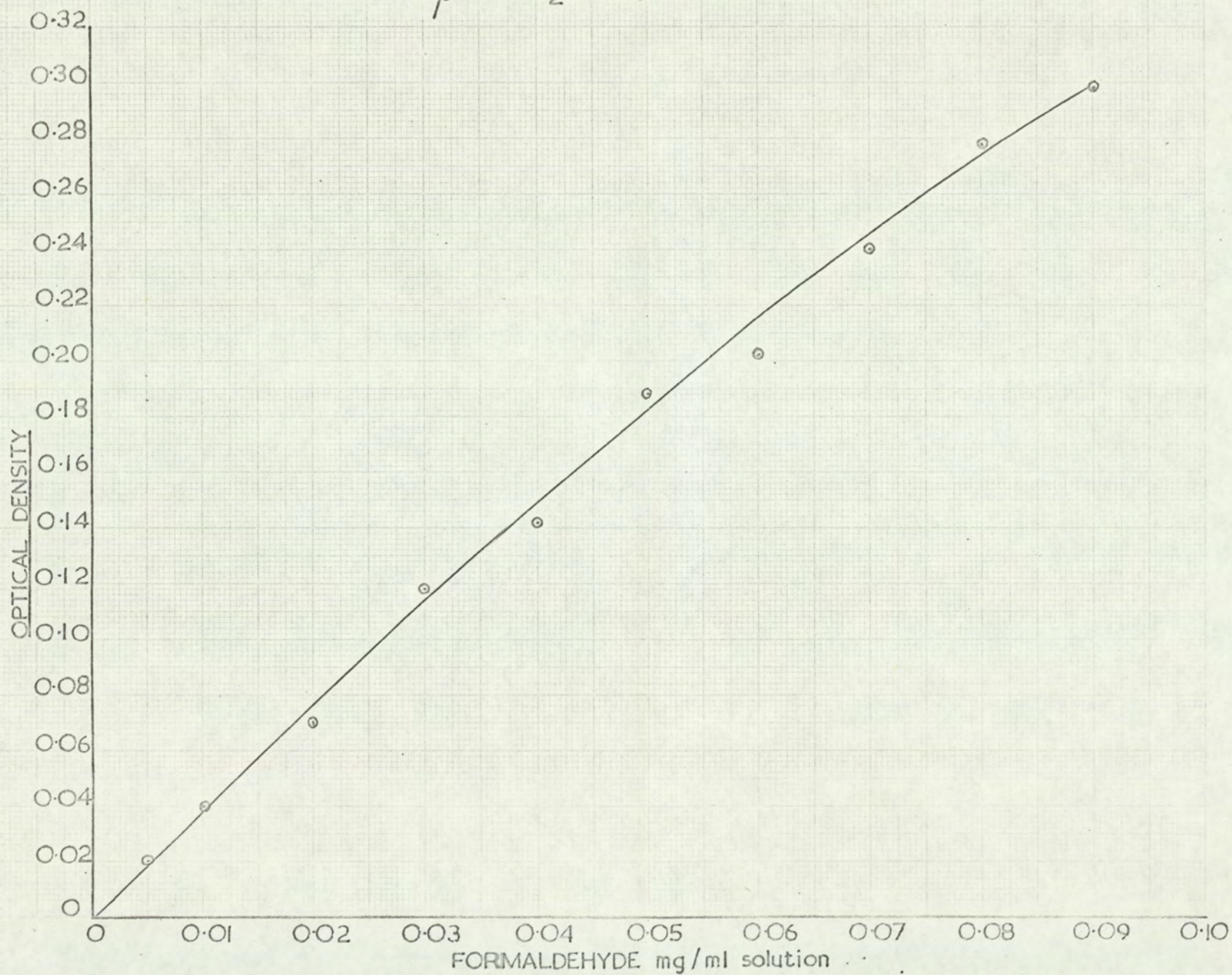
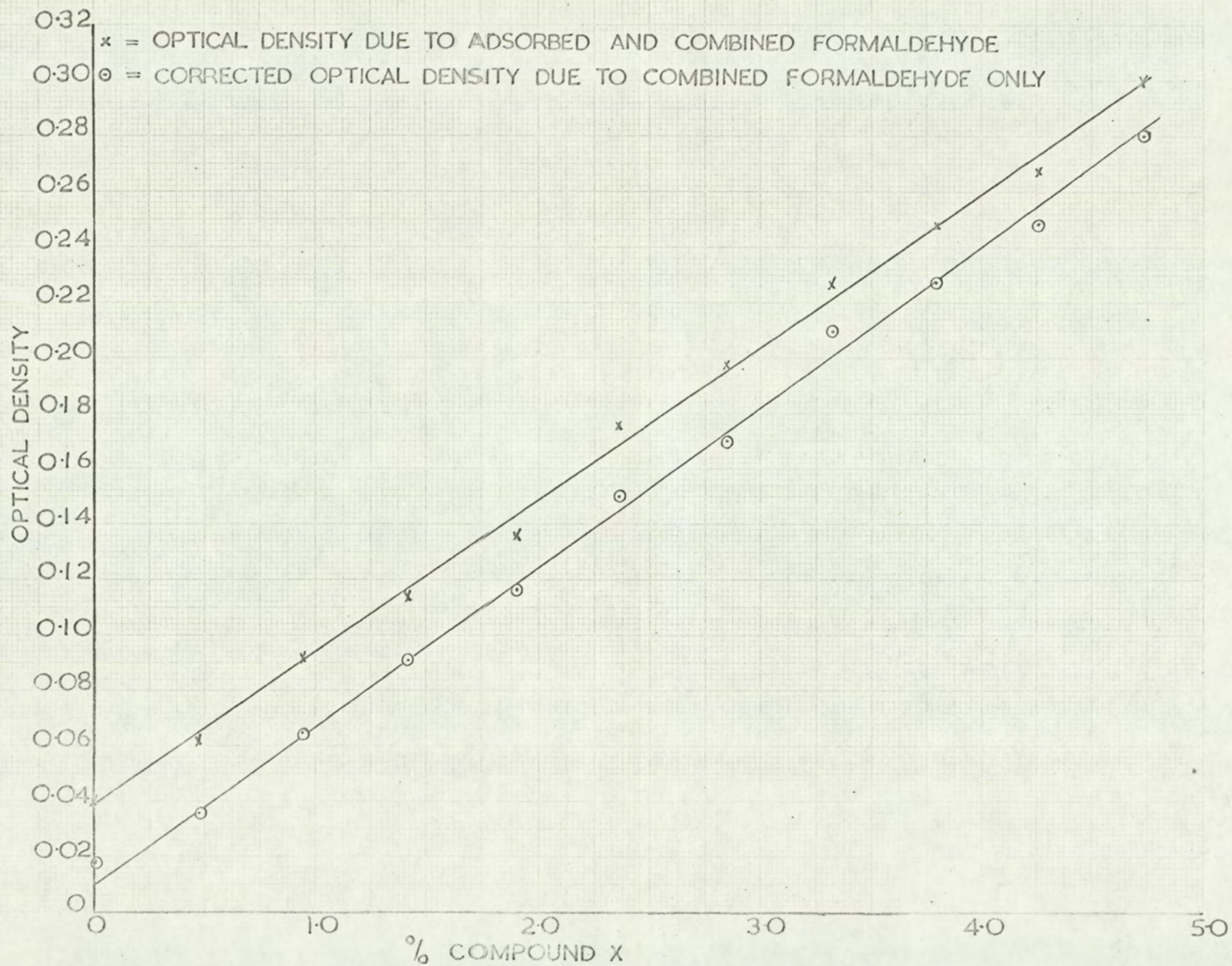


TABLE 7 : SPEKKER ABSORPTIOMETER - $\lambda = 570 \text{ m}\mu$ $\frac{1}{2}$ cm. cell

	Optical Density	Adsorbed HCHO mg./ml.	Corrected Optical Density
Pure P.E.	0.040	0.0054	0.018
P.E. + 0.47% Compound X	0.064	0.0066	0.036
P.E. + 0.94% "	0.092	0.0072	0.065
P.E. + 1.42% "	0.114	0.0060	0.091
P.E. + 1.89% "	0.136	0.0048	0.117
P.E. + 2.36% "	0.176	0.0075	0.150
P.E. + 2.84% "	0.198	0.0075	0.171
P.E. + 3.32% "	0.228	0.0051	0.210
P.E. + 3.79% "	0.248	0.0063	0.227
P.E. + 4.26% "	0.268	0.0060	0.248
P.E. + 4.73% "	0.300	0.0061	0.280

FIG. 8

SPEKKER ABSORPTIOMETER COMPOUND X CALIBRATION. $\lambda=570m\mu$ $\frac{1}{2}$ cm cell



A P P E N D I X B

manuscript

COULTER COUNTER DATA

Aqueous
0.9/NaCl +
8.5/Pure
ELECTROLYTE P.E.

TABLE 8 SAMPLE L.1 BEFORE GROWTH AT 70°C SOURCE BATCH A "PREPARED SEED"

GAIN INDEX	t'	l	F	VOLUME						n'' = $P\left(\frac{\bar{n}'}{1000}\right)^2$	APERTURE RESISTANCE	n = $\bar{n}' + n'' - \checkmark$	t = t'(F)	d = $k\sqrt[3]{t}$	CUM NO% OVERSIZE
				n'	n'	n'	n'	n'	n'						
			280	MANOMETER	2.0 ml.	COINCIDENCE	13.72							18.8	
				DIAMETER											
				Ultrasonics											
				DISPERSANT + TEMPERATURE											
				Nonidet P.40											
							8.71								
3	150	1	1.00000	2	2	2	2	2	0	2	0	150	100	0.20	
3	90	1	1.00000	2	2	2	2	2	0	2	0	90	84.2	7.89	
3	60	1	1.00000	8	6	17	10	0	0	2	8	60	73.5	29.8	
3	60	2	0.50074	229	159	544	311	1	1	2	310	30.0	58.4	44.6	
3	60	3	0.25100	874	545	2046	1155	18	18	2	1171	15.1	46.4	56.4	
3	60	4	0.12612	1276	762	3110	1716	40	40	3	1753	7.57	36.9	66.8	
3	60	5	0.06369	1585	842	4046	2158	64	64	4	2218	3.82	29.4	80.2	
3	60	6	0.03250	1857	1036	4732	2542	89	89	4	2627	1.95	23.5	91.0	
3	60	7	0.01688	2177	1182	5735	3031	126	126	10	3147	1.012	18.9	100	
3	60	8	0.00910	2596	1335	6360	3430	161	161	14	3577	0.546	15.4		
3	60	9	0.00524	2877	1515	6869	3754	192	192	16	3930	0.315	12.8		
3	60	10	0.00337	2789	1485	6230	3501	168	168	32	3637	0.202	11.0		

COULTER COUNTER DATA

Aqueous
0.9/NACL +
ELECTROLYTE 8.5/Pure
P.E.
CALIBRATION 18.8

TABLE 9 SAMPLE M.L. AFTER GROWTH AT 70°C SOURCE BATCH A "PREPARED SEED"

APERTURE 280 μ MANOMETER 2.0 ml. COINCIDENCE 13.72 FACTOR (P) 18.8
DIAMETER Ultrasonics VOLUME FACTOR (K)

DISPERSANT + TEMPERATURE 21.0°C APERTURE RESISTANCE 8.71 KΩ NOTES

GAIN INDEX	t'	F	n'	n'	n'	n'	n'	n'	n'' = $P\left(\frac{\bar{n}'}{1000}\right)^2$	n = $\bar{n}' + n'' - \sqrt{\quad}$	t = t'(F)	d = $k\sqrt[3]{t}$	CUM NO% OVERSIZE
3	210	1.00000	2	3	9	5	0	2	3	210	112	0.04	
3	150	1.00000	3	3	21	9	0	2	7	150	100	0.09	
3	90	1.00000	14	19	121	51	0	2	49	90	84.2	0.67	
3	60	1.00000	51	147	435	211	1	2	210	60	73.5	2.87	
3	60	0.50074	271	1076	1538	962	13	2	973	30.0	58.4	13.3	
3	60	0.25100	421	2588	2669	1893	49	2	1940	15.1	46.4	26.5	
3	60	0.12612	645	4320	3910	2958	120	3	3075	7.57	36.9	42.0	
3	60	0.06369	854	6384	5159	4132	234	4	4362	3.82	29.4	59.5	
3	60	0.03250	1016	8283	5770	5023	346	4	5365	1.95	23.5	73.3	
3	60	0.01688	1320	9970	6470	5920	481	10	6391	1.012	18.9	87.2	
3	60	0.00910	1520	11380	7280	6727	621	14	7334	0.546	15.4	100	
3	60	0.00524	1614	11320	6903	6612	598	16	7194	0.315	12.8		

FIG. 9

SIZE ANALYSIS AFTER BATCH CRYSTALLISATION

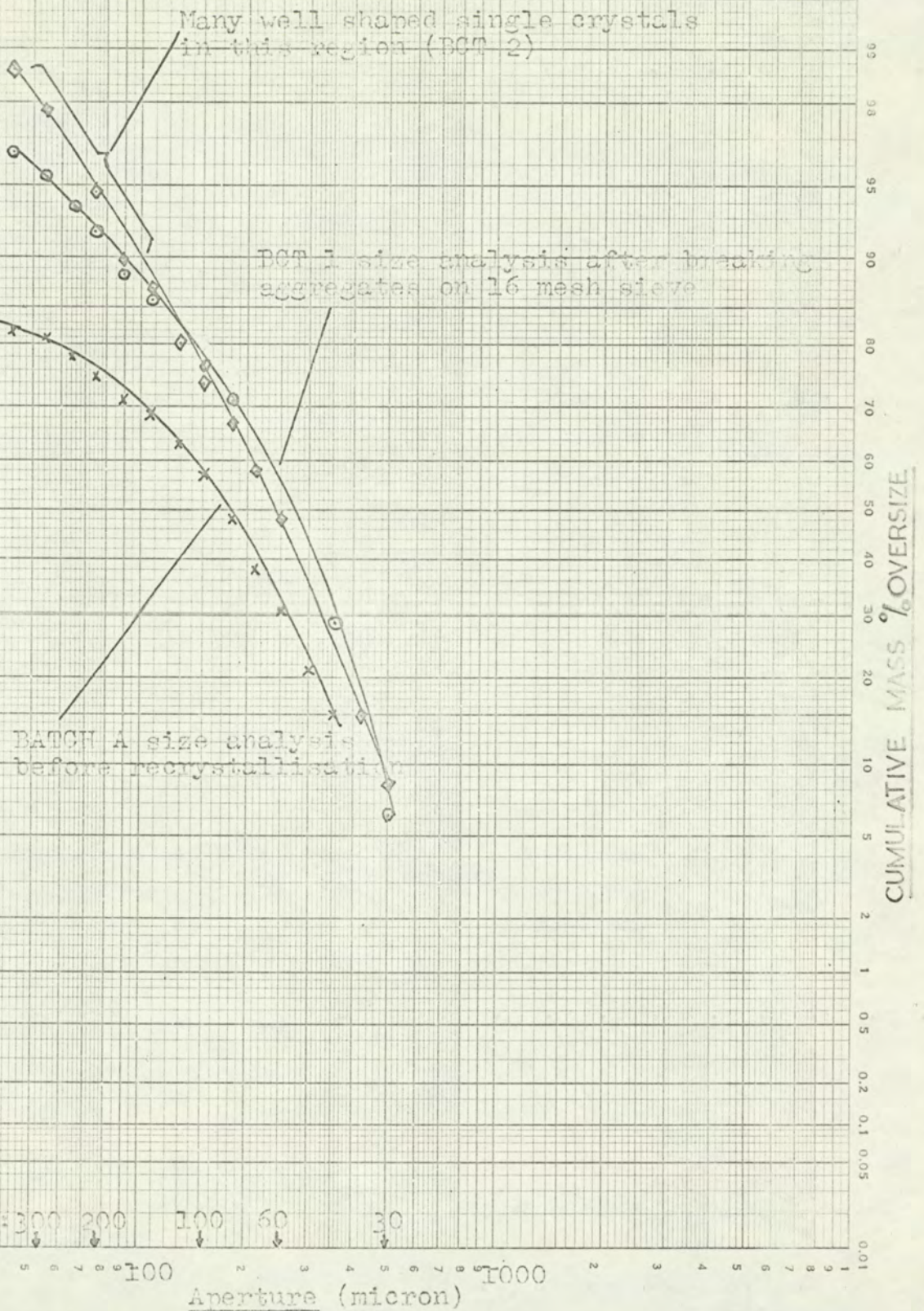


FIG. 12. Theoretical Fluidisation and Transport Velocities for Spheres (Monodisperse)

$\rho_s = 1.4 \text{ (g/cm}^3\text{)}$
 $\rho = 1.0 \text{ (g/cm}^3\text{)}$
 $\mu = 0.01 \text{ (P)}$

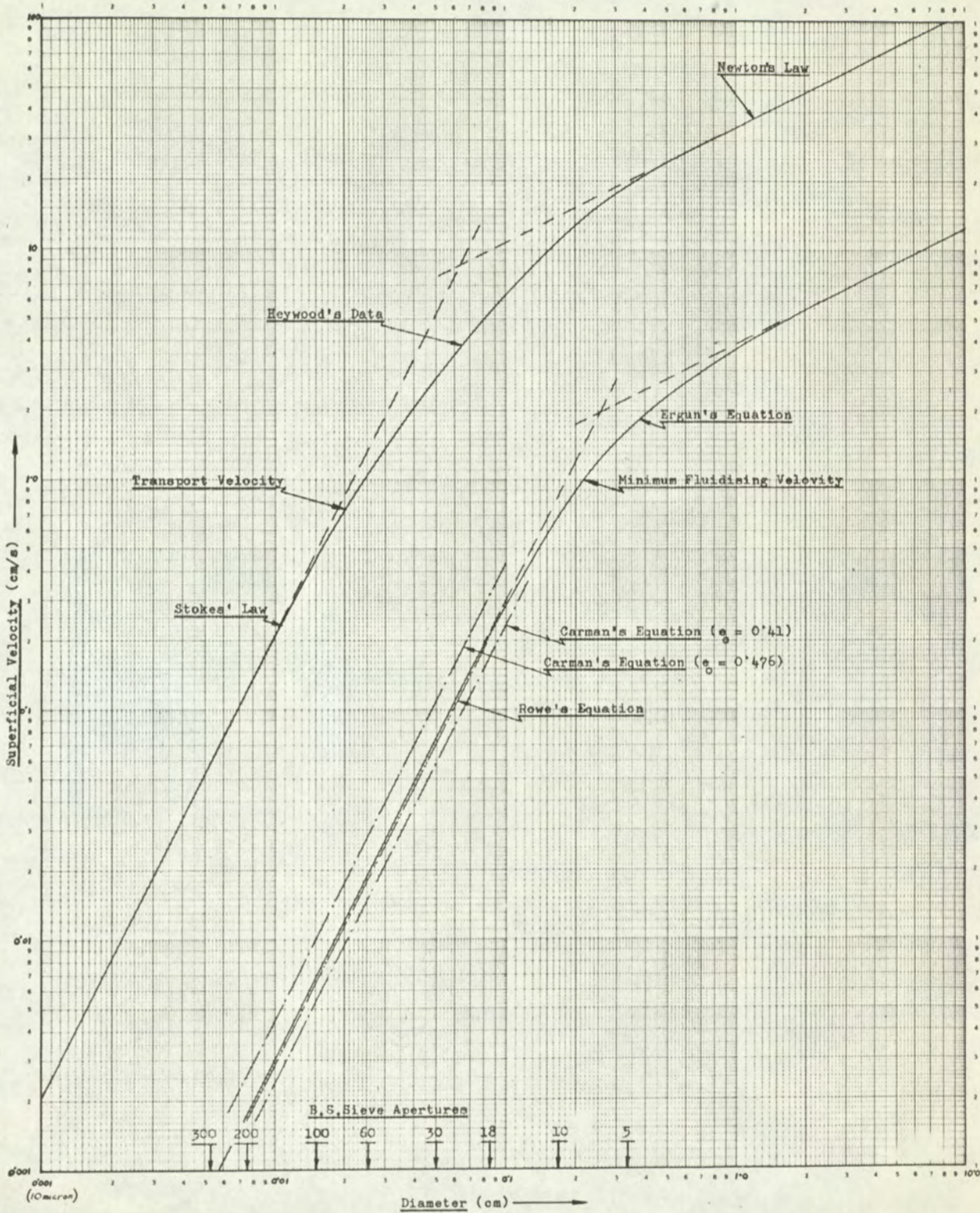
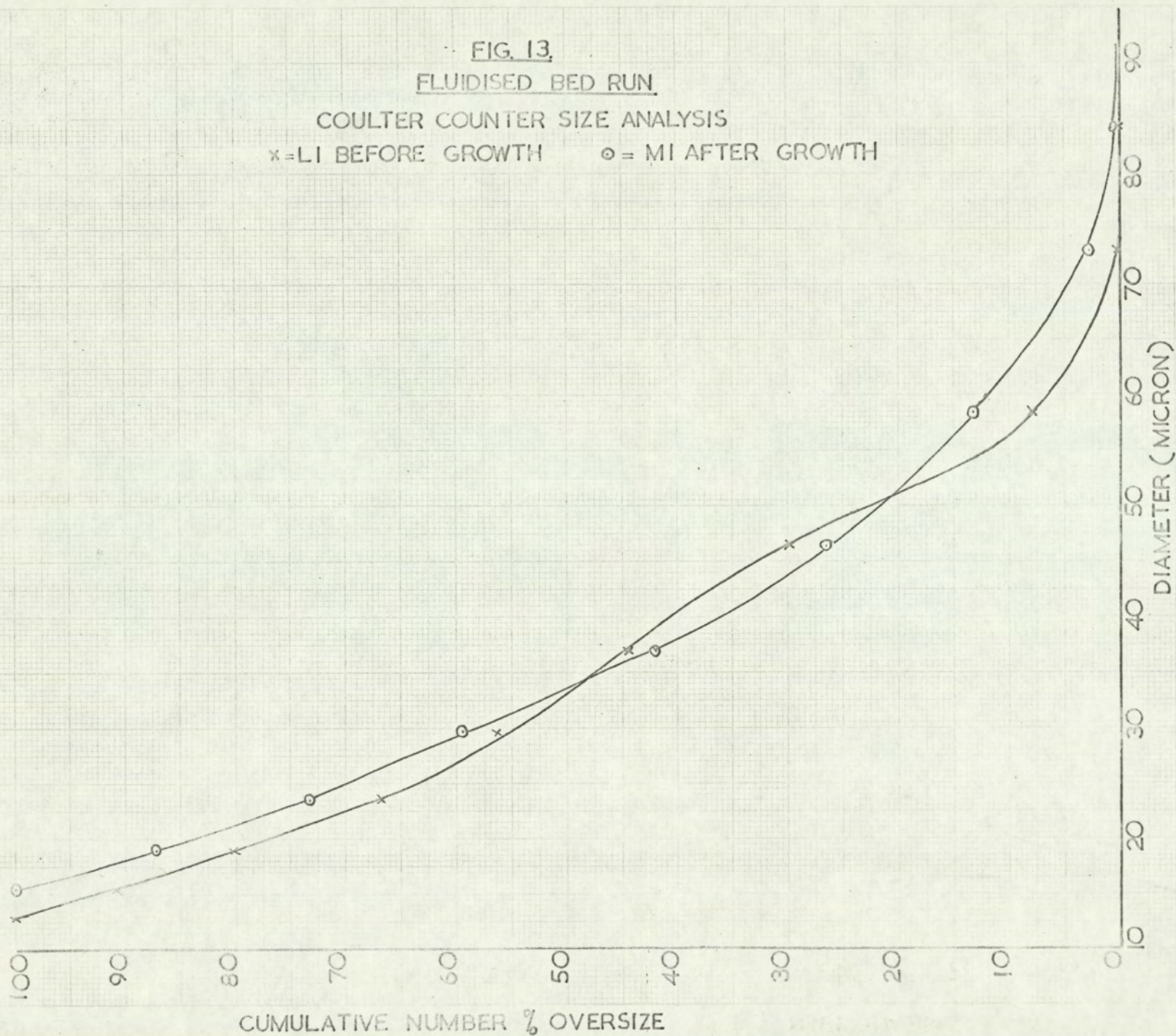


FIG. 13.
 FLUIDISED BED RUN
 COULTER COUNTER SIZE ANALYSIS
 x = LI BEFORE GROWTH ○ = MI AFTER GROWTH



A P P E N D I X C

aftercopy

APPENDIX C - COULTER COUNTER

C.1. Operation

It has been shown in Section 4.3.2. that for a given suspension the response of the Coulter Counter is proportional to particle volume provided the diameter of the particle does not exceed 40% of the aperture diameter. For each sample analysis a suitable orifice tube was chosen for the Coulter Counter so that the size range of particles in the sample would be within about 1½% to 40% of the aperture diameter. A small amount of sample (about 0.01g) was placed in about 250 mls of electrolyte previously filtered with a 0.45 μ porosity membrane filter. A few drops of non-ionic dispersant (NONIDET P40) were added and an ultrasonic probe operating at 20 Kc/s was immersed in the suspension for about one minute. This method of dispersion was compared in preliminary tests with (a) Violent agitation of the suspension and (b) mixing the sample with NONIDET P40 in the bottom of a beaker using a fine-haired paint brush. The ultrasonic method was found to give the most consistent results and was the easiest to apply. It was found to disperse loosely formed agglomerates but did not break up firmly held agglomerates formed during growth.

The suspension was then analysed by sucking successive equal volumes through the orifice at preset

threshold levels. After each count the reset switch was depressed which zeroed the counting units and changed the polarity of the electrodes to prevent excess polarization. For each threshold level an average of a number of counts was taken depending on the statistical variation. The suspension was stirred during the analysis to keep the particles in suspension. It was found that when the 50 μ tube was used the instrument had to have extra shielding from all external electrical devices such as stirrer motors to prevent interference at the more sensitive threshold levels.

C.2. Electrolyte

As P.E. is soluble in water a non-aqueous electrolyte was sought. The solvent would have to have a high dielectric constant to cause a dissolved salt to dissociate into ions and also be miscible with water to allow the analysis of aqueous suspensions. However no suitable non-aqueous electrolyte was found in which P.E. was completely insoluble. The most suitable non-aqueous electrolyte found was 4% Ammonium Thiocyanate in Isopropanol in which the solubility of Pure P.E. was 0.475 g/100g I.P.A. at 25^oC. It was therefore necessary to use a saturated solution for either aqueous or non-aqueous electrolyte. As the Isopropanol electrolyte required less P.E. than aqueous electrolytes, this was

first used saturated with P.E. at 25^oC. However this was found unsatisfactory because:-

- a) The thin film of liquid formed on the beaker walls above the solution during an analysis quickly evaporated forming crystals which dropped into the suspension being analysed.
- b) The change in solution strength due to evaporation during analysis altered the electrolyte calibration.
- c) A larger difference of the calibration constant K with temperature was found than with the 0.9% NaCl aqueous electrolyte.
- d) Air bubbles were easily formed when the electrolyte was passed through the 560 μ tube and these were counted as particles.

Consequently an aqueous electrolyte was used of 0.9 g NaCl/100 g H₂O and 8.5 g Pure P.E./100 g H₂O. This was such that the solution was saturated with P.E. at 25^oC and the small degrees of supersaturation involved during an analysis at room temperature would not effect the particle size during the short time required for analysis.

C.3. Coincidence

The possibility that two or more particles are in the sensing zone at the same time leads to what is called

coincidence error. This can be of two forms primary and secondary coincidence. Primary coincidence is the loss of count which results from only one pulse being generated for the passage of two or more particles.. Secondary coincidence is the counting of a particle whose size is the sum of two or more particles. For secondary coincidence caused by a doublet a narrow size range of both particles is required; i.e. two particles larger than 8 microns diameter are needed to give a count equivalent of 10 microns diameter. Also close proximity of the particles is required. So secondary coincidence is negligible for the low concentration used and primary coincidence correction only was required.

The primary coincidence correction is the addition of a number of n^{11} to the actual count n^1 . If the coincidence level lies between 1% and 10% i.e. $0.01 n^1 < n^{11} < 0.1 n^1$.

$$\text{Then } n^{11} = P \left(\frac{n^1}{1000} \right)^2$$

Where the coincidence factor P is obtained from the formula.

$$P = 2.5 \left(\frac{D}{100} \right)^3 \left(\frac{500}{V} \right)$$

where D is the aperture diameter in microns, and V is the metering manometer volume in microlitres. The factor 2.5 was obtained experimentally by Coulter

Electronics Limited using a 100 micron aperture and a 500 microlitre manometer volume at successive dilutions of counting on a mono-sized system. In order to avoid exceeding the 10% coincidence level n^1 must be less than $\frac{10^5}{P}$.

ORIFICE DIAMETER MICRONS	MANOMETER MLS.	COINCIDENCE FACTOR	MAXIMUM COUNT FOR 10% COINCIDENCE
560	2	109.76	910
280	2	13.72	7,288
50	0.5	0.3125	320,000
50	0.05	3.125	32,000

C.4. Calibration

The calibration factor, K, is used for conversion of threshold settings to particle volumes, or their cube roots to equivalent spherical diameters. The calibration factor is constant for a given aperture diameter and electrolyte resistivity.

A quantity of monosized particles, between 5% and 20% of the orifice diameter, such that the count obtained did not give more than 2% coincidence was dispersed in the electrolyte. The suspension was drawn through the

orifice with the threshold dial set on zero and the amplifier gain index on 3. The aperture current switch was adjusted to a value I^* where the pulses on the oscilloscope occupied about one quarter of the screen height. The threshold dial t was varied until the shadow line coincided with the height of the majority of pulses, and a count taken. Counts were taken at $\frac{1}{2} t^1$ and $1\frac{1}{2} t^1$ and averaged. The threshold value t^* was found by trial and error which corresponded to the average of $\frac{1}{2} t^*$ and $1\frac{1}{2} t^*$.

The aperture resistance was measured by measuring the voltage, V between the outer electrode and earth, and calculating the aperture resistance from $R = \frac{r \times V}{300 - V}$ ohms where r is the resistance of the aperture current switch in the position used. Values of r are:-

Aperture Current Setting	r (ohms)
10	65,000
9	115,000
8	215,000
7	415,000
6	815,000

From the Scale Expansion Factor, 'F', tables supplied by Coulter Electronics, F was found for this aperture resistance at current setting I and on Gain 3.

The Calibration factor K was then found from $K = d / (t^1 F)^{1/3}$ where d was the diameter of the monosized particles. The diameter corresponding to any threshold level t^1 can then be calculated from $d = K(\sqrt[3]{t^1 F})$. The appropriate interpolated 'F' values for particular current settings on Gain 3 are shown in the following pages tables 14, 15 and 16. For each consecutive lower gain index the F factor was multiplied by $\sqrt{2}$. Similarly for each consecutive higher gain index the F factor was divided by $\sqrt{2}$.

As the electrolyte resistivity changed with temperature the F factors are shown for the aperture resistances encountered and the calibrations were done over the temperature range expected.

For each size analysis thereafter the temperature of the electrolyte was taken and so the calibration known. The chart showing the Coulter Counter Data representation is shown on Table 10. The first three columns show the threshold settings. Column four shows the Scale Expansion Factors F for the particular gain index and aperture current. The product of this and the threshold setting t^1 gives the relative particle volume \mathcal{V} , column 12. Then using the calibration factor K, the diameter for this threshold is found from $d = K\sqrt[3]{\mathcal{V}}$ column 13. The average of a number of counts, n^1 , is taken above this

diameter, and is shown for three different samples columns 5, 6 and 7. The average of these readings \bar{n}^1 is taken column 8, and the coincidence error n^{11} calculated. The size analysis of particles present in the electrolyte as background count is shown column 10 and the count \bar{n}^1 then corrected by $n = \bar{n}^1 + n^{11} - \sqrt{\quad}$ Column 11. Finally the number percentage greater than d is calculated (Column 14).

TABLE 10
COULTER COUNTER DATA

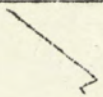
SAMPLE	APERTURE DIAMETER	MANOMETER VOLUME	TEMPERATURE	SOURCE	COINCIDENCE FACTOR (P)	ELECTROLYTE	CALIBRATION FACTOR (K)	NOTES	CUM NO% OVERSIZE	
										APERTURE RESISTANCE
GAIN INDEX									1	AMPLIFIER GAIN SETTING
	t'								2	THRESHOLD DIAL SETTING
	1								3	APERTURE CURRENT SETTING
	F								4	SCALE EXPANSION FACTORS
	n'								5	RAW COUNTS SAMPLE 1
	n'								6	RAW COUNTS SAMPLE 2
	n'								7	RAW COUNTS SAMPLE 3
	\bar{n}								8	AVERAGE OF RAW COUNTS
	$n'' = P \left(\frac{\bar{n}'}{1000} \right)^2$								9	COINCIDENCE CORRECTION
									10	BACKGROUND COUNT ON BLANK ELECTROLYTE
	$n = \bar{n}' + n'' - \sqrt{\dots}$								11	CORRECTED COUNT
	t								12	RELATIVE PARTICLE VOLUME
	d = $\frac{t}{k \sqrt[3]{t}}$								13	PARTICLE DIAMETER
									14	CUMULATIVE NUMBER % ABOVE STATED SIZE

TABLE 11 - CALIBRATION 50 μ TUBE

ELECTROLYTE : 0.9g NaCl/100g H₂O + 8.5g Pure P.E./100g H₂O

MONOSIZED PARTICLES : PUFF BALL SPORES $d = 3.62 \mu$

I* = 5 t* = 54 at 15°C to 25°C

Temp. °C	14	15	16	17	18	19	20	21	22	23	24	25
Voltage	53	52	51	50	50	49	48	47	46	46	45	44
I : 8	:	:	:	:	:	:	:	:	:	:	:	:
Resistance:	46.1	45.1	44.1	43.1	43.1	42.0	40.9	40.0	39.0	39.0	38.0	36.9
K _u	:	:	:	:	:	:	:	:	:	:	:	:
F ₅	:006616:	:006610:	:006604:	:006598:	:006598:	:006592:	:006586:	:006580:	:006574:	:006574:	:006568:	:006562
K	2.37:	2.37:	2.37:	2.37:	2.37:	2.37:	2.37:	2.37:	2.37:	2.37:	2.37:	2.37
:	:	:	:	:	:	:	:	:	:	:	:	:
:	:	:	:	:	:	:	:	:	:	:	:	:
:	:	:	:	:	:	:	:	:	:	:	:	:
:	:	:	:	:	:	:	:	:	:	:	:	:

TABLE 12

CALIBRATION 280 μ TUBE

ELECTROLYTE : 0.9g NaCl/100g H₂O + 8.5g Pure P.E./100g H₂O

MONOSIZED PARTICLES : LYCOPODIUM POWDER d = 28.0 μ

I* = 5 t* = 52 at 14°C to 25°C

Temp. °C	14	15	16	17	18	19	20	21	22	23	24	25
Voltage	12.7	12.6	12.4	12.3	12.1	12.0	11.8	11.7	11.5	11.4	11.3	11.1
I = 8	:	:	:	:	:	:	:	:	:	:	:	:
Resistance	9.53	9.43	9.28	9.20	9.04	8.96	8.78	8.71	8.56	8.48	8.41	8.26
K _a	:	:	:	:	:	:	:	:	:	:	:	:
F ₅	006376	006375	006374	006373	006372	006371	006370	006369	006368	006368	006367	006365
K	18.8	18.8	18.8	18.8	18.8	18.8	18.8	18.8	18.8	18.8	18.8	18.8

22

TABLE 13

CALIBRATION 560 μ TUBE

ELECTROLYTE : 0.9g NaCl/100g H₂O + 8.5g Pure P.E./100g H₂O

MONOSIZED PARTICLES : LYCOPODIUM POWDER d = 28.0 μ

I* = 9 t* = 36 at 14°C to 25°C

	14	15	16	17	18	19	20	21	22	23	24	25
Temp. °C	:	:	:	:	:	:	:	:	:	:	:	:
Voltage, I = 8	8.8	8.6	8.4	8.3	8.1	8.0	7.8	7.7	7.5	7.4	7.3	7.2
Resistance, K _a	6.50	6.35	6.20	6.13	5.97	5.90	5.74	5.65	5.50	5.44	5.36	5.28
F ₉	000507	000505	000504	000503	000502	000501	000499	000498	000497	000496	000496	000495
K	49.4	49.5	49.5	49.5	49.5	49.5	49.6	49.6	49.6	49.6	49.6	49.7

TABLE 14.

COULTER COUNTER 'F' SCALE EXPANSION FACTORS - FOR USE WITH 50 μ TUBE

Resistance K Ω	37	38	39	40	41	42	43	44	45	46	47
F ₁	1.00000	1.00000	1.00000	1.00000	1.00000	1.00000	1.00000	1.00000	1.00000	1.00000	1.00000
F ₂	0.50200	0.50200	0.50200	0.50200	0.50200	0.50200	0.50200	0.50200	0.50200	0.50200	0.50200
F ₃	0.25240	0.25260	0.25280	0.25300	0.25300	0.25300	0.25300	0.25300	0.25300	0.25300	0.25300
F ₄	0.12782	0.12788	0.12794	0.12800	0.12806	0.12812	0.12818	0.12824	0.12830	0.12836	0.12842
F ₅	0.06562	0.06568	0.06574	0.06580	0.06586	0.06592	0.06598	0.06604	0.06610	0.06616	0.06622
F ₆	0.03452	0.03458	0.03464	0.03470	0.03476	0.03482	0.03488	0.03494	0.03500	0.03506	0.03512
F ₇	0.01899	0.01906	0.01913	0.01920	0.01927	0.01934	0.01941	0.01948	0.01954	0.01960	0.01966
F ₈	0.01139	0.01146	0.01154	0.01161	0.01169	0.01176	0.01183	0.01191	0.01198	0.01205	0.01212
F ₉	0.00782	0.00791	0.00800	0.00809	0.00818	0.00827	0.00836	0.00845	0.00854	0.00863	0.00872
F ₁₀	0.00655	0.00667	0.00679	0.00691	0.00703	0.00715	0.00727	0.00739	0.00751	0.00763	0.00775

118

INTERPOLATED FROM COULTER ELECTRONICS LTD. DATA.

TABLE 15

COULTER COUNTER 'F' SCALE EXPANSION FACTORS - FOR USE WITH 280 μ TUBE

Resistance K Ω	9.5	9.4	9.3	9.2	9.1	9.0	8.9	8.8	8.7	8.6	8.5	8.4	8.3	8.2
F ₁	1.00000	1.00000	1.00000	1.00000	1.00000	1.00000	1.00000	1.00000	1.00000	1.00000	1.00000	1.00000	1.00000	1.00000
F ₂	0.50090	0.50088	0.50086	0.50084	0.50082	0.50080	0.50078	0.50076	0.50074	0.50072	0.50070	0.50068	0.50066	0.50064
F ₃	0.25100	0.25100	0.25100	0.25100	0.25100	0.25100	0.25100	0.25100	0.25100	0.25100	0.25100	0.25100	0.25100	0.25100
F ₄	0.12617	0.12616	0.12615	0.12615	0.12614	0.12614	0.12613	0.12612	0.12612	0.12611	0.12611	0.12610	0.12610	0.12609
F ₅	0.06376	0.06375	0.06374	0.06373	0.06372	0.06372	0.06371	0.06370	0.06369	0.06368	0.06368	0.06367	0.06366	0.06365
F ₆	0.03256	0.03255	0.03254	0.03253	0.03253	0.03252	0.03251	0.03251	0.03250	0.03249	0.03248	0.03247	0.03246	0.03245
F ₇	0.01695	0.01694	0.01693	0.01693	0.01692	0.01691	0.01690	0.01689	0.01688	0.01687	0.01687	0.01686	0.01685	0.01684
F ₈	0.00916	0.00915	0.00914	0.00913	0.00912	0.00912	0.00911	0.00910	0.00910	0.00909	0.00908	0.00907	0.00906	0.00905
F ₉	0.00530	0.00529	0.00528	0.00528	0.00527	0.00526	0.00525	0.00524	0.00524	0.00523	0.00522	0.00521	0.00520	0.00520
F ₁₀	0.00345	0.00344	0.00343	0.00342	0.00341	0.00340	0.00339	0.00338	0.00337	0.00336	0.00335	0.00334	0.00333	0.00332

INTERPOLATED FROM COULTER ELECTRONICS LTD. DATA.

TABIE 16.

COULTER COUNTER 'F' SCALE EXPANSION FACTORS - FOR USE WITH 560 μ TUBE

Resistance K _a	5.2	5.3	5.4	5.5	5.6.	5.7	5.8	5.9	6.0	6.1	6.2	6.3	6.4	6.5
	F ₁	1.00000	1.00000	1.00000	1.00000	1.00000	1.00000	1.00000	1.00000	1.00000	1.00000	1.00000	1.00000	1.00000
F ₂	0.50004	0.50006	0.50008	0.50010	0.50012	0.50014	0.50016	0.50018	0.50020	0.50022	0.50024	0.50026	0.50028	0.50030
F ₃	0.25100	0.25100	0.25100	0.25100	0.25100	0.25100	0.25100	0.25100	0.25100	0.25100	0.25100	0.25100	0.25100	0.25100
F ₄	0.12591	0.12591	0.12592	0.12592	0.12593	0.12593	0.12594	0.12594	0.12595	0.12595	0.12596	0.12596	0.12597	0.12597
F ₅	0.06342	0.06343	0.06344	0.06345	0.06346	0.06347	0.06348	0.06349	0.06350	0.06351	0.06352	0.06353	0.06354	0.06355
F ₆	0.03222	0.03223	0.03224	0.03225	0.03226	0.03227	0.03228	0.03229	0.03230	0.03231	0.03232	0.03233	0.03234	0.03235
F ₇	0.01661	0.01662	0.01663	0.01664	0.01665	0.01666	0.01667	0.01668	0.01669	0.01670	0.01671	0.01672	0.01673	0.01674
F ₈	0.00882	0.00883	0.00884	0.00885	0.00886	0.00887	0.00888	0.00889	0.00890	0.00891	0.00892	0.00893	0.00894	0.00895
F ₉	0.00494	0.00495	0.00496	0.00497	0.00498	0.00499	0.00500	0.00501	0.00502	0.00503	0.00504	0.00505	0.00506	0.00507
F ₁₀	0.00302	0.00303	0.00304	0.00305	0.00306	0.00307	0.00308	0.00309	0.00310	0.00311	0.00312	0.00313	0.00314	0.00315

INTERPOLATED FROM COULTER ELECTRONICS LTD. DATA

A P P E N D I X D

TABLE 17: RATE OF APPROACH TO EQUILIBRIUM.

STIRRING TIME :	1 h.	2 h.	4 h.
PURE P.E. S.G. at 25.0°C	1.01749	1.01738	1.01738
PURE P.E. + 1.0% Di-P.E. S.G. at 25.0°C		1.01787	
PURE P.E. + 2.0% Di-P.E. S.G. at 25.0°C	1.01849	1.01847	1.01847

BATCH A (P.E. + 4.73% COMPOUND X).

Approached from Undersaturation:

Stirring time : 4 h. 5 h.
 S.G. at 25.0°C : 1.02042 1.02079

The solution was left overnight and then stirring resumed:

Stirring time: 3 h. 6 h.
 S.G. at 25.0°C : 1.02183 1.02268

Approached from Supersaturation:

Stirring time: 1 h. 2 h. 3 h. 4 h. 5 h. 6 h.
 S.G. at 25.0°C: 1.03257 1.02703 1.02415 1.02326 1.02255 1.02229
 Difference : - 0.00554 - 0.00388 - 0.00089 - 0.00071 - 0.00026

The solution was left overnight and then stirring resumed:

Further 8 h. stirring :
 S.G. at 25.0°C : 1.02290
 Difference : +0.00061

FIG. 14

THE VARIATION OF SPECIFIC GRAVITY WITH
P.E. CONCENTRATION IN AQUEOUS SOLUTION

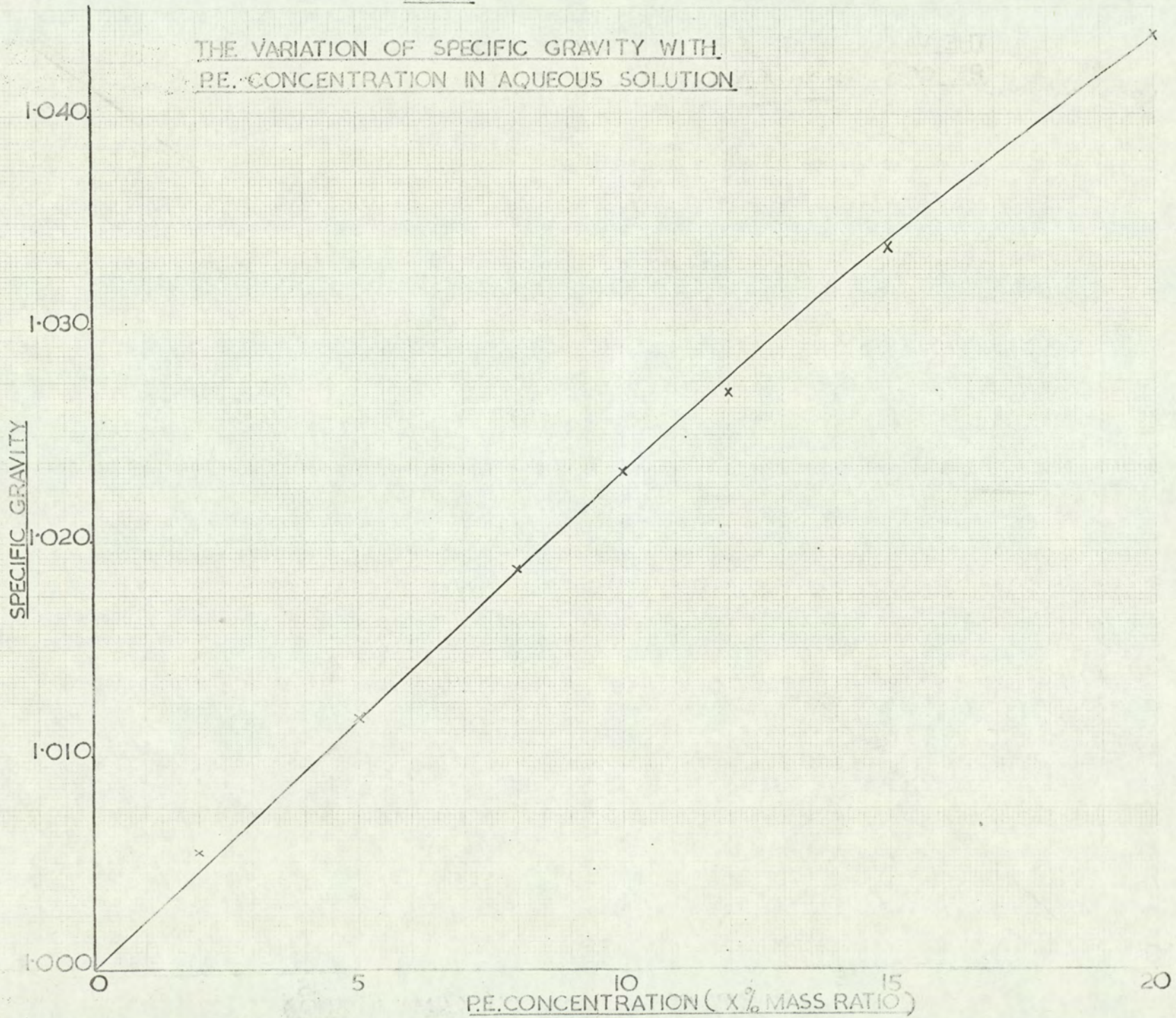


TABLE 18: CONCENTRATION EQUIVALENT OF S.G. AT EQUILIBRIUM

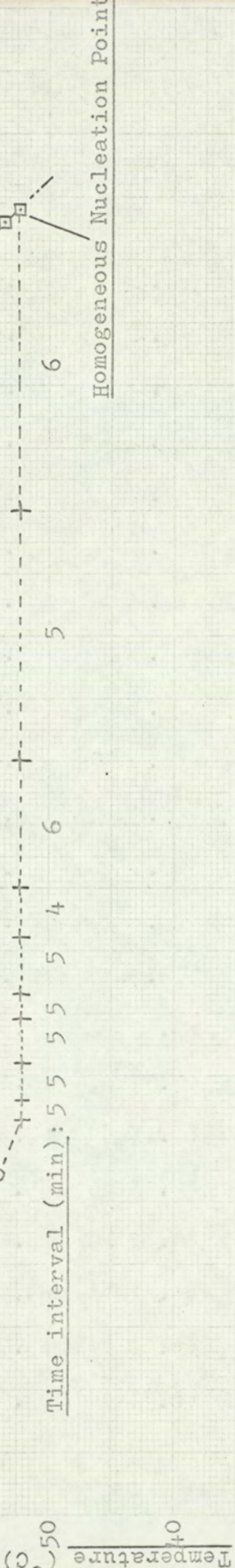
SAMPLE	X % MASS RATIO	% MASS FRACTION.
PURE P.E.	7.4	6.9
PURE P.E. + 1% Di-P.E.	7.65	7.2
PURE P.E. + 2% Di-P.E.	7.9	7.4
BATCH A. approached from undersaturation for a total of 11 h. stirring	9.65	8.8
BATCH A. approached from supersaturation for 6 h.	9.50	8.7
BATCH A. approached from supersaturation allowed to stand overnight and then further 8 h. stirring.	9.75	8.9

TABLE 19: SOLUBILITY DETERMINATIONS BY EVAPORATION

TEMPERATURE:	25.0°C	40.0°C	60.0°C	80.0°C
PURE P.E. % MASS RATIO:	7.34	11.35	23.6	43.0
" " " " "	7.42	11.34		
" " " " "	7.65	11.18		
" " " " "	7.67			
PURE P.E. AVERAGE % MASS RATIO	7.52	11.29	23.6	43.0
PURE P.E. AVERAGE % MASS FRACTION:	7.0	10.2	19.2	30.1
BATCH A. % MASS RATIO:		13.65	24.9	46.0
" " " " "		14.02		47.2
" " " " "		14.55		45.9
BATCH A. AVERAGE % MASS RATIO:		14.07	24.9	46.4
BATCH A. AVERAGE % MASS FRACTION		12.4	20.0	31.8

TABLE 20: INTERPOLATED CALIBRATION OF REFRACTOMETERS

n_D	% SUGAR FROM I.C.T. (74)	INDICATED % SUGAR ON 583215(A)	INDICATED % SUGAR ON 583213(B)	n_D	% SUGAR FROM I.C.T. (74)	INDICATED % SUGAR ON 583215(A)	INDICATED % SUGAR ON 583213(B)
1.333	0.00	0.40	0.05	1.355	14.55	15.55	15.30
1.334	0.70	1.15	0.80	1.356	15.20	16.20	15.95
1.335	1.40	1.90	1.55	1.357	15.80	16.80	16.55
1.336	2.05	2.60	2.25	1.358	16.40	17.40	17.15
1.337	2.75	3.30	2.95	1.359	17.00	18.05	17.80
1.338	3.40	4.05	3.70	1.360	17.60	18.65	18.40
1.339	4.15	4.80	4.45	1.361	18.25	19.20	18.95
1.340	4.80	5.50	5.15	1.362	18.90	19.85	19.60
1.341	5.45	6.20	5.85	1.363	19.45	20.45	20.25
1.342	6.15	6.90	6.60	1.364	20.05	21.00	20.80
1.343	6.80	7.60	7.30	1.365	20.70	21.60	21.40
1.344	7.45	8.30	8.00	1.366	21.30	22.15	21.95
1.345	8.10	8.95	8.65	1.367	21.90	22.70	22.50
1.346	8.75	9.60	9.30	1.368	22.45	23.25	23.10
1.347	9.40	10.30	10.00	1.369	23.05	23.80	23.65
1.348	10.05	11.00	10.70	1.370	23.65	24.30	24.15
1.349	10.75	11.70	11.40	1.371	24.25	24.85	24.70
1.350	11.40	12.35	12.05	1.372	24.80	25.40	25.25
1.351	12.00	13.00	12.70	1.373	25.40	25.95	25.80
1.352	12.60	13.65	13.35	1.374	26.00	26.50	26.35
1.353	13.25	14.30	14.00	1.375	26.55	27.05	26.90
1.354	13.95	14.90	14.60	1.376	27.10	27.60	27.45



Homogeneous Nucleation Point

FIG. 16.

CALIBRATION TEST - C7

Inst. No.: 583 215-----A

Material: (PE + 4.7 %X)

Concentration: 26.0 mass %

○ = Heating
 □ = Cooling
 + = Constant Temperature
 E = Equilibrium assumed
 ↓ = Interpolation concentration for every Δn = 0.001 change in refractive index

Indicated % Sugar

TABLE 21a

Interpolated Calibration Data (Pure PE) - °C

Test No :		C28	C25	C29	C26	C27
% m/v:		8.08	10.54	14.35	18.08	22.16
% mass:		7.9	10.2	13.7	17.2	20.9
n_D	Indicated % Sugar on 583 215					
1.333	0.40	78.0				
34	1.15	73.5				
35	1.90	69.0				
36	2.60	65.0				
37	3.30	60.5	73.0			
38	4.05	55.0	68.5			
39	4.80	50.0	64.0			
1.340	5.50	44.5	59.5			
41	6.20	39.0	55.0	76.5		
42	6.90	33.0	50.0	72.5		
43	7.60	26.5	45.5	68.0		
44	8.30	19.0	40.5	64.0		
45	8.95	10.5	35.0	59.5	81.0	
46	9.60		28.0	55.0	77.0	
47	10.30		18.5	50.0	73.0	
48	11.00			44.5	69.0	
49	11.70			39.5	64.5	
1.350	12.35			34.0	60.5	80.0
51	13.00			27.5	56.5	77.0
52	13.65			21.0	52.0	73.5
53	14.30			N	47.5	69.5
54	14.90				42.5	66.0
55	15.55				35.0	61.5
56	16.20				N	56.5
57	16.80					51.5
58	17.40					46.0
59	18.05					N

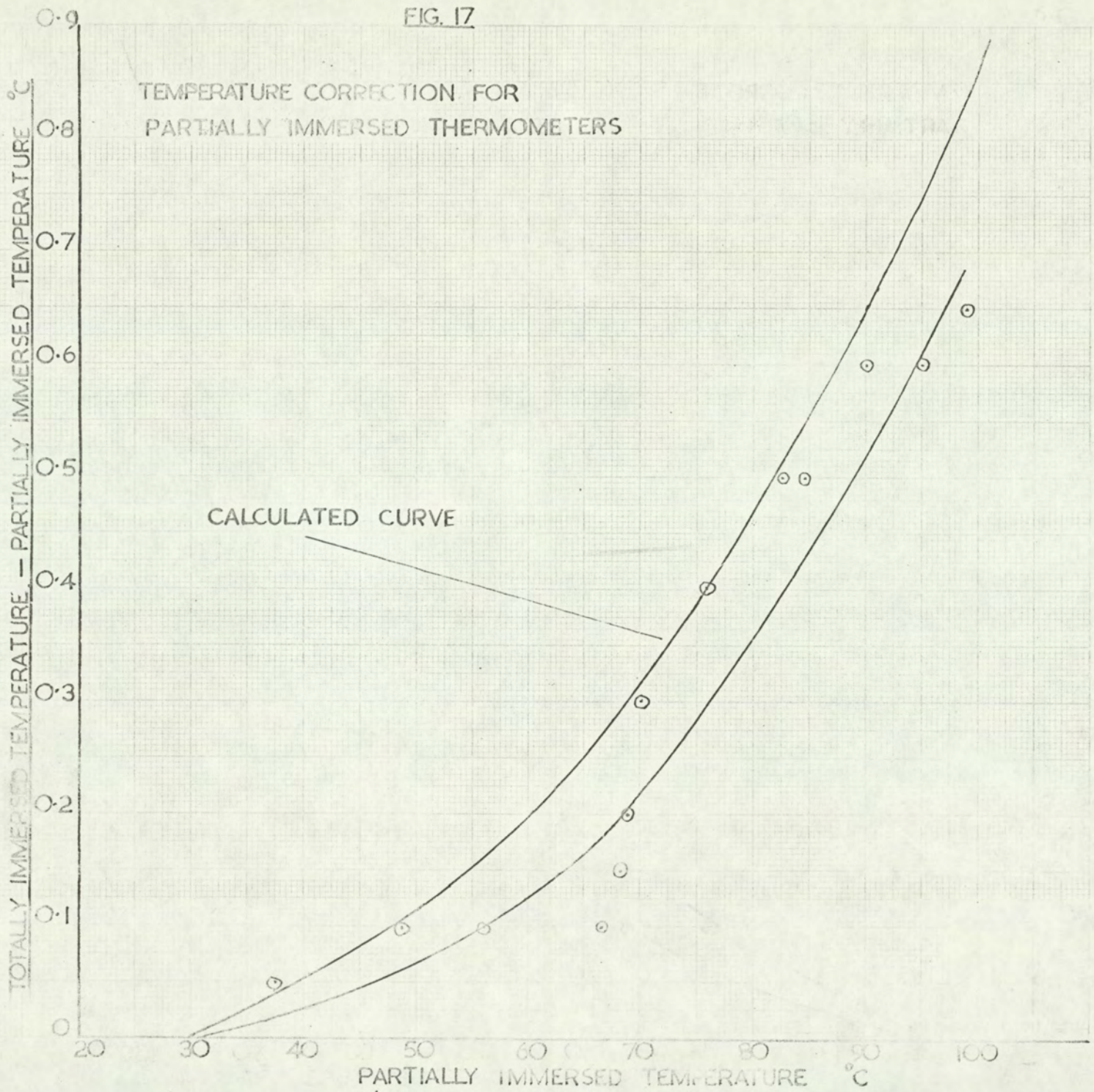
TABLE 21d: NUCLEATION AND EQUILIBRIUM DATA

TEST NO.	MATERIAL	T°C	% mass fraction	t(h)	Growth + Dissolution -
C.26	Pure P.E.	34.0	17.2	N	
C.26	Pure P.E.	44.5	12.2	0.8	-
C.26	Pure P.E.	50.0	14.1	1.0	-
C.26	Pure P.E.	31.1	8.6	40.0	+
C.27	Pure P.E.	46.0	20.9	N	
C.29	Pure P.E.	18.5	13.7	N	
C.29	Pure P.E.	27.8	7.7	17.5	+
C.29	Pure P.E.	38.0	10.3	3.0	-
C.29	Pure P.E.	23.4	7.0	315.0	+
C.5	Batch A	18.0	15.2	N	
C.5	Batch A	40.7	11.4	14.0	-
C.5	Batch A	51.0	14.7	0.8	-
C.6	Batch A	37.5	22.4	N	
C.6	Batch A	55.5	17.5	1.0	-
C.6	Batch A	60.5	19.4	0.5	-
C.6	Batch A	64.5	21.5	0.5	-
C.7	Batch A	52.5	26.0	N	
C.7	Batch A	70.0	24.5	0.3	-
C.7	Batch A	72.2	24.8	0.3	-
C.8	Batch A	40.0	12.1	(N)0.3	+
C.9	Batch A	1.8	13.5	N	
C.9	Batch A	17.0	7.4	14.0	+
C.11	Batch A	2.5	14.8	N	
C.11	Batch A	25.0	8.7	70.0	+
C.11	Batch A	29.8	10.0	5.3	-
C.11	Batch A	33.5	11.0	16.5	-
C.12	Batch A	27.5	19.0	N	
C.12	Batch A	35.5	12.1	0.5	-
C.12	Batch A	40.5	13.3	1.0	-
C.12	Batch A	45.7	14.3	0.5	-
C.12	Batch A	55.0	17.0	0.5	-

TABLE 21d (CONTINUED)

TEST NO.	MATERIAL	T°C	% mass fraction	t(h)	Growth + Dissolution -
C.13	Batch A	69.5	34.9	N	
C.13	Batch A	86.5	34.7	0.3	-
C.14	Batch C	27.8	19.2	N	
C.14	Batch C	47.2	13.7	0.8	-
C.14	Batch C	57.0	17.6	0.5	-
C.15	Batch C	3.0	13.7	N	
C.15	Batch C	23.4	7.5	240.0	+
C.16	Batch C	42.5	24.3	N	
C.16	Batch C	49.8	14.4	0.5	+
C.16	Batch C	60.5	19.5	1.3	-
C.16	Batch C	42.2	12.9	13.0	+
C.18	Batch C	64.3	31.1	N	
C.18	Batch C	70.0	24.7	3.0	+
C.18	Batch C	77.6	29.7	0.5	-
C.20	Batch C	11.8	16.2	N	
C.20	Batch C	18.0	6.8	0.1	+
C.20	Batch C	52.5	15.7	13.5	-
C.21	Batch C	58.0	27.8	N	
C.21	Batch C	64.6	23.0	0.8	+
C.21	Batch C	69.0	25.0	0.5	-
C.22	Batch C	67.7	34.7	N	
C.22	Batch C	74.5	30.2	0.5	+

FIG. 17



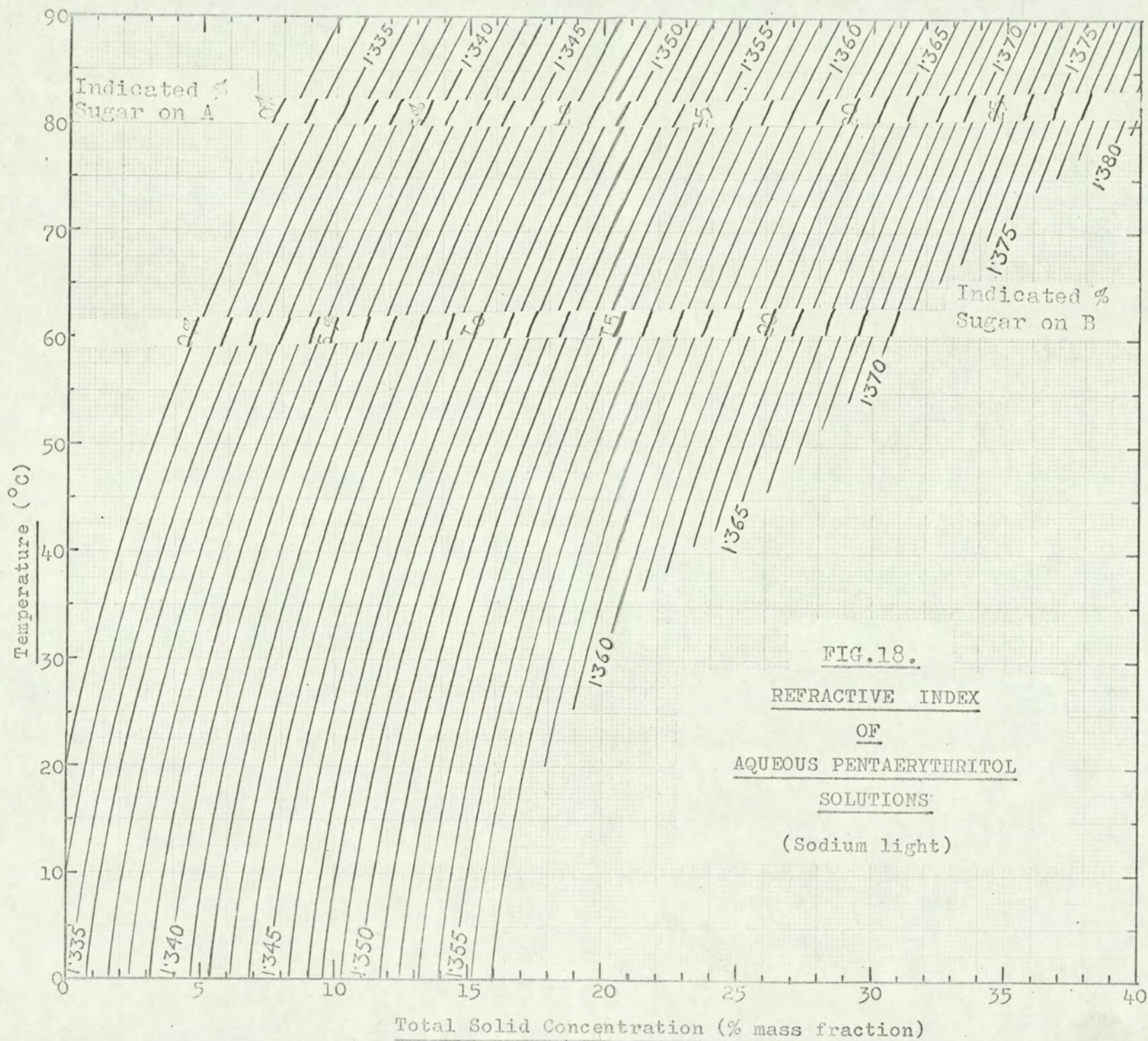


FIG.18.
REFRACTIVE INDEX
OF
AQUEOUS PENTAERYTHRITOL
SOLUTIONS
(Sodium light)

TABLE 22: EQUILIBRIUM DATA OBTAINED FROM GROWTH RATE TESTS

TEST	MATERIAL	T°C	% Sugar Indicated on A or B	Initial Concentration % m/v	Time of Growth (h)	Seed g	Stirrer speed r.p.m.	x % m/m
R2	Batch A	51.0	11.8A	24.0	20 $\frac{1}{3}$	2	1200	15.4
R3	Batch A	51.0	11.8A	24.0	19 $\frac{1}{4}$	2	1200	15.4
R4	Batch A	51.0	11.8A	24.0	40	2	1010	15.4
R13	Batch A	50.0	11.6A	17.6	120	2	500	15.0
R15	Batch A	55.4	12.9A	Nuclea- tion	19 $\frac{2}{3}$	-	500	17.1
R17	Batch A	38.8	9.2A	"	25	-	300	11.1
R20	Batch A	70.0	17.8A	30.0	115	2	500	24.7
R21	Batch A	55.0	14.0A	21.5	51 $\frac{1}{2}$	2	500	18.2
R23	Batch A	80.0	22.15A	37.0	49	2	500	31.4
R24	Batch A	60.0	14.1B	24.0	51	2	600	19.5
R25	Batch A	60.0	14.5A	24.0	16	2	500	19.6
R26	Batch A	60.0	14.2B	24.0	29	2	500	19.6
R27	Pure P.E.	60.0	13.2B	24.0	28	2	500	18.2
R29	Pure P.E.	70.0	16.9B	29.0	8	2	500	23.8
R30	Pure P.E.	80.0	21.15B	37.0	5 $\frac{1}{2}$	2	500	30.2

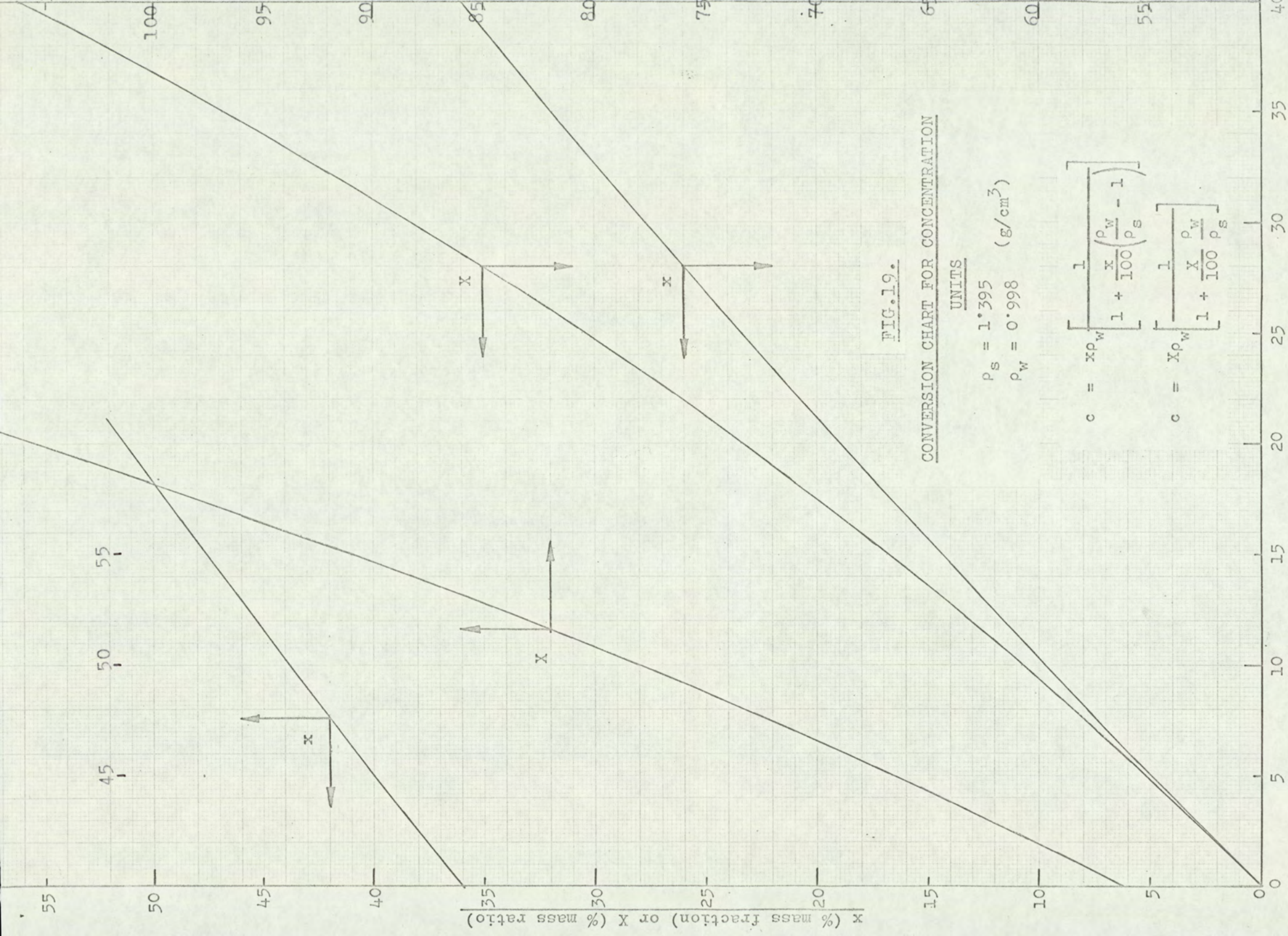


FIG. 19.

CONVERSION CHART FOR CONCENTRATION

UNITS

$$P_S = 1.395 \quad (\text{g/cm}^3)$$

$$P_W = 0.998$$

$$c = x\rho_W \left[\frac{1}{1 + \frac{x}{100} \left(\frac{\rho_W}{\rho_S} - 1 \right)} \right]$$

$$c = X\rho_W \left[\frac{1}{1 + \frac{X}{100} \frac{\rho_W}{\rho_S}} \right]$$

c (% m/v at 20°C, undissolved)

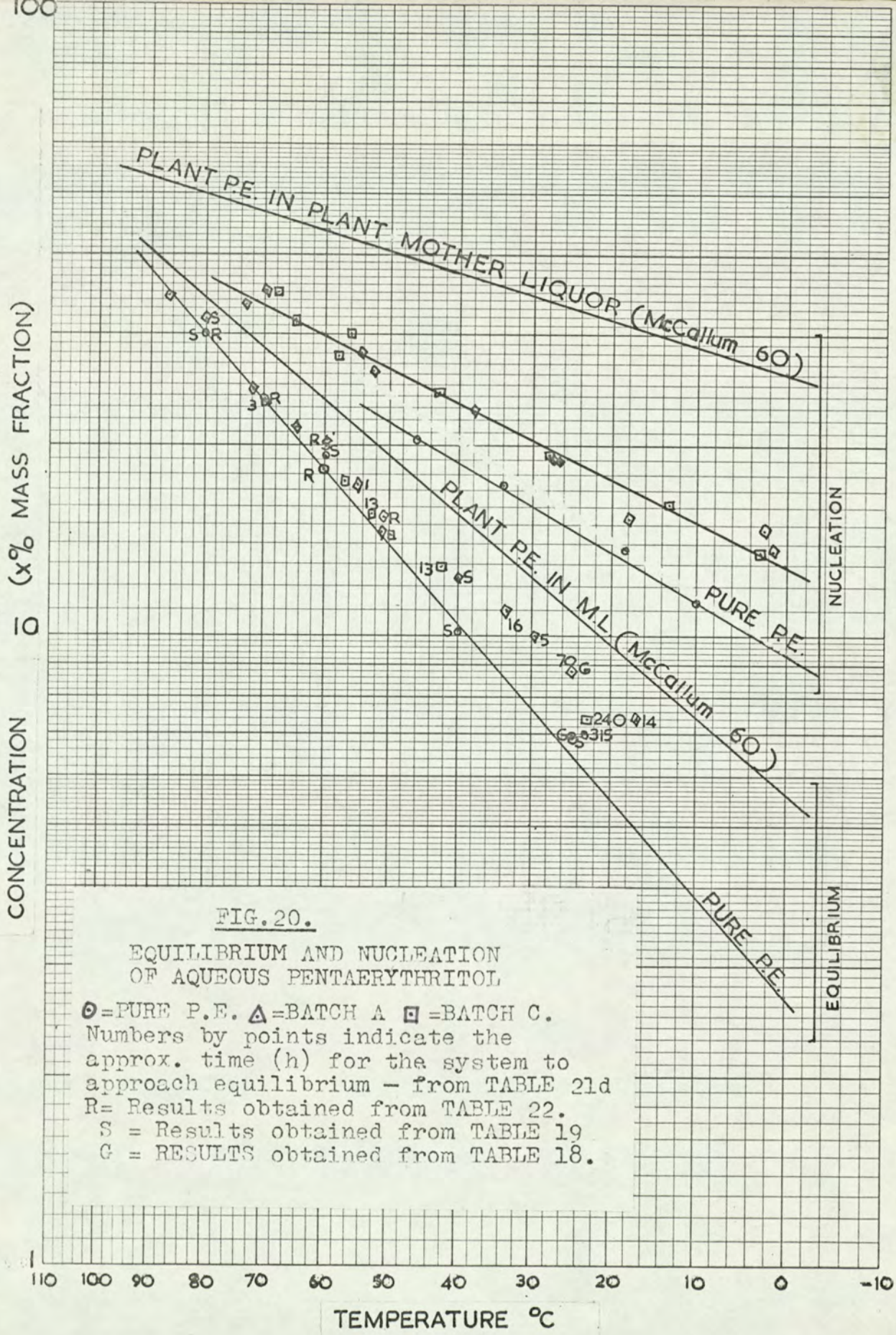
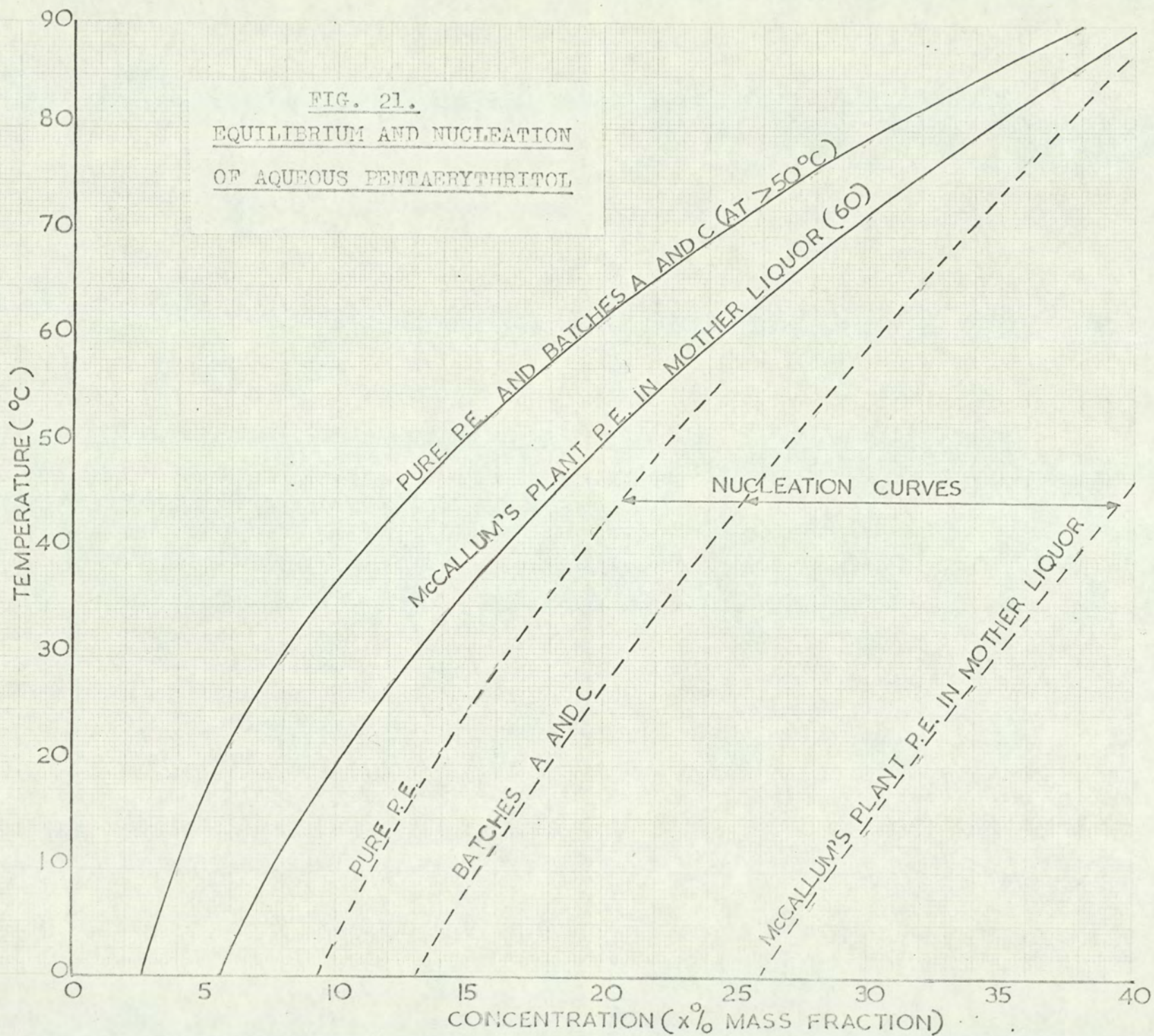


FIG. 20.

EQUILIBRIUM AND NUCLEATION
OF AQUEOUS PENTAERYTHRITOL

- = PURE P.E. △ = BATCH A □ = BATCH C.
- Numbers by points indicate the approx. time (h) for the system to approach equilibrium - from TABLE 21d
- R = Results obtained from TABLE 22.
- S = Results obtained from TABLE 19
- G = RESULTS obtained from TABLE 18.

FIG. 21.
EQUILIBRIUM AND NUCLEATION
OF AQUEOUS PENTABRYTHRITOL



A P P E N D I X E

TABLE 23

BATCH A. SEED: SIEVE FRACTION 44.53 μ EFFECT OF STIRRER SPEED 60.0 $^{\circ}$ C

From Fig. 24 $c = 1.142 n + 4.24$

$n_{\infty} = 14.4$

Indicated % Sugar on A	% P.E. m/v	R.7.220RPM		R11.300RPM		R9.400RPM		R12.500RPM		R8600RPM		R10.750RPM	
		t(min)	K ¹ x 10 ⁴	t(min)	K ¹ x 10 ⁴	t(min)	K ¹ x 10 ⁴	t(min)	K ¹ x 10 ⁴	t(min)	K ¹ x 10 ⁴	t(min)	K ¹ x 10 ⁴
17.30	24.00	0		0		0		0		0		0	
17.20	23.88	14	11.6			7	23.3	7	23.3	7	23.3		
17.10	23.77	40	5.94	12	27.1	18	14.1	17	15.5	13	25.8	5	65.1
17.00	23.65	70	4.97			30	12.4	30	11.5	30	8.77	7	74.5
16.90	23.54	85	9.50			45	9.5	45	9.5	45	9.5	31	5.94
16.80	23.43	100	9.10			58	10.5	57	11.4	60	9.1	54	5.94
16.70	23.31	120	6.55	116	5.48	71	10.1			72	10.9	70	8.2
16.60	23.20	140	6.75	130	9.65	83	11.2			84	11.2	85	9.0
16.50	23.08	155	8.90	138	16.7					94	13.4	94	14.8
16.40	22.97	168	10.20	150	11.1			110	10.1	104	13.3	106	11.1
16.30	22.85			160	13.2			125	8.8	112	16.5	116	13.2
16.20	22.74	195	9.90	180	6.83			155	4.55	128	8.53	135	7.2
16.10	22.63	230	3.94	220	3.45	180	6.93	180	5.52	148	6.9	165	4.6
16.00	22.51			245	5.58	202	6.38	205	5.60	170	6.38	195	4.76
15.90	22.40	320	3.15	290	3.25	240	3.85	255	2.92			215	7.3
15.80	22.28	340	7.45	330	3.72							230	9.95
15.70	22.17	360	7.90	435	1.51	330	3.42	290	8.79				
15.60	22.06	380	8.00			360	5.33						
15.50	21.94	410	5.67	500	2.43	380	8.50	330	3.95			290	8.28
15.40	21.83			520	9.20	420	4.60	350	9.20				
15.30	21.71			540	9.85	440	9.85					315	15.4
15.20	21.60			565	8.65			450	4.14			335	10.8
15.10	21.48											410	3.18
15.00	21.37											460	5.43
14.90	21.26											495	8.95
$\bar{K}^{-1} \times 10^4 \text{ min}^{-1} (\text{g seed})^{-1}$		7.284		7.373		7.089		7.039		10.41		12.03	
Std. Deviation x 10 ⁴ :		±2.221		±4.332		±2.982		±2.872		±3.042		±15.50	

TABLE 24: METASTABLE LIMIT OF BATCH A IN AQUEOUS SOLUTION STIRRED AT 500 rpm

$T^{\circ}\text{C}$	c_0 %m/v	x_0 %m/m	n_0	n_{∞}	x_{∞} %m/m	$n_0 - n_{\infty}$	$x_0 - x_{\infty}$	Approx. Time to nucleate (h)
60.0	24.0	22.5	17.3	14.4	19.4	2.9	3.1	> 68
58.8	24.0	22.5	17.6	13.9	18.6	3.7	3.9	> 48
57.0	24.0	22.5	17.8	13.5	18.0	4.3	4.5	19
55.0	24.0	22.5	18.1	12.9	16.9	5.2	5.4	12
53.0	24.0	22.5	18.4	12.4	16.3	6.0	6.2	8
50.0	24.0	22.5	18.9	11.6	15.0	7.3	7.5	1

- 133 -
TABLE 25

BATCH A. COMPARISON OF DIFFERENT SEED MATERIALS - Sieve Fraction 44-53 μ

From Fig. 24 $c = 1.142 n + 4.24 n = 14.4$ 60.0°C 500 r.p.m.

Indicated % Sugar on A	% P.E. m/v	R14 Prepared Seed		R12 BATCH A Sieve fraction.		R25.BATCH A Milled for 3h		R26.BATCH A Milled for 20min.	
		t(min)	K ¹ x10 ⁴	t(min)	K ¹ x10 ⁴	t(min)	K ¹ x10 ⁴	t(min)	K ¹ x10 ⁴
17.30	24.00	0		0		0			
17.20	23.88	9	18.1	7	22.3				
17.10	23.77	80	2.18	17	15.5	4	81.5	7	46.6
17.00	23.65	130	2.98	30	11.5	6	74.5	22	9.95
16.90	23.54	195	2.20	45	9.5	10	35.7	33	13.0
16.80	23.43	240	3.03	57	11.4	15	27.3	43	13.6
16.70	23.31	300	2.18			23	16.4		
16.60	23.20					32	15.0	67	10.8
16.50	23.08	400	2.66			38	22.2		
16.40	22.97			110	10.1	43	26.6		
16.30	22.85			125	8.8	55	11.0	115	8.45
16.20	22.74			155	4.55	65	13.6		
16.10	22.63			180	5.52				
16.00	22.51			205	5.60	96	8.94	190	5.60
15.90	22.40			255	2.92	110	9.98		
15.80	22.28							220	9.77
15.70	22.17			290	8.79				
15.60	22.06								
15.50	21.94			330	3.95				
15.40	21.83	1440	1.52	350	9.20				
15.30	21.71	1500	3.25					420	8.85
15.20	21.60	1800	0.715	450	4.14				
15.10	21.48								
15.00	21.37								
$K^{-1} \times 10^4 \text{min}^{-1}$ (g.seed) ⁻¹		2.546		7.039		23.75		10.00	
Std.Deviation x10 ⁴		±0.6107		±2.872		± 18.39		± 2.558	

TABLE 26: SIZE DISTRIBUTION 1 (280 μ TUBE)

BATCH A								PURE P.E.
Before Attrition NO%O.S	Attrition: d_{μ}	6min NO%O.S	3 $\frac{1}{2}$ h NO%O.S	20 h NO%O.S	35h NO%O.S	48h NO%O.S	72h NO%O.S	10min NO%O.S
0.14	73.5	0	0.08	0	0	0	0.02	0.04
12.2	58.4	1.02	1.72	0	0.64	0.09	0.16	1.63
32.1	46.4	7.55	12.6	1.8	2.88	0.54	1.15	4.91
42.7	36.9	14.2	19.4	16.7	5.43	1.40	2.94	5.48
54.4	29.4	17.2	25.6	30.7	9.32	4.3	6.60	6.82
63.8	25.5	26.4	30.9	45.7	12.22	10.1	11.9	8.70
73.9	18.9	33.4	40.5	52.2	18.7	17.4	20.6	13.7
87.6	15.4	45.6	50.9	61.4	26.4	27.0	31.3	19.9
100	12.8	55.9	64.8	80.0	36.9	39.7	41.7	30.3
	11.0	69.6	77.3	83.4	50.0	50.6	53.1	45.2
	8.75	82.2	86.6	89.9	67.3	69.2	68.3	73.6
	7.80	92.0	89.8	95.6	77.0	79.3	79.5	84.0
	6.95	99.1	94.3	95.6	93.6	88.5	91.3	94.0
	6.22	100	100	100	100.0	100	100	100
	a =	26	24	16.5	45	44	42	45

FIG. 23d

SIZE DISTRIBUTION I (280 μ COULTER COUNTER ORIFICE)
AFTER 6 MINS. ATTRITION

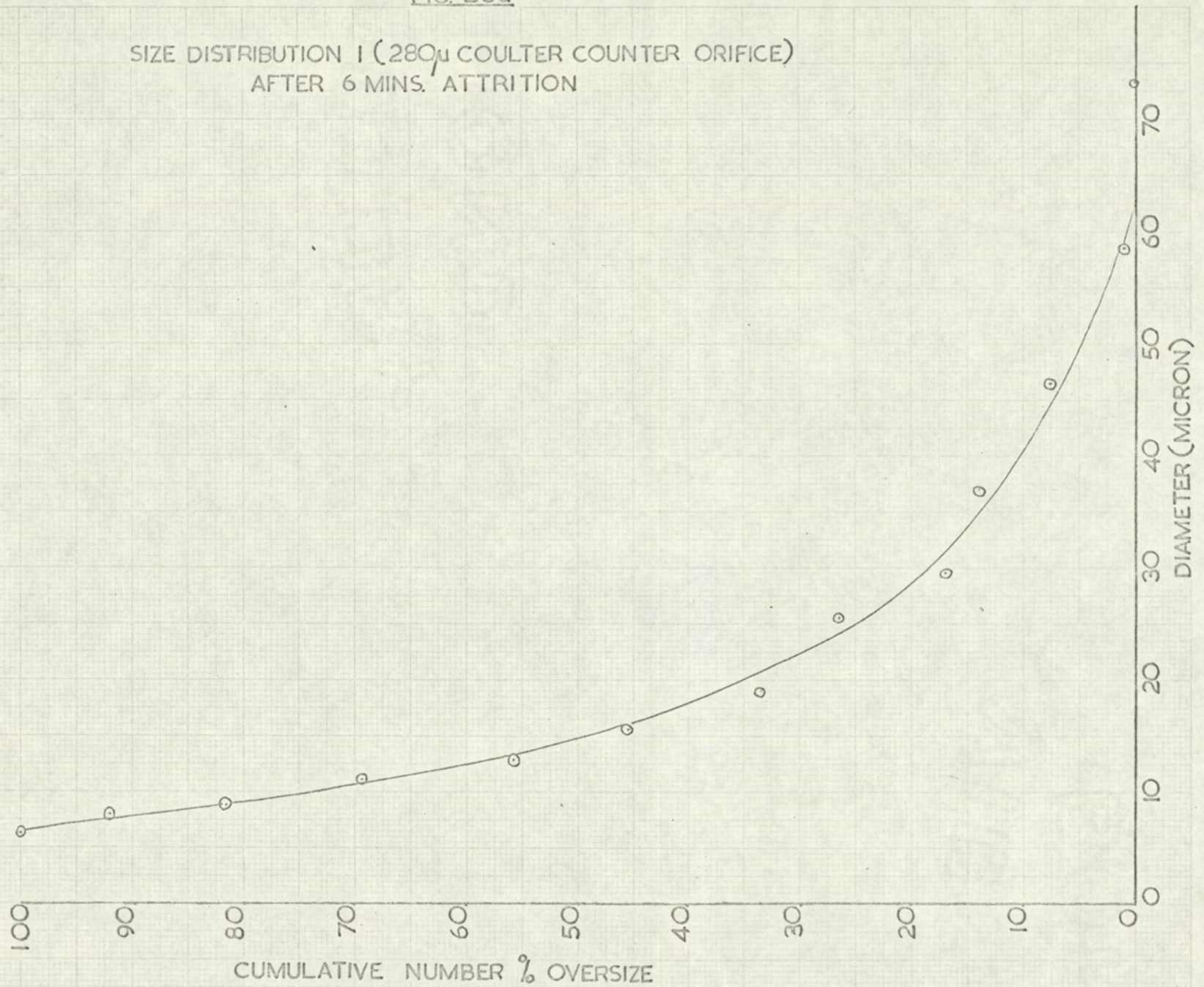


TABLE 27: SIZE DISTRIBUTION 2 (50 μ TUBE)

ATTRITION: d μ	BATCH A					PURE P.E.
	6 min NO%O.S	2oh NO%O.S	35h NO%O.S	48h NO%O.S	72h NO%O.S	10 min NO%O.S
14.1	1.47	0	1.29	0	0	1.43
12.6	4.1	2.63	3.14	1.71	0	2.14
10.6	5.47	2.63	4.52	2.99	0.715	2.32
9.3	7.05	2.63		3.42	2.14	5.35
7.35	8.74	2.63	6.9	4.70	4.28	6.44
5.87	13.6	7.90	10.0	6.84	5.71	7.5
4.68	27.0	10.5	15.1	12.8	5.71	26.1
3.76	38.8	14.5	20.5	15.8	14.3	66.6
3.03	60.0	35.5	39.3	27.8	26.5	66.6
2.50	80.6	57.8	53.4	52.6	51.4	100
2.12	83.7	79.0	82.2	82.0	74.4	
1.88	100	100	100	100	100	
b	6.0	1.50	5.3	3.0	4.0	2.8
l	12.1	7.2	9.7	6.2	4.7	5.8

FIG. 23b

SIZE DISTRIBUTION 2 (50 μ COULTER COUNTER ORIFICE)
 AFTER 6 MINS. ATTRITION

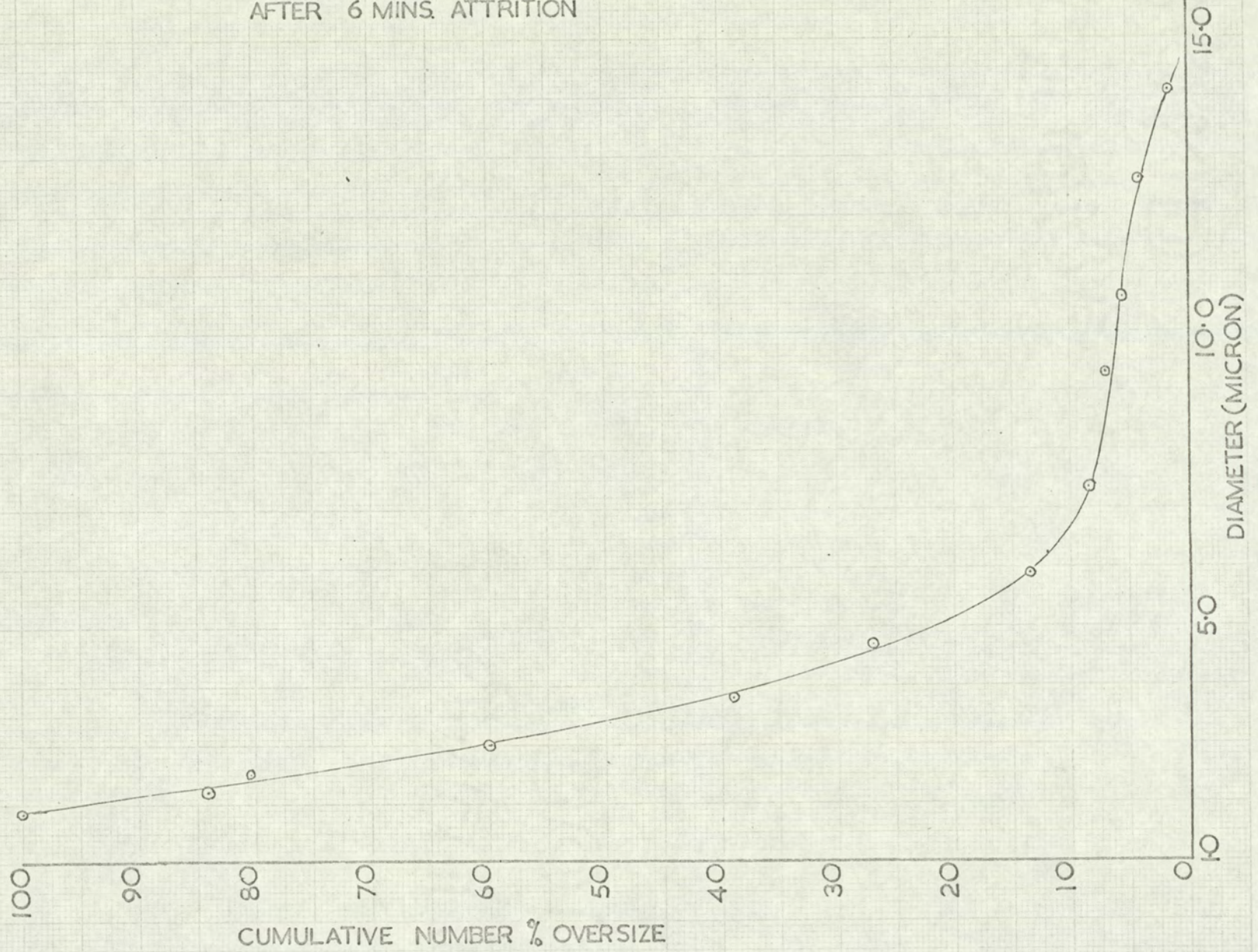


TABLE 28: COMBINED SIZE DISTRIBUTION

BATCH A						PURE P.E.
ATTRITION:	6 min	20h	35h	48h	72h	10 min
d μ	NO%O.S	NO%O.S	NO%O.S	NO%O.S	NO%O.S	NO%O.S
58.4	0.2	0	0	0	0	0.65
46.4	1.57	0.478	0.33	0.03	0.07	1.95
29.4	3.51	8.14	1.08	0.29	0.43	2.72
18.9	6.95	13.85	2.16	1.17	1.34	5.45
12.8	11.6	21.2	4.26	2.68	2.70	12.1
8.75	17.1	23.9	7.75	4.66	4.43	29.4
6.95	20.2	25.4	10.8	5.96	5.93	37.5
5.87	22.1	27.1	11.8	7.4	9.55	40.9
4.68	34.3	29.1	16.8	13.3	9.55	52.8
3.76	44.8	32.3	22.1	16.4	17.8	79.0
3.03	64.0	48.9	40.6	28.2	29.5	79.0
2.50	82.1	66.6	54.4	52.9	53.5	100
2.12	85.3	83.3	82.7	81.7	75.7	
1.88	100	100	100	100	100	
Specific Surface cm^2/g	1295	1325	1620	2490	2160	1210

Specific Surface original Batch A seed = 855 cm^2/g .

TABLE 29a

R.32 PURE P.E.

SEED: SIEVE FRACTION 44-53 μ 500 r.p.m. 50.0°C

Indicated % Sugar on A	% P.E. m/v	From Fig. 24: $c = 1.125n + 2.65$ $n_{\infty} = 10.9$				
		M(g)	$\left(\frac{M + dM}{M}\right)^{\frac{2}{3}}$	A cm ²	t(min)	K x 10 ⁷ min ⁻¹ cm ⁻²
13.90	18.500	2.000		2420	0	
13.80	18.175	2.937	1.290	3120	25	4.82
13.70	18.063	3.262	1.072	3350	60	3.38
13.60	17.950	3.587	1.066	3570	120	1.78
13.50	17.838	3.912	1.059	3780	300	0.860

$\bar{K} = 2.007 \times 10^{-7} \text{ min}^{-1} \text{ cm}^{-2}$ Standard Deviation: $\pm 1.276 \times 10^{-7}$

TABLE 29b

R.27 PURE P.E. SEED: SIEVE FRACTION 44-53 μ 500 r.p.m. 60.0°C

Indicated % Sugar on A	% P.E. m/v	From Fig. 24: $c = 1.142n + 4.24$ $n = 13.5$				
		M(g)	$\left(\frac{M + dM}{M}\right)^3$	A cm ²	t(min)	K x 10 ⁷ min ⁻¹ cm ⁻²
17.30	24.00	2.000		2420	0	
17.20	23.88	2.362	1.118	2705	7	15.3
17.10	23.77	2.694	1.091	2950	26	5.08
17.00	23.65	3.056	1.088	3210	140	0.78
16.80	23.43	3.720	1.136	3640	165	6.79
16.60	23.20	4.470	1.110	4040	190	6.47
16.10	22.63	6.178	1.246	5030	270	4.79

$\bar{K} = 4.707 \times 10^{-7} \text{ min}^{-1} \text{ cm}^{-2}$ Standard Deviation: $\pm 2.761 \times 10^{-7}$

- 139 -
TABLE 29c

R.29 PURE P.E. SEED: SIEVE FRACTION 44-53 μ 500 r.p.m. 70.0°C

Indicated % Sugar on A.	% P.E. m/v	From Fig. 24: $c = 1.275n + 4.1$ $n_{90} = 16.9$				
		M(g)	$\left(\frac{M + dm}{M}\right)^3$	A cm ²	t(min)	K x 10 ⁷ min ⁻¹ cm ⁻²
19.55	29.000	2.000		2420	0	
19.45	28.899	2.402	1.132	2740	3	49.0
19.25	28.644	3.204	1.21	3310	95	2.94
19.05	28.389	4.004	1.16	3840	115	12.18
18.55	27.751	6.000	1.31	5040	150	16.85
18.45	27.623	6.404	1.045	5260	163	9.44
18.35	27.496	6.802	1.040	5470	175	10.3
18.15	27.241	7.594	1.076	5880	200	10.5
18.05	27.113	7.990	1.034	6080	215	9.31
17.95	26.986	8.385	1.032	6280	230	9.82
17.55	26.476	9.969	1.123	7070	310	9.01
17.45	26.348	10.363	1.025	7250	325	15.55
17.35	26.221	10.755	1.024	7430	375	5.46
17.25	26.093	11.147	1.023	7600	425	6.70
17.15	25.966	11.539	1.023	7790	480	7.93

$\bar{K} = 1.144 \times 10^{-6} \text{ min}^{-1} \text{ cm}^{-2}$. Standard Deviation: $\pm 0.414 \times 10^{-6}$

TABLE 29d

R.30 PURE P.E. SEED: SIEVE FRACTION 44-53 μ 500 r.p.m. 80.0°C

Indicated % Sugar on A	% P.E. m/v	From Fig. 24: $c = 1.245n + 6.8$ $n_{90} = 21.2$				
		M(g)	$\left(\frac{M + dM}{M}\right)^2$	A(cm ²)	t(min)	K x 10 ⁶ min ⁻¹ cm ⁻²
23.25	36.000	2.000		2420	0	
22.80	35.186	4.770	1.785	4.320	26	2.82
22.60	34.937	5.605	1.113	4810	45	1.53
22.30	34.564	6.853	1.143	5500	85	1.17
22.20	34.439	7.265	1.040	5720	97	1.42
22.00	34.190	8.087	1.074	6150	120	1.635
21.80	33.941	8.909	1.067	6550	160	1.13
21.70	33.817	9.320	1.032	6770	170	2.75
21.50	33.568	10.141	1.059	7160	215	1.62
21.40	33.443	10.550	1.026	7340	270	0.983

$\bar{K} = 1.378 \times 10^{-6} \text{ min}^{-1} \text{ cm}^{-2}$ Standard Deviation: $\pm 0.2214 \times 10^{-6}$

R34 (Repeat R30) PURE P.E. 500 r.p.m.

80.0°C

Indicated % Sugar on A	% P.E. m/v	From Fig. 24: $c = 1.245n + 6.8$ $n_{90} = 21.2$				
		M(g)	$\left(\frac{M + dM}{M}\right)^3$	A(cm ²)	t(min)	K x 10 ⁶ min ⁻¹ cm ⁻²
23.30	36.000	2.000		2420	0	
23.10	35.560	3.485	1.450	3510	4	8.4
23.00	35.435	3.902	1.078	3780	7.5	4.21
22.90	35.311	4.319	1.069	4040	11	4.19
22.80	35.186	4.736	1.064	4300	20	1.60
22.70	35.062	5.152	1.058	4550	28	1.835
22.60	34.937	5.568	1.053	4790	36	1.837
22.40	34.688	6.398	1.096	5250	45	3.41
22.30	34.564	6.812	1.044	5480	52	2.315
22.20	34.439	7.226	1.039	5700	59	2.44
22.10	34.315	7.640	1.038	5920	68	2.01
22.00	34.190	8.053	1.035	6120	95	0.723
21.90	34.065	8.466	1.033	6330	114	1.125
21.80	33.941	8.878	1.032	6540	124	1.21

$\bar{K} = 2.242 \times 10^{-6} \text{ min}^{-1} \text{ cm}^{-2}$ Standard Deviation: $\pm 1.148 \times 10^{-6}$

R33 BATCH A PREPARED SEED: SIEVE FRACTION 44-53 μ 500 R.P.M. 50.0°C

Indicated % Sugar on A	% P.E. m/v	From Fig. 24: $c = 1.125n + 2.65$ $n = 11.6$				
		M(G)	$\left(\frac{M + dM}{M}\right)^3$	A(cm ²)	t(min)	K x 10 ⁸ min ⁻¹ cm ⁻²
15.00	19.500	2.000		2590	0	
14.60	19.075	3.235	1.38	3580	960	4.22
14.50	18.963	3.561	1.066	3810	1140	5.16
14.40	18.850	3.887	1.058	4030	1380	3.74

$\bar{K} = 4.373 \times 10^{-8} \text{ min}^{-1} \text{ cm}^{-2}$ Standard Deviation: $\pm 1.004 \times 10^{-8}$

TABLE 30b

R21 BATCH A. PREPARED SEED: SIEVE FRACTION 44-53 μ 500 r.p.m. 55.0°C

Indicated % Sugar on A	% P.E. m/v	From Fig. 24: $c = 1.145n + 3.20$ $n_{90} = 12.9$				
		M(g)	$\left(\frac{M + dm}{M}\right)^3$	A(cm ²)	t(min)	$k \times 10^8 \text{ min}^{-1} \text{ cm}^{-2}$
16.00	21.500	2.000		2590	0	
15.90	21.405	2.251	1.082	2810	10	126
15.80	21.291	2.590	1.097	3080	25	77.5
15.70	21.177	2.929	1.086	3340	110	12.9
15.60	21.062	3.268	1.075	3590	255	7.37
14.90	20.261	5.603	1.435	5160	1110	8.02
14.80	20.146	5.937	1.039	5360	1230	8.01
14.70	20.032	6.271	1.038	5560	1470	4.09
14.20	19.459	7.937	1.170	6510	2550	5.00
14.10	19.345	8.269	1.028	6680	2790	4.98
14.00	19.230	8.601	1.026	6850	3090	4.28

$\bar{K} = 8.078 \times 10^{-8} \text{ min}^{-1} \text{ cm}^{-2}$ Standard Deviation: $\pm 3.149 \times 10^{-8}$

TABLE 30c

R 14 BATCH A. PREPARED SEED: SIEVE FRACTION 44-53 μ 500 R.P.M. 60.0°C

Indicated % Sugar on A	% P.E. m/v	From Fig. 24: $c = 1.142n + 4.24$ $n_{90} = 14.4$				
		M(g)	$\left(\frac{M + dM}{M}\right)^3$	A(cm ²)	t(min)	K x 10 ⁷ min ⁻¹ cm ⁻²
17.30	24.00	2.000		2590	0	
17.20	23.88	2.362	1.118	2900	9	13.95
17.10	23.77	2.694	1.091	3160	80	1.71
17.00	23.65	3.056	1.088	3440	130	2.25
16.90	23.54	3.388	1.072	3690	195	1.69
16.80	23.43	3.720	1.066	3930	240	2.335
16.70	23.31	4.080	1.066	4190	300	1.70
16.50	23.08	4.829	1.110	4660	400	2.05
15.40	21.83	8.664	1.470	6840	1440	1.17
15.30	21.71	9.018	1.027	7020	1500	2.51
15.20	21.60	9.343	1.023	7180	1800	0.552

$\bar{K} = 1.956 \times 10^{-7} \text{ min}^{-1} \text{ cm}^{-2}$ Standard Deviation: $\pm 4.657 \times 10^{-8}$

TABLE 30d

R.20 BATCH A. PREPARED SEED: SIEVE FRACTION 44-53 μ 500 r.p.m. 70.0°C

Indicated % Sugar on A	% P.E. m/v	From Fig. 24: $c = 1.275n + 4.1$ $n_{90} = 17.8$				
		M(g)	$\left(\frac{M + dM}{M}\right)^3$	A(cm ²)	t(min)	K x 10 ⁶ min ⁻¹ cm ⁻²
20.30	30.000	2.000		2590	0	
20.20	29.855	2.406	1.129	2925	5	2.97
20.10	29.728	2.812	1.111	3250	14	1.475
20.00	29.600	3.218	1.093	3550	25	1.175
19.90	29.473	3.623	1.085	3850	37	1.100
19.80	29.345	4.028	1.072	4130	46	1.40
19.70	29.218	4.432	1.066	4410	60	1.19
19.50	28.963	5.240	1.119	4930	75	1.59
19.40	28.835	5.643	1.051	5180	86	1.097
19.30	28.708	6.046	1.046	5420	96	1.242
19.20	28.580	6.447	1.045	5650	125	0.428
19.10	28.453	6.849	1.041	5880	158	0.395
19.00	28.325	7.251	1.039	6110	195	0.359
18.80	28.070	8.051	1.072	6560	300	0.275
18.70	27.943	8.446	1.033	6780	350	0.313
18.10	27.178	10.806	1.179	7990	1230	0.169
18.00	27.050	11.201	1.025	8180	1560	0.147

$\bar{K} = 8.256 \times 10^{-7} \text{ min}^{-1} \text{ cm}^{-2}$ Standard Deviation: $\pm 5.041 \times 10^{-7}$

TABLE 30e

R.23 BATCH A. PREPARED SEED: SIEVE FRACTION 44-53, 500 r.p.m. 80.0°C

Indicated % Sugar on A	% P.E. m/v	From Fig. 24: $c = 1.245n + 6.8$ $n_{90} = 22.15$				
		M(g)	$\left(\frac{M + dM}{M}\right)^3$	A(cm ²)	t(min)	K x 10 ⁶ min ⁻¹ cm ⁻²
24.20	37.000	2.000		2590	0	
24.10	36.805	2.665	1.213	3140	2.5	7.4
24.00	36.680	3.087	1.104	3480	4.5	7.79
23.90	36.556	3.509	1.090	3790	8	4.22
23.80	36.431	3.931	1.079	4090	15	2.15
23.70	36.307	4.353	1.070	4380	24	1.65
23.20	35.684	6.453	1.300	5680	74	1.55
23.10	35.570	6.863	1.043	5940	90	1.07
23.00	35.445	7.273	1.040	6160	105	1.225
22.80	35.196	8.103	1.077	6640	150	0.94
22.60	34.947	8.933	1.065	7060	210	0.895
22.50	34.823	9.345	1.031	7310	243	1.06

$\bar{K} = 2.574 \times 10^{-6} \text{ min}^{-1} \text{ cm}^{-2}$ Standard Deviation: $\pm 2.353 \times 10^{-6}$

TABLE 31

R.31 BATCH C. PREPARED SEED: SIEVE FRACTION 44-53 μ 500 R.P.M. 60.0°C
 A ASSUMED = 2590 cm²

Indicated % Sugar on A	% P.E. m/v	From Fig. 24: $c = 1.142n + 4.24$ $n_{90} = 14.7$				
		M(g)	$\left(\frac{M + dM}{M}\right)^3$	A(cm ²)	t(min)	K x 10 ⁷ min ⁻¹ cm ⁻²
17.30	24.00	2.000		2590	0	
17.20	23.88	2.362	1.118	2900	25	5.70
17.10	23.77	2.694	1.091	3165	40	5.17
16.60	23.20	4.470	1.310	4140	100	10.5
16.40	22.97	5.159	1.101	4570	145	5.63
16.30	22.85	5.518	1.058	4830	170	5.20
16.10	22.63	6.178	1.078	5200	220	5.31
16.00	22.51	6.536	1.038	5400	250	4.78
15.80	22.28	7.222	1.069	5770	290	7.44
15.70	22.17	7.650	1.030	5940	315	6.52

$\bar{K} = 6.483 \times 10^{-7} \text{ min}^{-1} \text{ cm}^{-2}$ Standard Deviation: $\pm 1.987 \times 10^{-7}$

TABLE 32

BATCH A. PREPARED SEED: SIEVE FRACTION 44-53 μ EFFECT OF STIRRER SPEED

From Fig.24: $c = 1.142n + 4.24$ $n_{90} = 14.4$ 60.0°C

Indicated % Sugar on A	% P.E m/v	R14.500 rpm.		R.22 400 rpm.		R.24 600 rpm.	
		t(min)	$K^1 \times 10^4$	t(min)	$K^1 \times 10^4$	t(min)	$K^1 \times 10^4$
17.30	24.00	0		0		0	
17.20	23.88	9	18.1	10	16.3		
17.10	23.77	80	2.18	45	4.41	8	40.7
17.00	23.65	130	2.98	65	7.45	27	7.85
16.90	23.54	195	2.20	150	1.68	75	2.96
16.80	23.43	240	3.03	260	1.24	100	5.47
16.70	23.31	300	2.18	320	2.18		
16.60	23.20						
16.50	23.08	400	2.66				
16.40	22.97						
16.30	22.85						
16.20	22.74						
16.10	22.63						
16.00	22.51			1140	1.17		
15.90	22.40			1380	0.608		
15.80	22.28			1620	0.620		
15.70	22.17						
15.60	22.06						
15.50	21.94						
15.40	21.83	1440	1.52	2520	0.754		
15.30	21.71	1500	3.25				
15.20	21.60	1800	0.715				
15.10	21.48						
15.00	21.37						
14.70	21.03					1260	3.64
$K^1 \text{ min}^{-1} (\text{g seed})^{-1}$		2.546×10^{-4}		2.678×10^{-4}		5.427×10^{-4}	
Standard Deviation		$\pm 0.6107 \times 10^{-4}$		$\pm 2.437 \times 10^{-4}$		$\pm 2.445 \times 10^{-4}$	

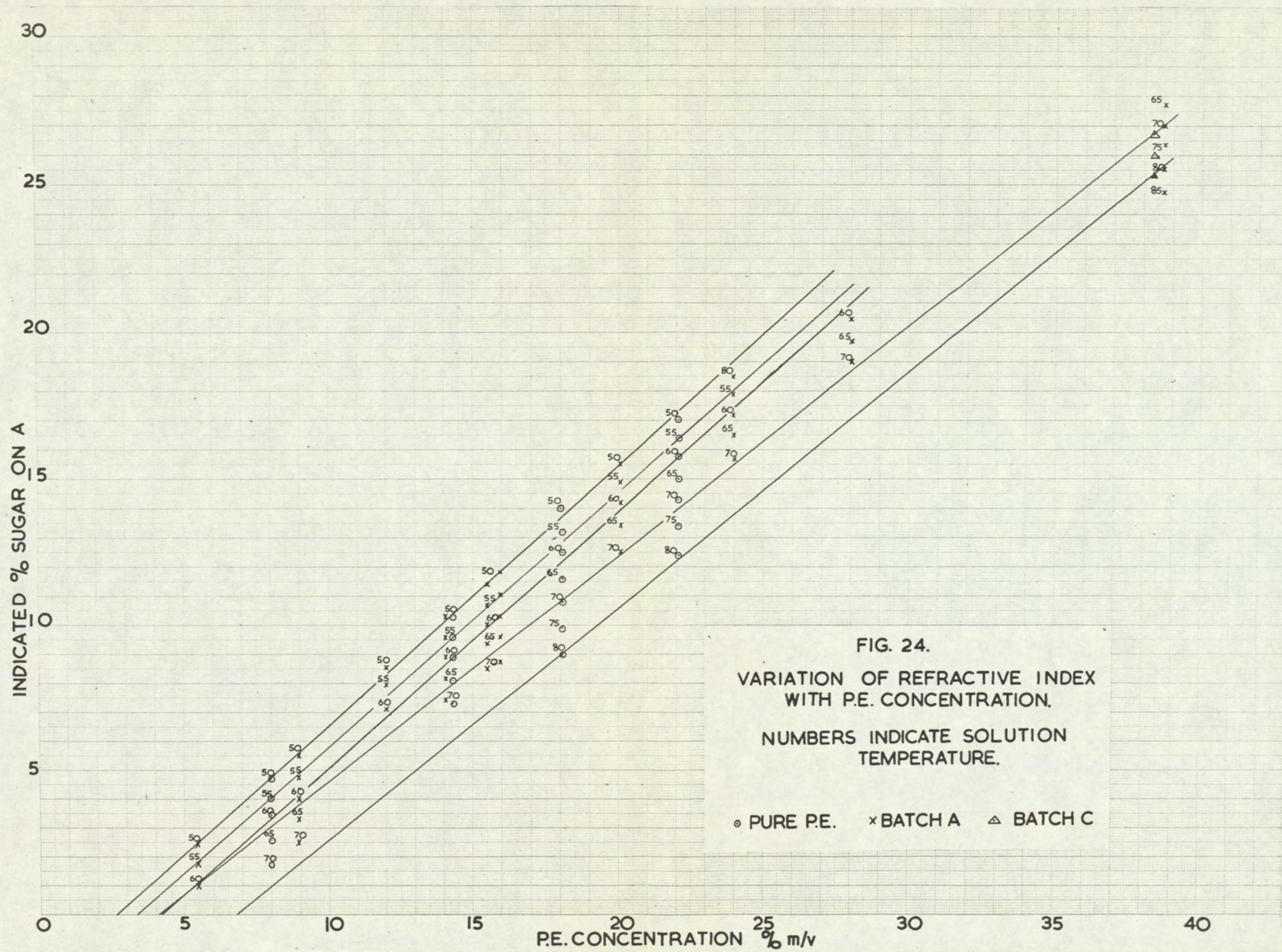
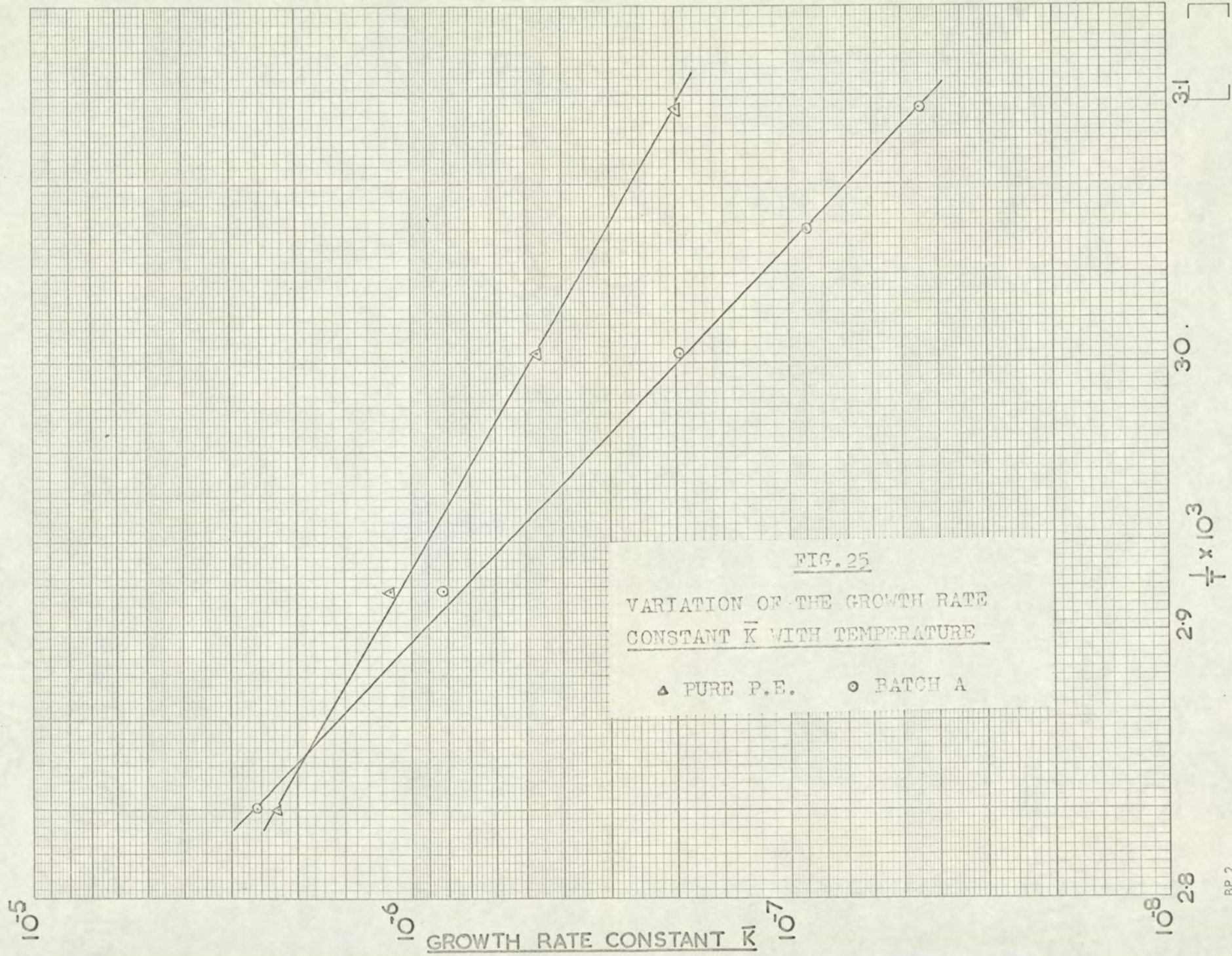


FIG. 24.
 VARIATION OF REFRACTIVE INDEX
 WITH P.E. CONCENTRATION.
 NUMBERS INDICATE SOLUTION
 TEMPERATURE.
 ○ PURE P.E. × BATCH A △ BATCH C



Conversion of K to K_L and K_M

$$\frac{dc}{dt} = -KA (C - C_\infty)$$

$$\text{but } C = \frac{100m}{\frac{m}{\rho} + v} = \frac{100m}{250} \text{ g/Cm}^3$$

$$\therefore dc = \frac{100v \, dm}{\left(\frac{m}{\rho} + v\right)^2}$$

$$\therefore \frac{100v \, dM}{dt \left(\frac{m}{\rho} + v\right)^2} = KA (C - C_\infty)$$

$$\text{But } \frac{dr}{dt} = K_L (C - C_\infty)$$

$$\therefore dM = \frac{KA \left(\frac{m}{\rho} + v\right)^2}{v K_L \times 100} dr$$

$$\text{But } \frac{dM}{dr} = \rho_S 4\pi r^2$$

$$\rho_S 4\pi r^2 = \frac{K}{K_L} \frac{4\pi r^2 (250)^2}{\left(250 - \frac{m}{\rho_S}\right) 100}$$

$$K_L = K \frac{250^2}{(250\rho_S - m) 100}$$

Similarly, where $\frac{dm}{dt} = -K_m A (C - C_\infty)$

$$K_m = K \frac{250^2}{\left(250 - \frac{m}{\rho_S}\right) 100}$$

NOMENCLATURE USED IN SECTIONS 3 TO 7

<u>SYMBOL</u>	<u>MEANING</u>	<u>UNITS</u>
a	Cumulative number % smaller than 10.0 μ diameter (on 280 μ Coulter Counter orifice)	-
A	Total surface area of crystal sample	cm ²
A	Arrhenius equation constant	-
b	Difference in size distribution on the 50 μ orifice between the number % greater than 10 μ diameter and the number % greater than the diameter of the lower limit of the 280 μ Coulter Counter orifice.	-
c	% mass volume.	g(100cm) ⁻³
E	Activation Energy for growth.	K. Cals (g.mole) ⁻¹
K	Growth rate constant	min. ⁻¹ cm. ⁻²
\bar{K}	Average value of K	min. ⁻¹ cm. ⁻²
K _L ⁸	Growth rate constant (linear basis).	cm/min(g/100cm ³)
K _M	Growth rate constant (mass basis).	g/min cm ² (mass fraction)
K ¹	Growth rate constant.	min. ⁻¹ (g. seed) ⁻¹
l	Cumulative number % on the 50 μ Coulter Counter orifice greater	-

<u>SYMBOL</u>	<u>MEANING</u>	<u>UNITS</u>
	than the diameter of the lower limit of the 280 μ orifice.	
m	Mass of solute in solution	g.
M	Crystal mass in suspension	g.
n_D	Refractive Index for mean sodium D lines.	-
n	Refractive Index as Indicated % Sugar.	-
n_∞	Refractive Index as Indicated % Sugar at equilibrium.	-
n	Number of growth rate constants K used in obtaining \bar{K} .	-
R	Universal Gas Constant.	cals (g.mole) ⁻¹ °K ⁻¹
S	Specific Surface	cm ² g ⁻¹
t	Time.	min.
t	Mean temperature of emergent stem of partially immersed thermometer.	°C.
T	Temperature.	°K.
T _o	Observed temperature	°C.
v	Total volume of solution.	cm ³
V	Volume of solvent.	cm ³
x	% mass fraction.	g (100g) ⁻¹
X	Number % oversize on combined size distributions.	-

<u>SYMBOL</u>	<u>MEANING</u>	<u>UNITS</u>
X	% Mass ratio.	$g (100g)^{-1}$
Y	Number % oversize using 280 μ Coulter Counter orifice.	-
y	Correction to be added to T_o to correct partially immersed thermometer.	$^{\circ}C.$
Z	Number % oversize using 50 μ Coulter Counter orifice.	-
λ	Wavelength of light.	millimicron
m μ	Millimicron	10^{-7} cm.
ρ_s	Density of solute.	$g.cm^{-3}$
ρ_w	Density of solvent.	$g.cm^{-3}$

NOMENCLATURE USED WITH COULTER COUNTER

SIZE ANALYSER

<u>SYMBOL</u>	<u>MEANING</u>	<u>UNITS</u>
A	The orifice area normal to the flow axis.	cm ²
a	The projected area, parallel to the orifice axis, of the particle as it is oriented in passing through the orifice.	cm ²
D	The orifice diameter.	micron
d	The diameter of the particle.	micron
F	Scale Expansion Factor.	-
I	The aperture current setting.	
I *	The aperture current setting used in calibration.	
K	The calibration factor.	-
n ¹	The average of counts of a particular sample.	-
\bar{n}^1	The average of counts n ¹ of each sample.	-
n ¹¹	The coincidence correction.	-
n	The corrected count.	-
P	Coincidence factor.	-
R	The aperture resistance.	ohms.
Δ R	The change in aperture resistance	ohms.

<u>SYMBOL</u>	<u>MEANING</u>	<u>UNITS</u>
	produced by the particle.	
r	The resistance of the aperture current switch in the position used.	ohms.
t	The relative particle volume (t^1 .F.)	-
t^1	The threshold level.	-
t^*	The threshold value found for the monosized particles used in the calibration.	-
V	The voltage between the outer electrode and earth when immersed in the electrolyte.	volts.
v	The particle volume.	cm^3
✓	Background count of blank electrolyte.	-
ρ	The particle resistivity	microhms cm^{-3}
ρ_0	The electrolyte resistivity	microhms cm^{-3}

REFERENCES

1. OSTWALD, W., "Lehrbuck," Vol. II, Leipzig, Englemann, 1896 - 1902.
2. MIERS, H.A., J. Inst. Metals, 37, 331, 1927.
3. FREUNDLICH, H., "Colloid and Capillary Chemistry", p. 155, New York, Dutton & Co., 1922.
4. KNAPP, L.F., The Solubility of small particles and the stability of Colloids, Trans. Faraday Soc., 17, (1922) 457.
5. DUNDON, M.L., Surface Energy of Several Salts, J. Amer. Chem. Soc., 45 (1923) 2658.
6. ROLLER, J. PHYS. CHEM. 35, 1931, 1133.
7. VAN HOOK, A., and FRULLA, F., Ind. Eng. Chem., 44, No. 6. (1952).
8. GIBBS, J.W., Collected Works, 1928, London: Longmans Green.
9. BECKER, R., and DOERING, W., Ann. Phys., 32, 128, (1938)
10. BECKER, R. VON, Ann. Phys. Lpz. 32. (1938) 128.
11. UHLMANN, D.R., and CHALMERS, B., The Energetics of Nucleation. Ind. Eng. Chem., 57, 9, 1965 19 - 31.
12. VAN HOOK, A., "Crystallisation": Theory and Practice, 1961 (New York : Rheinhold Publishing Corporation).
13. MELIA, T.P., Crystal Nucleation from Aqueous Solutions. J. Appl. Chem., 15. 1965 345.

14. VOLMER, M., Kinetik der Phasenbildung, Dresden, T. Steinkopff, 1939.
15. PRECKSHOT, G.W. and BROWN, G.G., Ind. Eng. Chem. 44, No. 6, 1952. p 1314.
16. TELKES, M., Ibid. p. 1308.
17. VAN HOOK, A and FRULLA, F. Ibid. p. 1305.
18. MULLIN, J.W. and RAVEN, K.D., Nature, 195, 1962, p.35.
19. STRICKLAND-CONSTABLE, R.F., and MASON, R.E.A., Nature London 1963, 197, 897.
20. MELIA, T.P., and MOFFITT, W.P., I. & E.C. FUNDAMENTALS. Vol. 3. No. 4. 1964. p.313.
21. BRANSOM, S.H., DUNNING, W.J., and MILLARD, B. Symposium on Crystal Growth, Disc. Faraday Soc., No. 5 (1949).
22. RANDOLPH, A.D., and LARSON, M.A., A.I. Ch. E.J., 1962, 8, 639.
23. BUCKLEY, H.E., Crystal Growth, 1952, London : Chapman and Hall.
24. MARC, R., UBER DIE KRISTALLISATION AUS WASSERIGEN LOSUNGEN, Z. PHYS. CHEM., 61 (1908), 385; 67 (1909), 470.
25. VOLMER, M., Z. PHYSIK. CHEM., 1922, 102, 267 - 275.
26. BRANDES, H., Z. PHYSIK. CHEM., 1927, 126, 196 - 210.
27. BRAVAIS, A., ETUDES CRISTALLOGRAPHIQUES? PARIS, GAUTHIER VILLARS, 1866.
28. KOSSEL, W., in FALKENHAGEN, Quantentheorie und Chemie, Leipzig, 1928, 46pp.

29. STRANSKI, I.N., Z. PHYSIK. CHEM., 1928, 136, 259 - 278.
30. FRANK, F.E., The Influence of Dislocations on Crystal Growth, Ref. 4 p. 48.
31. NOYES, A.A. and WHITNEY, W.R., J. Amer. Chem. Soc., 19, (1897), 930. Z. Phys. Chem., 23 (1897), 689.
32. NERNST, W., Z. Phys. Chem., 47 (1904), 52.
33. MULLIN, J.W., Crystallisation, 1961, London: Butterworths.
34. BERTHOUD, A., J. Chim. Phys., 10 (1912), 624.
35. VALETON, J.J.P., Z. Kristallogr., 59 (1923), 135, 335; 60 (1924), 1.
36. CARTIER, R., PINDZOLA, D and BRUINS, P.F., Ind. Eng. Chem., 51 (1959), 1409.
37. AMELINCKX, S., J. Chim. Phys., 47 (1950), 213.
38. BRANSOM, S.H., DUNNING, W.J., MILLARD, B., Ref. 4.
39. JENKINS, J.D., J. Am. Chem. Soc. (1925) 47, 1, 903-922.
40. McCABE, W.L. and STEPHENS, R.P., Chem. Eng. Prog., 47, No. 4, pp. 168.
41. VAN HOOK, A., Kinetics of Crystallisation, "Principles of Sugar Technology", Vol. 2, P. Honig, 1959, Amsterdam: Elsevier.
42. RUMFORD, F. and BAIN, J., Trans. Inst. Chem. Eng. Vol. 38, 1960.
43. HIXON, A.W., and KNOX, K.L., Ind. Eng. Chem. 43, (1951) 2144.
44. BRANSOM, S.H., Brit. Chem. Eng., December, 1960.

45. BRANSOM, S.H., and PALMER, A.G.C., Brit. Chem. Eng. 9, No. 10, 1964.
46. BENNETT, R.C., Chem. Eng. Prog., 58, No. 9, 1962.
47. VON GROTH, P., Chemische Krystallographie, Vol. 3., 385, Leipzig, 1915.
48. BERLOW, E., BARTH, R.H., and SNOW, J.E.,
The Pentaerythritols, A.C.S. Monograph No. 136,
Rheinhold, New York, 1958.
49. SHINOD, R., CRUICKSHANK, D.W.J., and COX, E.C.,
Acta. Cryst. 11, 389 - 91 (1958).
50. EVANS, Crystal Chemistry, p. 321.
51. International Critical Tables, 5, 70.
52. BRADLEY, R.S. and COTSON, S., J. Chem. Soc. 1953,
1984 - 88.
53. NITTA, I., SEKI, S., and SUZUKI, K., Bull. Chem. Soc.
Japan, 2463 - 9 (1951).
54. BRIGHT and CARSON, I.C.I. [REDACTED] *
55. WYLER, J.A., WERNETT, E.A., (Trojan Powder Company),
U.S. Patent (2,299,048), 1942.
56. I.C.I. [REDACTED] *
57. I.C.I. [REDACTED] *

58. I.C.I. [REDACTED] *
[REDACTED]
59. I.C.I. [REDACTED] *
[REDACTED]
60. I.C.I. [REDACTED] *
61. I.C.I. [REDACTED] *
[REDACTED]
[REDACTED] *
62. SALKIND, M., AHERN, H.F. and ALBERT, A.A., Ind. Eng. Chem., 50, No. 8, 1106 - 14, 1958.
63. WIERSMA, D.S., HOYLE, R.E. and REMPIS, H., Anal. Chem. Vol. 34, No. 12, 1533, (1962).
64. BARTH, R.H. and SNOW, J.E., U.S. Patent 2,464,430.
65. WILLIAMS, A.F., I.C.I. Private Communication.
66. SPIREK and STROUTS, I.C.I. [REDACTED] *
[REDACTED]
67. SPREK and WILLIAMS, I.C.I. [REDACTED] *
[REDACTED]
[REDACTED] *
68. MACINNES and ALLAN. I.C.I. [REDACTED] *
[REDACTED]
69. I.C.I. [REDACTED] *
70. I.C.I. N.A.M.B. M.189. d. 1 - 9.
71. WALKER, J.F., "Formaldehyde", 3rd. Ed., A.C.S. Monograph. No. 159, Rheinhold.

* Private communication

72. WYLER, J.A., and WERNETT, E.A., (Trojan Powder Company), U.S. Patent (2,299,048), 1942.
73. PHOENIX, L., I.C.I. [REDACTED]
[REDACTED]
[REDACTED] *
74. International Critical Tables. 2. 337.
75. COOKE, E.G., Paint Manufacture. 18, 125 (1948).
76. Analytical Chemistry, Vol. 1. p.95. Editors: Strouts, C.R.N. Gilfillan, J.H., Wilson, H.N.
77. WHITTIER, E.O., and GOULD, S.P., Ind. Eng. Chem. 23, No. 6, p.670. (1931).
78. VAN HOOK, A., Ind. Eng. Chem. 37, No. 8., p.782 (1945).
79. BRANSOM, S.H., Chem. Proc. Eng. 46, No. 12, p.647, (1965).

* Private communication